REMARKS/ARGUMENTS

Claims 1, 2, 10, 11, and 20 are pending.

Claim 1 and claim 20 have been amended to include that the subject is suffering from BMP-induced osteogenesis characterized by heterotopic ossification, and that human noggin SEQ ID NO:2 is for local administration, whereas human noggin mutant SEQ ID NO:10 is for systemic or local administration. Claim 10 has been amended to include that human noggin SEQ ID NO:2 is for local administration whereas human noggin mutant SEQ ID NO:10 is for systemic or local administration. Support for the amendments to the claims can be found in the claims and specification as filed. Support for the amendments to claims 1, 10, and 20 can be found, for example, at paragraph [0030]. The amendments to the claims add no new matter and place the claims in condition for allowance; thus the Examiner is respectfully requested to enter them.

III. Rejections Under 35 USC § 112, first paragraph.

The Examiner withdrew the enablement rejection regarding the scope of the noggin polypeptides of the claims. Accordingly, this subject matter will not be addressed.

The Examiner sustained the remaining enablement rejections interposed in the Office Action dated 28 November 2006. Briefly, the Examiner asserted that the specification does not enable using a noggin polypeptide to affect a patient already suffering from a bone disorder. The Examiner also asserted that the prior art teaches that noggin may induce increased bone density and bone formation rates, a feature not expected of a BMP antagonist, citing Yanagita (2005) Cytokine and Growth Factor Reviews 16:309-317, 314. The Examiner also asserted that the prior art does not disclose the functions of BMPs after birth and thus such functions are unpredictable, and the claims are extremely broad because they do not specify the BMP-related disorder to be treated or the effect that noggin administration is expected to have.

Applicants respectfully disagree with the Examiner and refer the Examiner to arguments made of record in Applicants' response to the Non-final Office Action dated 28 November 2006. Applicants submit that the amendments to the claims render the

Examiner's rejections moot. Applicants below address the Examiner's rejections to the extent that they might be applied to the amended claims.

Applicants respectfully disagree with the Examiner that "[n]o working examples directed to protein therapy of patients already suffering from FOP or any other BMP-related disorder are provided." (Office Action of 28 November 2006, page 3, final paragraph).

A working model of a BMP disorder is presented in the specification as filed. The specification presents a percutaneous bone induction model of BMP-induced osteogenesis used to evaluate the effectiveness of noggin as an inhibitor of heterotopic ossification (see, e.g., paragraph [0030]) that reproduces the characteristic stages of rhBMP-induced endochondral bone formation and mimics all the stages of heterotopic ossification seen during ectopic bone induction in FOP (see, e.g., paragraph [0030]). The model presents inflammatory and angiogenic, fibroproliferative stages as well as mineralization of the cartilage matrix and mature heterotopic bone growth with marrow elements (see, e.g., paragraph [0031]). The Examiner has not provided any rational basis as to why the above-mentioned model would not be understood by a person of ordinary skill as a model for FOP and/or a BMP-related disorder. The Examiner has not provided any rational basis, has made no findings regarding whether the model mimics FOP, and has not asserted that the model described in the specification is an unacceptable model for FOP. The Examiner has not provided any rational basis, has made no findings regarding the role of BMP in the model, and has not asserted that the model does not represent a BMP-related disorder.

Treatment of the BMP disorder described above, by systemic (intraperiotoneal) and local administration of ***noggin protein***, is disclosed in the specification (see, e.g., paragraph [0032]). Local administration of ***noggin protein*** was effective, whereas systemic administration was not (see Id.). Systemic administration of noggin is ineffective due to its poor bioavailability and low half-life (see paragraph [0033]).

The inventors of the pending claims presented an example of successful treatment of the BMP disorder by ***systemic administration of human noggin mutant protein*** hNOGΔB2 (SEQ ID NO:10), which deletes the heparin-binding domain of human noggin (see, for example, paragraph [0034]). The specification discloses in this example that

administration of intraperitoneal injection of the mutant noggin protein of the pending claims resulted in longer half-life and improved bioavailability over wild type human noggin.

Thus, the specification provides evidence that (1) noggin ***protein*** administered locally effectively inhibited BMP-induced heterotopic ossification (paragraph [0032]); (2) noggin ***protein*** systemically administered has a low half-life and low bioavailability due to its heparin-binding function (paragraph [0033]) but that a mutant noggin ***protein*** lacking a heparin-binding domain displayed improved half-life and higher bioavailability than wild-type noggin (paragraph [0033] and [0034]). The Examiner has not indicated any reasonable basis to doubt the veracity of these examples.

The Examiner has not articulated a reasonable basis to question the veracity of Applicants' enablement of a method for treating BMP-induced osteogenesis characterized by heterotopic ossification using the recited antagonists of the claims (*i.e.*, noggin and mutant noggin). No reasonable basis has been articulated by the Examiner that would call into question the ability of the recited noggins to treat rather than prevent the recited disorder. Applicants submit that the Examiner's mere disbelief—absent a clearly articulated reasonable basis—is insufficient to support the enablement rejection. Regarding the Examiner's reliance on Glaser's finding (Glaser (2003) The Journal of Bone and Joint Surgery 85-A/12:2332-2342) that systemic administration of noggin is not effective in preventing BMP4-induced heterotopic ossification, this observation has no bearing on efficacy of local administration using noggin, or on efficacy of systemic administration using the claimed noggin mutant, as taught by Applicants' own specification (see, *e.g.*, paragraphs [0032]-[0033]). Accordingly, Applicants' reliance on Glaser to support a nonenablement rejection is misplaced.

Applicants respectfully submit that the Examiner has mischaracterized the Yanagita reference (Yanagita (2005) Cytokine & Growth Factor Reviews 16:309-317. Yanagita expressly endorses that

> Noggin antagonizes the action of BMPs ... [n]oggin binds to BMP-2 and BMP-4 with high affinity and BMP-7 with low affinity, and prevents BMPs from binding to its receptors.
>
> * * *

> [t]ransgenic mice overexpressing noggin in mature osteocalcin-positive osteoblasts showed dramatic decreases in bone mineral density and bone formation rates.

Yanagita at page 313-314, citations omitted. Yanagita notes that noggin belongs to the class of BMP antagonists (Yanagita at pages 309-310). Accordingly, Yanagita could not provide a reasonable basis to doubt the veracity of the enablement of the pending claims.

Based on the examples described above, the inventors transfered the structural gene for the noggin mutant lacking the heparin-binding domain into a mouse using an adenoviral construct to demonstrate how noggin protein delivered through gene therapy could prevent BMP-induced heterotopic ossification in a mouse (see, *e.g.,* paragraph [0035] and Example 6). Examples in the specification describe the efficacy of the approach of generating mutant noggin protein *in vivo* retrovirally in an implant model to prevent BMP-mediated heterotopic ossification. The Examiner has not articulated a reasonable basis as to why exogenously introduced noggin or mutant noggin protein would not inhibit or prevent the process of heterotopic ossification mediated by BMP, regardless of whether the noggin or mutant noggin was introduced by injection or retrovirally, and regardless of what stage (*e.g.*, histologic stages 1A, 1B, 1C, 2A, 2B, or 2C; specification at paragraph [0030]) the noggin or mutant noggin was introduced. Accordingly, Applicants submit that there is no reasonable basis to doubt the enablement of the claimed method of treating a BMP-induced osteogenesis characterized by heterotopic ossification using the recited noggin proteins.

The Examiner indicated that she would consider evidence of data wherein noggin polypeptides are used to treat BMP-related disorders in subjects suffering from BMP-related disorders. Applicants provide as exhibits the following publications:

(1) Hannalla et al. (2004) The Journal of Bone and Joint Surgery 86-A(1) 80-91), attached as Exhibit A, which shows that exogenously added noggin protein in mice will inhibit heterotopic ossification following Achilles tenotomy (page 85, right column), and which shows that some heterotopic ossification can occur but the amount is influenced by the presence of noggin (page 89, left column, first full paragraph), indicating that noggin can not only prevent heterotopic ossification but also retard its progress;

(2) Lories et al. (2005) The Journal of Clinical Investigation 115(6):1571-1579, attached as Exhibit B, which shows that exogenously added noggin in a mouse model of a heterotopic ossification disorder (ankylosis) that mimics endochondral bone formation (see page 1576, left column, first full paragraph);

(3) Warren et al (2003) Nature 422:625-629, attached as Exhibit C, which shows noggin's role in ongoing bone development and the possibility of using noggin therapeutically in post-natal skeletal development (see final sentence on page 628, left column, before "Methods"); and

(4) Rosenberg, L (2003) The Journal of Bone and Joint Surgery 85-A(Suppl 3):1-2, attached as Exhibit D, which describes new therapeutic approaches to human BMP-related disease by administration of noggin (page 1, right column, final two paragraphs); and

(5) Devlin et al (2003) Endocrinology 144(5):1972-1978, attached as Exhibit E, which describes a noggin transgene under control of the osteocalcin promoter, which exhibited phenotypes in post-natal animals that are in agreement with what would be predicted from blocking the known effects of BMPs (see, *e.g.*, page 1976, right column).

Conclusion

It is believed that this document is fully responsive to the Final Office Action mailed 02 May 2007. In light of the above, it is believed that the claims are in condition for allowance, and such action is respectfully urged.

Fees

It is believed that no fee is due with the submission of this response. In the event it is determined that a fee is due, the Commissioner is hereby authorized to charge Deposit Account Number 18-0650 for the amount of that fee.

Respectfully submitted

Tor Smeland Ph.D., Reg. No. 43,131
Regeneron Pharmaceuticals, Inc.
777 Old Saw Mill River Road
Tarrytown, New York 10591
(914) 345-7435 (direct)

EXHIBIT A

RETROVIRAL DELIVERY OF NOGGIN INHIBITS THE FORMATION OF HETEROTOPIC OSSIFICATION INDUCED BY BMP-4, DEMINERALIZED BONE MATRIX, AND TRAUMA IN AN ANIMAL MODEL

BY DAVID HANNALLAH, MD, MSC, HAIRONG PENG, MD, PHD, BRETT YOUNG, BSC, ARVYDAS USAS, MD, BRIAN GEARHART, BSC, AND JOHNNY HUARD, PHD

Investigation performed at the Department of Orthopaedic Surgery, University of Pittsburgh, School of Medicine, Pittsburgh, and the Growth and Development Laboratory, Children's Hospital of Pittsburgh, Pittsburgh, Pennsylvania

Background: The heterotopic ossification of muscles, tendons, and ligaments is a common problem faced by orthopaedic surgeons. We investigated the ability of Noggin (a BMP [bone morphogenetic protein] antagonist) to inhibit heterotopic ossification.

Methods: Part 1: A retroviral vector carrying the gene encoding human Noggin was developed and used to transduce muscle-derived stem cells. Part 2: Cells transduced with BMP-4 were implanted into both hind limbs of mice along with either an equal number, twice the number, or three times the number of Noggin-expressing muscle-derived stem cells (treated limb) or with nontransduced muscle-derived stem cells (control limb). At four weeks, the mice were killed and radiographs were made to look for evidence of heterotopic ossification. Part 3: Eighty milligrams of human demineralized bone matrix was implanted into the hind limbs of SCID (severe combined immunodeficiency strain) mice along with 100,000, 500,000, or 1,000,000 Noggin-expressing muscle-derived stem cells (treated limbs) or nontransduced muscle-derived stem cells (control limbs). At eight weeks, the mice were killed and radiographs were made. Part 4: Immunocompetent mice underwent bilateral Achilles tenotomy along with the implantation of 1,000,000 Noggin-expressing muscle-derived stem cells (treated limbs) or nontransduced muscle-derived stem cells (control limbs). At ten weeks, the mice were killed and radiographs were made.

Results: Part 1: An in vitro BMP inhibition assay demonstrated that Noggin was expressed by muscle-derived stem cells at a level of 280 ng per million cells per twenty-four hours. Part 2: Three varying doses of Noggin-expressing muscle-derived stem cells inhibited the heterotopic ossification elicited by BMP-4-expressing muscle-derived stem cells. Heterotopic ossification was reduced in a dose-dependent manner by 53%, 74%, and 99%, respectively ($p < 0.05$). Part 3: Each of three varying doses of Noggin-expressing muscle-derived stem cells significantly inhibited the heterotopic ossification elicited by demineralized bone matrix. Heterotopic ossification was reduced by 91%, 99%, and 99%, respectively ($p < 0.05$). Part 4: All eleven animals that underwent Achilles tenotomy developed heterotopic ossification at the site of the injury in the control limbs. In contrast, the limbs treated with the Noggin-expressing muscle-derived stem cells had a reduction in the formation of heterotopic ossification of 83% and eight of the eleven animals had no radiographic evidence of heterotopic ossification ($p < 0.05$).

Conclusions: The delivery of Noggin mediated by muscle-derived stem cells can inhibit heterotopic ossification caused by BMP-4, demineralized bone matrix, and trauma in an animal model.

Clinical Relevance: Gene therapy to deliver Noggin may become a powerful method to inhibit heterotopic ossification in targeted areas of the body.

The heterotopic ossification of muscles, tendons, and ligaments can be a problem following trauma, neurologic injury, severe burns, and elective surgery and in certain diseases such as fibrodysplasia ossificans progressiva[1-11]. Reports of radiographic heterotopic ossification following total hip arthroplasty have ranged from 15% to 90% of patients,

with 1% to 27% of patients reporting clinically important pain and loss of motion[12]. The prevalence of heterotopic ossification associated with all burn injuries has ranged between 1% and 3% but can be as high as 35% for larger, more severe burns[10,13,14]. The development of heterotopic ossification after spinal cord injury has been reported in 16% to 53% of patients, one-third of whom had clinically important manifestations[15,16]. Heterotopic ossification has also been reported in nonskeletal tissues such as the gastrointestinal tract[17].

While the exact etiology of heterotopic ossification remains unclear, it is possible that the overexpression of certain bone morphogenetic proteins (BMPs), such as BMP-2 and BMP-4, plays a role in heterotopic ossification formation. It has been demonstrated that the addition of BMPs to normal skeletal muscle can induce heterotopic ossification[18-21]. BMP-4, in particular, seems to be upregulated in diseases such as fibrodysplasia ossificans progressiva, a rare autosomal dominant disease characterized by the progressive ossification of skeletal muscle, ligaments, and tendons[7,22-26].

In addition to overactive BMP, the downregulation of growth factors such as Noggin, a BMP antagonist, may contribute to heterotopic ossification[27]. Some patients with fibrodysplasia ossificans progressiva have been found to have mutations in the Noggin gene, and mice with deletions of the Noggin gene develop many features similar to those of fibrodysplasia ossificans progressiva[27,28].

We hypothesized that heterotopic ossification may be inhibited by the local delivery of Noggin to tissue predisposed to form heterotopic ossification. To test our hypothesis, we developed a retroviral vector carrying the gene encoding Noggin. The vector was used to transduce skeletal muscle-derived stem cells[29] and then was tested against three different models of heterotopic ossification formation (BMP-4, demineralized bone matrix, and trauma), all of which previously have been shown to induce heterotopic ossification[18,30-37]. Specifically, we evaluated the in vivo ability of Noggin-expressing muscle-derived stem cells to prevent BMP-4-expressing muscle-derived stem cells from forming heterotopic ossification. We also tested the Noggin-expressing muscle-derived stem cells against demineralized bone matrix. Finally, we investigated the ability of the Noggin-expressing muscle-derived stem cells to block heterotopic ossification in immunocompetent mice subjected to Achilles tenotomy, a traumatic animal model of heterotopic ossification initially described by Buck in 1953[33] and later substantiated by McClure[32] and Rooney et al.[34].

Materials and Methods

Part 1: Development of a Retroviral Vector and Genetic Engineering of Muscle-Derived Stem Cells to Express Noggin

Polymerase chain reaction-amplified Noggin human cDNA was cloned into a murine leukemia virus-based retroviral vector pCLX at the Not I and Bgl II sites, resulting in pCLNog. pCLX had been previously created from pLXSN (obtained from A. Dusty Miller of Fred Hutchinson Cancer Research Center, Seattle, Washington) by removing the SV40 promoter and the neomycin resistance gene, and replacing the U3 in the 5′ LTR with the human cytomegalovirus promoter as described by Peng et al.[36,37].

The CLNog vector DNA was converted into replication defective retrovirus by cotransfection, with calcium-phosphate precipitation, into a packaging cell line GP-293 (Clontech, Palo Alto, California) with a plasmid, pVSVG, that expressed vesicular stomatitis virus glycoprotein as the viral envelope[36,37]. The conditioned medium containing the retrovirus expressing Noggin (RetroNog) was centrifuged at 3000 rpm for five minutes to remove cellular debris and then was stored at –80°C in small aliquots until use.

RetroNog was used to transduce muscle-derived stem cells that had been isolated previously with use of the preplate technique[38,39], which separated the muscle-derived cells into six different populations (PP1 to PP6) according to their ability to adhere to type-I collagen-coated flasks. The specific muscle-derived stem cells used in this experiment are a clonal population of PP6 cells, termed mc13 cells, that display the capacity to differentiate into both myogenic and osteogenic lineages in vitro and in vivo[29]. The mc13 cells used in this experiment were at passage 14 and were found to be nontumorigenic as previously described[29]. The cells were grown in culture medium made from Dulbecco modified Eagle medium, 10% fetal bovine serum, 10% horse serum, and 1% L-glutamine. The isolation and extensive characterization of mc13 cells have been previously reported[29]. After transduction, the muscle-derived stem cells were tested for the ability to express Noggin with use of an in vitro BMP-4 inhibition alkaline phosphatase assay. Serial dilutions of conditioned media, taken from flasks containing Noggin-expressing muscle-derived stem cells, were used to inhibit the ability of BMP-4 to activate alkaline phosphatase in C2C12 cells (CRL-1772; American Type Culture Collection, Manassas, Virginia), a mouse myoblast cell line[40,41]. The C2C12 cells were used for the bioassay because of their ability to express alkaline phosphatase in a dose-dependent manner in response to BMP-4 stimulation[36]. Each BMP-4 inhibition alkaline phosphatase assay was performed in triplicate, and the average number of positive cells was used to calculate the concentration of Noggin expressed by the muscle-derived stem cells. Known amounts of recombinant mouse Noggin (R and D Systems, Minneapolis, Minnesota) were used as a control.

Part 2: In Vivo Evaluation of the Ability of Noggin to Inhibit Heterotopic Ossification Induced by BMP-4

Next, we evaluated the capacity of the Noggin-expressing muscle-derived stem cells engineered in Part 1 to inhibit the ability of BMP-4-expressing muscle-derived stem cells to form heterotopic ossification. The BMP-4-expressing muscle-derived stem cells used in this experiment previously have been shown to induce heterotopic ossification formation and secrete BMP-4 at a level of 115 ng per million cells every twenty-four hours[35-37]. These prior studies also showed that the resultant heterotopic ossification was attributable to the BMP-4 secretion and not to the vector itself, since the control retro-

TABLE I Part-2 Animal Groups and Corresponding Results

Group	No. of Mice	Ratio of BMP to Noggin Cells	Ratio of BMP to Noggin Protein	Implants Used in Control Limb†	Implants Used in Treated Limb†	Area of Heterotopic Ossification*		
						Control Limb† (mm^2)	Treated Limb† (mm^2)	Reduction of Area
A	5	1:1	1:2.4	200,000 BMP-4-expressing MDSC and 200,000 nontransduced MDSC	200,000 BMP-4-expressing MDSC and 200,000 Noggin-expressing MDSC	26.47 ± 8.5	12.47 ± 7.85	53%
B	6	1:2	1:4.8	200,000 BMP-4-expressing MDSC and 400,000 nontransduced MDSC	200,000 BMP-4-expressing MDSC and 400,000 Noggin-expressing MDSC	19.83 ± 5.46	5.07 ± 6.52	74%
C	5	1:3	1:7.2	200,000 BMP-4-expressing MDSC and 600,000 nontransduced MDSC	200,000 BMP-4-expressing MDSC and 600,000 Noggin-expressing MDSC	26.21 ± 11.25	0.29 ± 0.64	99%

*The difference between the treated and control limbs with respect to the formation of heterotopic ossification reached significance for groups A, B, and C ($p < 0.05$). The dose-dependent nature of the inhibition also reached significance between groups B and C as well as between groups A and C ($p < 0.05$). †MDSC = muscle-derived stem cells. ‡The values are given as the mean and the standard deviation.

viral vector expressing only the marker gene (LacZ) did not elicit any heterotopic ossification formation[35-37].

On day 0, 5 × 5 × 2-mm biodegradable collagen sponges (Gelfoam; Pharmacia and Upjohn, Peapack, New Jersey) were loaded with either BMP-4-expressing muscle-derived stem cells and Noggin-expressing muscle-derived stem cells or BMP-4-expressing muscle-derived stem cells and nontransduced muscle-derived stem cells as outlined in Table I. The ratio of BMP-4-expressing muscle-derived stem cells to Noggin-expressing muscle-derived stem cells was 1:1 in group A, 1:2 in group B, and 1:3 in group C. Since the BMP-4-expressing muscle-derived stem cells and the Noggin-expressing muscle-derived stem cells did not express their transgenes at the same level, Table I also shows the ratio of BMP-4 to Noggin protein. The collagen sponges were then incubated overnight at 37°C in culture medium.

On day 1, eighteen immunocompetent inbred mice (C57BL16J; Jackson Laboratories, Bar Harbor, Maine) were anesthetized with use of an intraperitoneal injection of 3 mg of ketamine and 0.3 mg of xylazine. A posterior approach to the femur was used to develop a pocket in the hamstring muscle on both the left and right sides. The surgeon was then handed one of the 5 × 5 × 2-mm collagen sponges that had been prepared the previous day. The sponge was briefly immersed in Hanks balanced salt solution to wash away any proteins from the culture medium, and then it was inserted into the appropriate pocket created in the mouse limb. Each mouse received a sponge from the control group on one side and a sponge from the treatment group on the contralateral side. The surgeon was blinded with regard to which limb received which sponge during the surgery. Care was taken not to cross-contaminate the treatment sponges with the control sponges. The skin was closed with use of 4-0 Prolene nonabsorbable suture (Ethicon, Somerville, New Jersey).

At four weeks after the surgery, the mice were killed and both lower extremities were removed by cutting across the proximal part of the femur. The skin was carefully removed without disrupting any of the musculature, and radiographs of the limbs were made with use of a Faxitron x-ray cabinet (Faxitron X-Ray, Wheeling, Illinois) for forty seconds at 40 kVp to look for evidence of heterotopic ossification. The radiographs were digitized at a resolution of 2400 pixels/in (945 pixels/cm), and the amount of heterotopic ossification formation was measured with use of the National Institutes of Health imaging software to calculate the two-dimensional area of the heterotopic ossification. After the radiographs were made, both thighs were flash-frozen in 2-methylbutane precooled in liquid nitrogen and then were sectioned into 10-μm sections with use of a cryostat (Microm, Waldorf, Germany). Histological analysis with von Kossa staining followed by hematoxylin and eosin staining[42] was performed to evaluate for heterotopic ossification; however, no attempt was made to distinguish different populations of cells with use of cell-specific markers. The interval between killing the mice and flash-freezing the specimens was approximately one hour, during which time the specimens were maintained in cooled Dulbecco phosphate-buffered solution. All comparisons between treated and untreated limbs were made in the same animals so that animal-to-animal variations in the ability to form heterotopic ossification would not affect the results. The significance between the treated and untreated limbs was determined with use of a paired two-tailed t test. The significance

TABLE II Part-3 Animal Groups and Corresponding Results

Group	No. of Mice	Implants Used in Control Limb†	Implants Used in Treated Limb†	Area of Heterotopic Ossification*		
				Control Limb† (mm^2)	Treated Limb† (mm^2)	Reduction of Area
A	5	80 mg human demineralized bone matrix and 100,000 nontransduced MDSC	80 mg human demineralized bone matrix and 100,000 Noggin-expressing MDSC	42.71 ± 15.33	3.97 ± 4.88	91%
B	5	80 mg human demineralized bone matrix and 500,000 nontransduced MDSC	80 mg human demineralized bone matrix and 500,000 Noggin-expressing MDSC	27.47 ± 5.27	0.16 ± 0.36	99%
C	4	80 mg human demineralized bone matrix and 1,000,000 nontransduced MDSC	80 mg human demineralized bone matrix and 1,000,000 Noggin-expressing MDSC	32.94 ± 9.7	0.28 ± 0.56	99%

*The difference between treated and control limbs with respect to the formation of heterotopic ossification reached significance in groups A, B, and C ($p < 0.05$). The effect of varying the dose of Noggin, however, did not reach significance. †MDSC = muscle-derived stem cells. †The values are given as the mean and the standard deviation.

between the different doses of Noggin was determined with use of a general linear model.

Part 3: In Vivo Evaluation of the Ability of Noggin to Block Heterotopic Ossification Induced by Demineralized Bone Matrix

On day 0, 5 × 5 × 2-mm biodegradable collagen sponges (Gelfoam; Pharmacia and Upjohn) were loaded with either 100,000 (group A), 500,000 (group B), or 1,000,000 (group C) Noggin-expressing muscle-derived stem cells or nontransduced muscle-derived stem cells as outlined in Table II. The sponges were then incubated overnight at 37°C in culture medium.

On day 1, a pocket was developed in the hamstring muscles of fifteen SCID (severe combined immunodeficiency strain) mice with use of the same approach to the femur as described in Part 2. All mice had 80 mg of human demineralized bone matrix (Osteotech, Eatontown, New Jersey) placed into both the left and right thighs. No carrier was used for the demineralized bone matrix. In addition, each mouse received a collagen sponge from the control group on one side and a collagen sponge from the treatment group (Noggin-expressing muscle-derived stem cells) on the contralateral side. The sponges were briefly rinsed in Hanks balanced salt solution and then were placed into the developed hamstring pocket, on top of and in direct contact with the demineralized bone matrix. The surgeon was blinded with regard to which limb received which sponge (a control sponge or one containing Noggin-expressing cells) during the surgery. Care was taken not to cross-contaminate the treatment sponges with the control sponges. The skin was closed with use of 4-0 Prolene nonabsorbable suture (Ethicon).

At eight weeks after surgery, the mice were killed. The limbs were harvested, radiographs were made, and then the limbs were flash-frozen for histological analysis as described in Part 2. The amount of heterotopic ossification was calculated as described in Part 2.

Part 4: In Vivo Evaluation of the Ability of Noggin to Inhibit Heterotopic Ossification After Achilles Tenotomy

On day 0, 5 × 5 × 2-mm biodegradable collagen sponges (Gelfoam; Pharmacia and Upjohn) were loaded with either 1,000,000 Noggin-expressing muscle-derived stem cells (treatment group) or with 1,000,000 nontransduced muscle-derived stem cells (control group). The sponges were then incubated overnight at 37°C in culture medium.

On day 1, eleven mice underwent bilateral midpoint Achilles tenotomy through a posterior approach. In addition, a pocket was developed in the triceps surae. The sponges that were prepared the previous day were briefly rinsed in Hanks balanced salt solution and then inserted into the developed mouse pocket. Each mouse received a sponge from the control group on one side and a sponge from the treatment group on the contralateral side. The surgeon was blinded with regard to which limb received which sponge (a control sponge or one containing Noggin-expressing cells) during the surgery. Care was taken not to cross-contaminate the treatment sponges with the control sponges. The skin was closed with use of 4-0 Prolene nonabsorbable suture (Ethicon).

At ten weeks after surgery, the mice were killed. The limbs were harvested, radiographs were made, and then the limbs were flash-frozen for histological analysis as described in Part 2. The amount of heterotopic ossification was calculated as described in Part 2.

Results

Part 1: In Vitro Evaluation of the Noggin-Expressing Muscle-Derived Stem Cells

The BMP-4 alkaline phosphatase inhibition assay demonstrated the ability of the Noggin-expressing muscle-derived stem cells to inhibit BMP-4 in vitro. The number of assayed C2C12 cells that expressed alkaline phosphatase is

TABLE III Part-4 Animal Groups and Corresponding Results

No. of Mice	Implants Used in Control Limb†	Implants Used in Treated Limb†	Area of Heterotopic Ossification*		
			Control Limb‡ (mm^2)	Treated Limb‡ (mm^2)	Reduction of Area
11	Achilles tenotomy and 1,000,000 nontransduced MDSC	Achilles tenotomy and 1,000,000 Noggin-expressing MDSC	0.53 ± 0.3	0.09 ± 0.2	83%

*The difference between the treated and control limbs with respect to the formation of heterotopic ossification reached significance ($p < 0.05$). †MDSC = muscle-derived stem cells. ‡The values are given as the mean and the standard deviation.

shown in Figure 1 as a percentage of the number of cells that expressed alkaline phosphatase when exposed only to BMP-4 and not to Noggin. Varying ratios of BMP-4 to Noggin are shown. When the ratio of BMP-4 to Noggin-expressing cells was 1:1, only 17% of the assayed C2C12 cells were positive for alkaline phosphatase (an 83% reduction). This reduction fell to 36% when the ratio of BMP-4 to Noggin was increased to 16:1 (1:0.0625). A dose-dependent effect was observed since the reduction in alkaline phosphatase activity, mediated by Noggin, decreased as the ratio of BMP-4 to Noggin increased (Fig. 1). By comparing the results of the Noggin-expressing muscle-derived stem cells to the Noggin protein control, the calculated concentration of Noggin secreted by the muscle-derived stem cells was 280 ng per million cells every twenty-four hours. In other words, the inhibitory effect of one million Noggin-expressing muscle-derived stem cells on BMP-4 was comparable with adding 280 ng of purified Noggin protein to the BMP-4-expressing cells once every twenty-four hours.

Part 2: In Vivo Evaluation of the Ability of Noggin to Inhibit Heterotopic Ossification Induced by BMP-4

Two mice (one from group A and one from group B) died because of anesthetic complications during the immediate postoperative period. At four weeks after surgery, the remaining sixteen mice displayed radiographic evidence of heterotopic ossification formation in the untreated limbs. The treated limbs, however, exhibited significantly less heterotopic ossification formation with a 53%, 74%, and 99% reduction in the two-dimensional area of heterotopic ossification for groups A, B, and C, respectively (Table I). The differences between the treated and untreated limbs reached significance in each group ($p = 0.0003$ for group A, $p = 0.002$ for group B, and $p = 0.007$ for group C), as did the differences between groups B and C ($p = 0.0273$) and groups A and C ($p = 0.0246$). When the ratio of BMP-4-expressing muscle-derived stem cells to Noggin-expressing muscle-derived stem cells was 1:3 (group C), only one of the five mice had any radiographic evidence of heterotopic ossification in the treated limbs. The results are summarized in Table I, and representative radiographs are shown in Figure 2. The collagen sponge had been absorbed by the time the mice were killed and thus was not present in any of the histologic sections.

Part 3: In Vivo Evaluation of the Ability of Noggin to Block Heterotopic Ossification Induced by Demineralized Bone Matrix

One mouse from group C died because of anesthetic complications during the immediate postoperative period. At eight weeks after surgery, the remaining fourteen mice displayed

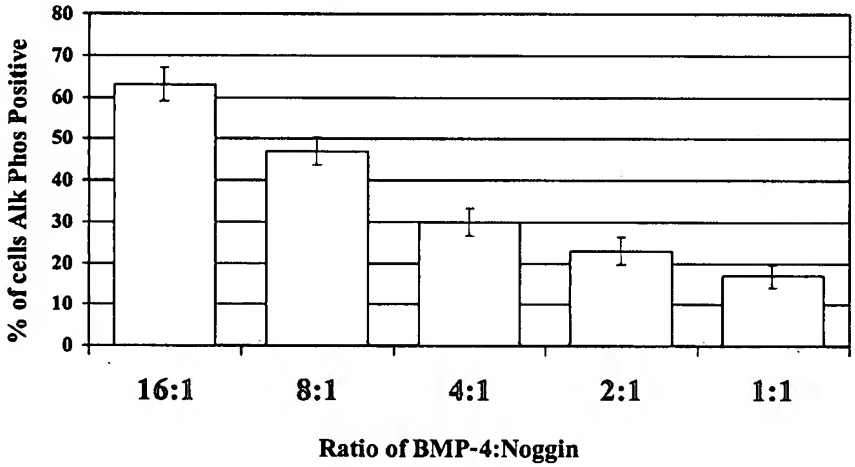

Fig. 1
Results of an in vitro alkaline phosphatase BMP-4 inhibition assay. The number of cells that expressed alkaline phosphatase is shown as a percentage of the control cells (BMP-4 without Noggin). When the ratio of BMP-4 to Noggin was 1:1, only 17% of the cells were positive for alkaline phosphatase (an 83% reduction). This inhibition fell (36% of the cells were positive) when the ratio of BMP-4 to Noggin was 16:1 (1:0.0625).

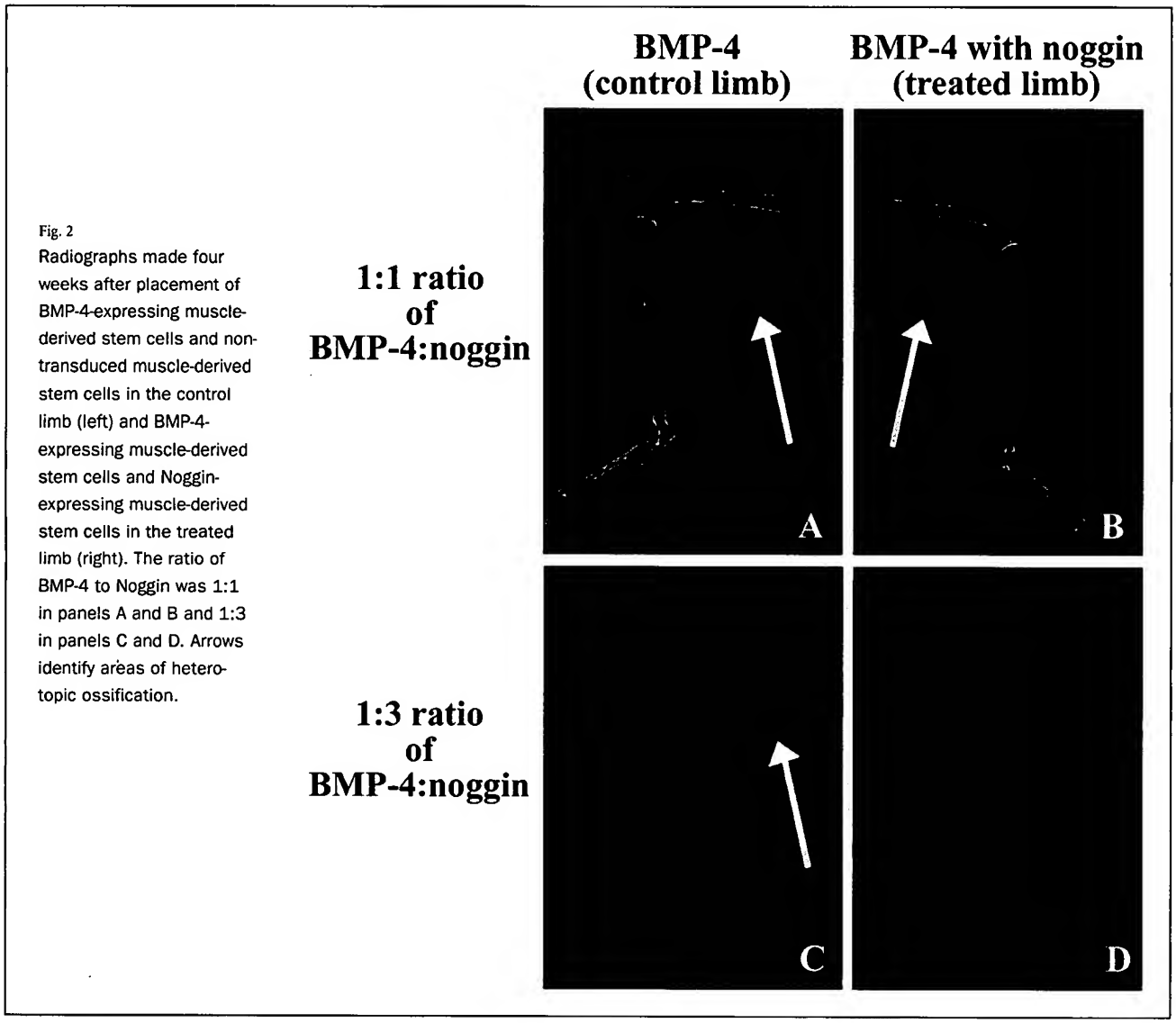

Fig. 2
Radiographs made four weeks after placement of BMP-4-expressing muscle-derived stem cells and non-transduced muscle-derived stem cells in the control limb (left) and BMP-4-expressing muscle-derived stem cells and Noggin-expressing muscle-derived stem cells in the treated limb (right). The ratio of BMP-4 to Noggin was 1:1 in panels A and B and 1:3 in panels C and D. Arrows identify areas of heterotopic ossification.

radiographic evidence of heterotopic ossification in the untreated limbs. Significantly less heterotopic ossification was observed in the treated limbs, however, with 91%, 99%, and 99% less heterotopic ossification in each of the three groups, respectively ($p = 0.004$ for group A, $p = 0.0004$ for group B, and $p = 0.006$ for group C). Furthermore, only one of the five animals in group B and one of the four animals in group C had any evidence of heterotopic ossification formation in the treated limb. The differences between the outcomes of groups A, B, and C did not reach significance—i.e., the different doses of Noggin did not behave significantly differently from one another. The results are summarized in Table II, representative radiographs are shown in Figure 3, and cross sections with von Kossa staining for calcium deposits followed by hematoxylin and eosin staining are shown in Figure 4. The collagen sponge had been absorbed by the time the mice were killed and thus was not present in any of the histologic sections.

Part 4: In Vivo Evaluation of the Ability of Noggin to Inhibit Heterotopic Ossification After Achilles Tenotomy

At ten weeks following the Achilles tenotomy, all eleven mice displayed radiographic evidence of heterotopic ossification in the untreated limbs at the proximal stump of the cut Achilles tendon. In the treated limbs, however, eight of eleven mice had no radiographic evidence of heterotopic ossification at the proximal end of the cut tendon. The overall reduction in heterotopic ossification for all eleven mice was 83% ($p = 0.0007$). The results are summarized in Table III. Representative radiographs made at ten weeks after surgery are shown in Figure 5, and cross sections with von Kossa staining for cal-

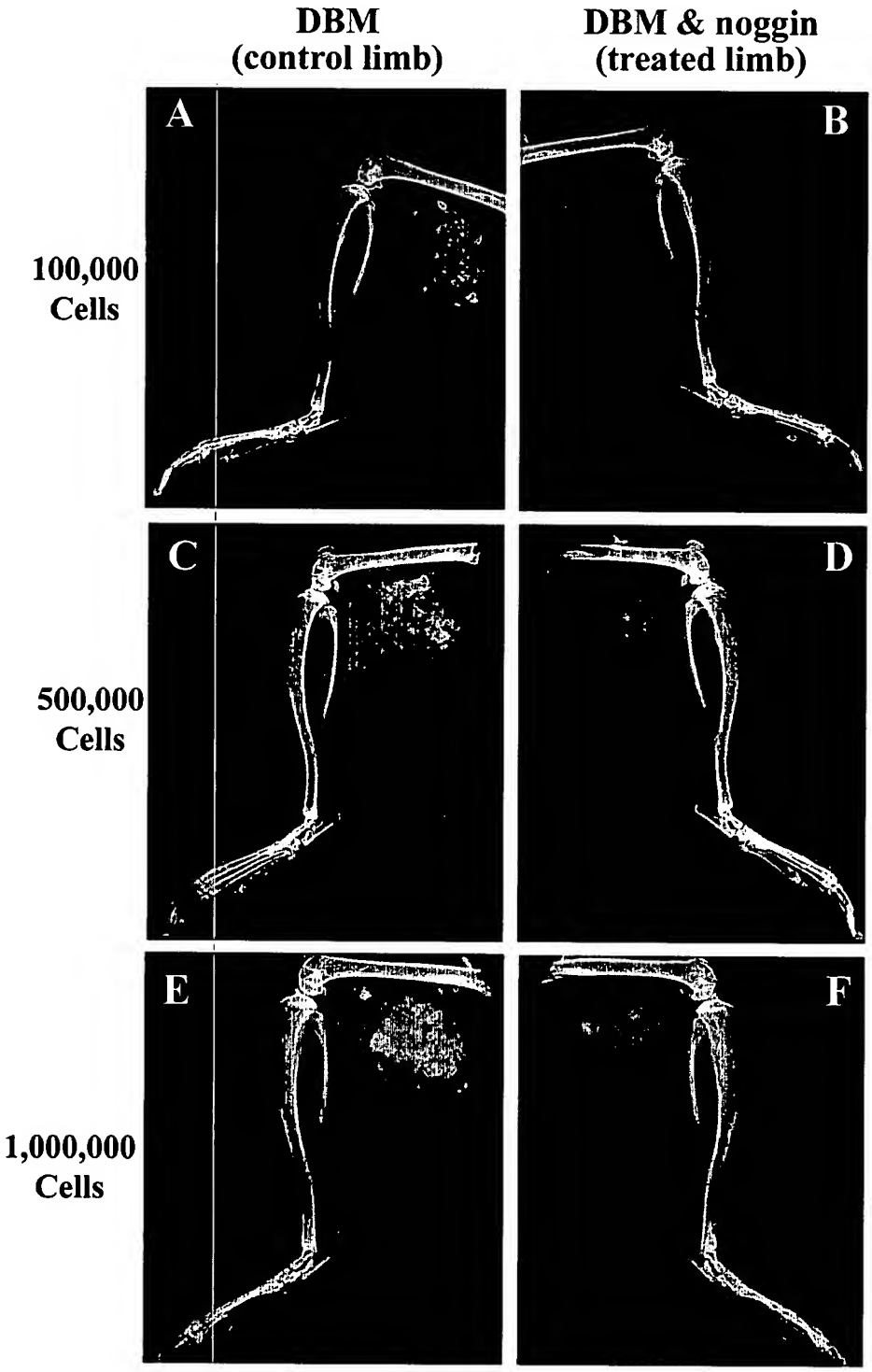

Fig. 3

Radiographs made eight weeks after bilateral implantation of 80 mg of human demineralized bone matrix in the hind limbs of SCID (severe combined immunodeficiency strain) mice. The limbs treated with Noggin-expressing muscle-derived stem cells showed less bone formation (panels B, D, and F). *A:* 80 mg demineralized bone matrix with 100,000 nontransduced muscle-derived stem cells. *B:* 80 mg demineralized bone matrix with 100,000 Noggin-expressing muscle-derived stem cells. *C:* 80 mg demineralized bone matrix with 500,000 nontransduced muscle-derived stem cells. *D:* 80 mg demineralized bone matrix with 500,000 Noggin-expressing muscle-derived stem cells. *E:* 80 mg demineralized bone matrix with 1,000,000 nontransduced muscle-derived stem cells. *F:* 80 mg demineralized bone matrix with 1,000,000 Noggin-expressing muscle-derived stem cells.

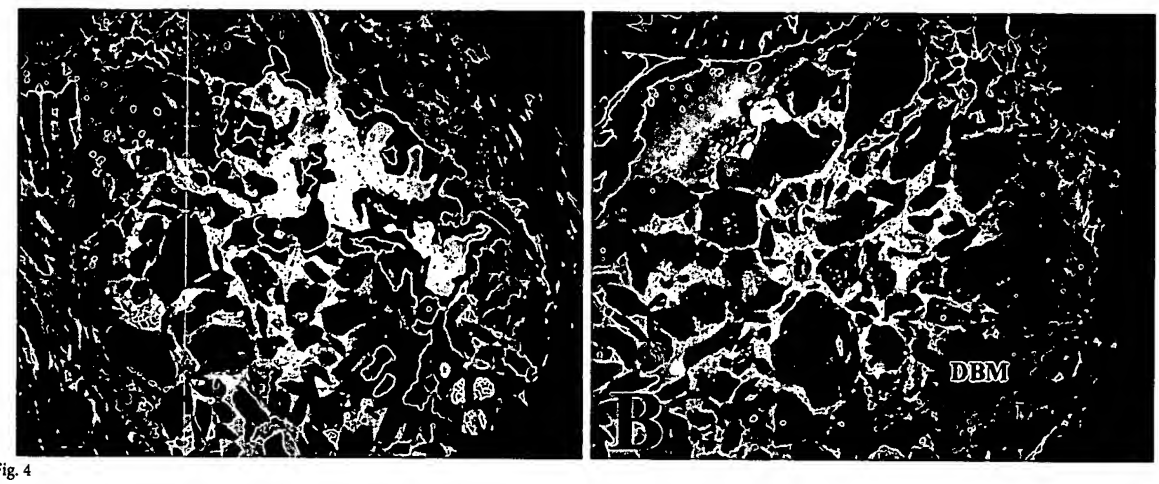

Fig. 4

Sections of muscle obtained eight weeks after implantation of demineralized bone matrix (DBM) and stained with von Kossa stain followed by hematoxylin and eosin (original magnification, ×40). Muscle (stained red) is seen on the periphery surrounding the demineralized bone matrix (DBM) in the middle of the field (stained pink). *A:* A control limb in which demineralized bone matrix was implanted with 500,000 nontransduced muscle-derived stem cells showing ossification of the demineralized bone matrix (stained black). *B:* A treated limb in which demineralized bone matrix was implanted with 500,000 Noggin-expressing muscle-derived stem cells, showing no ossification.

cium deposits followed by hematoxylin and eosin staining are shown in Figure 6. The collagen sponge had been absorbed by the time the mice were killed and thus was not present in any of the histologic sections.

Discussion

Noggin derives its name from the initial observation that frogs that had an overexpression of Noggin during development grew larger heads[43]. Noggin is an extracellular

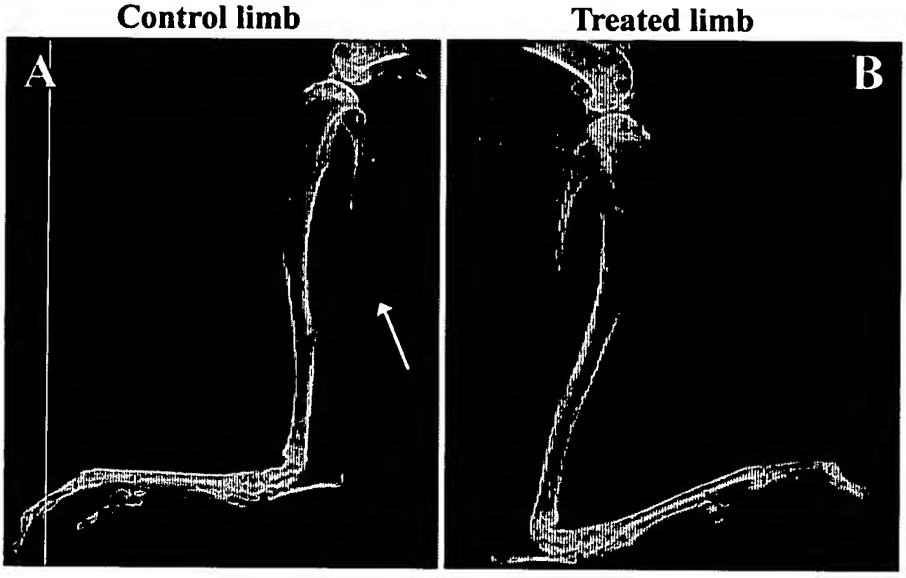

Fig. 5

Radiographs of control *(A)* and treated *(B)* limbs made ten weeks after the Achilles tenotomy. The arrow points to the area of heterotopic ossification at the proximal end of the cut tendon that developed in the untreated, control limb. No evidence of heterotopic ossification is seen in the treated limb.

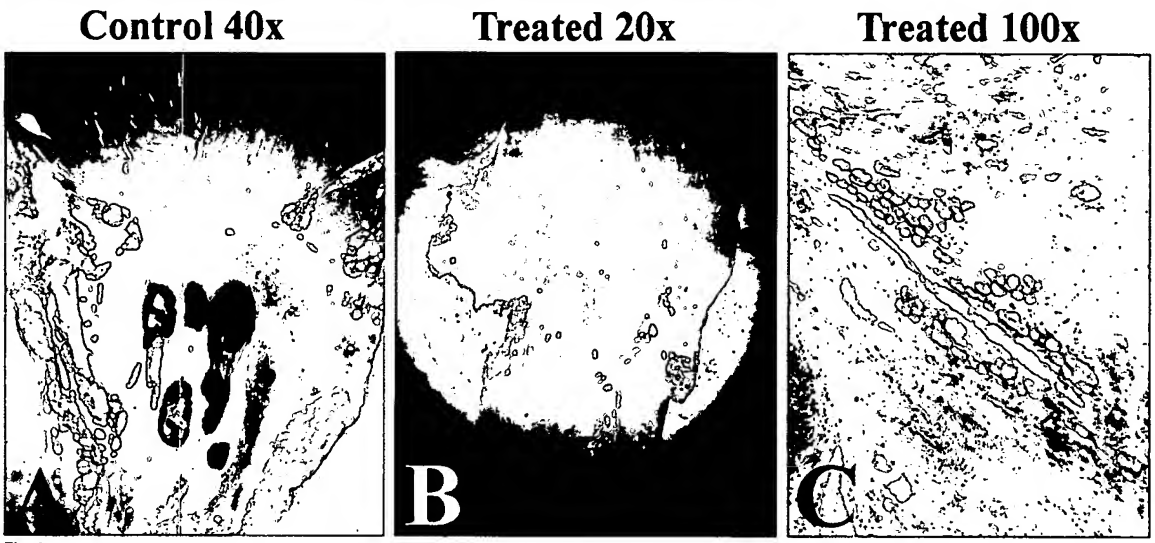

Fig. 6

Longitudinal sections of the Achilles myotendinous junction obtained ten weeks after the Achilles tenotomy and stained with von Kossa stain followed by hematoxylin and eosin. Heterotopic ossification is stained black. *A:* The control limbs showed bone formation in the healing Achilles tendon at 40× magnification. *B:* No heterotopic ossification was seen in the treated limbs at 20× magnification (shown) or at 40× magnification (not shown). C: At 100× magnification, tiny particles of bone that were stained black were seen in the treated limbs; these particles were not seen radiographically or at lower magnifications.

polypeptide that binds to and antagonizes members of the transforming growth factor (TGF)-β superfamily of proteins, including BMPs such as BMP-2 and BMP-4. It inhibits by binding directly to the BMP and preventing the BMP from binding to its receptor[44]. Noggin is normally expressed by tissues such as skeletal muscle and cartilage during embryonic development and is required for normal development of the skeleton[45-47]. It is often co-expressed with BMP during development, presumably to limit the range over which BMP exerts its action. Knock-out mice that lack the Noggin gene develop larger, thicker bones and synostoses in the axial joints, including the elbows and phalangeal joints[27]. Humans who have heterozygous missense mutations of the Noggin gene develop multiple synostoses syndrome, interphalangeal synostoses, and other skeletal abnormalities of the cervical spine and femoral neck[48].

Aspenberg et al. recently showed that an engineered form of the Noggin protein can be used to inhibit bone growth into a diffusion chamber screwed into a rat tibia[49]. In order to increase the pharmacokinetic profile of Noggin, these researchers deleted certain binding sites and added a portion of the human immunoglobulin G1 protein to it. To our knowledge, however, Noggin has not been used to inhibit the formation of heterotopic ossification and there have been no published reports describing the use of Noggin to inhibit heterotopic ossification caused by BMP-4, demineralized bone matrix, or trauma.

We chose to use gene therapy to deliver the Noggin because gene therapy provides a constant delivery of lower, more physiologic doses of proteins that would otherwise be quickly degraded by natural proteases[50]. We used a retroviral vector to transduce the muscle-derived stem cells to express Noggin because retroviral vectors have low antigenicity, which allows them to be used in immunocompetent animals[35-37,50]. Parts 2 and 4 of this study demonstrated that the in vivo expression of Noggin persists long enough to influence the formation of heterotopic ossification in immunocompetent animals. In contrast to the work of Aspenberg et al., who used a genetically engineered form of Noggin, we used wild-type Noggin to further limit the immunogenicity and to try to replicate the normal physiologic interaction between Noggin and BMPs[49]. SCID mice were used in Part 3 of our study to prevent an immune response to the human demineralized bone matrix.

The finding in Part 2 of our study that Noggin is capable of inhibiting the formation of heterotopic ossification caused by BMP-4 is consistent with the fact that Noggin binds to and directly antagonizes BMP-4. Noggin has been shown to have a much higher affinity for BMP-4 and BMP-2 compared with other BMPs, such as BMP-7[44]. We chose to use BMP-4 to test Noggin because of specific evidence indicating that BMP-4 may play a role in the formation of heterotopic ossification[24,25]. Part 3 of our study, which suggested that Noggin is capable of inhibiting the formation of heterotopic ossification induced by demineralized bone matrix, provided further evidence that BMPs are the primary component of demineralized bone matrix responsible for ossification.

Several trauma-induced animal models for heterotopic ossification have been reported in the literature, with variable predictability of heterotopic ossification formation[31,51-54]. We

chose to use the Achilles tenotomy model for heterotopic ossification because of its relative simplicity and excellent predictability in the development of heterotopic ossification. This model for heterotopic ossification was first described in the rat by Buck in 1953[33]. In 1983, McClure applied the model to 150 mice and found that heterotopic ossification developed in 60% by five weeks after injury and in 100% by ten weeks after injury[32]. After the tenotomy, the proximal portion of the tendon retracts, and foci of heterotopic ossification eventually develop at the proximal stump of the cut tendon, which was where our implants containing the muscle-derived stem cells were placed.

The exact mechanism by which Achilles tenotomy, or any type of trauma, causes heterotopic ossification is unclear. However, since Part 4 of this study suggested that the formation of heterotopic ossification is inhibited when BMPs are blocked with use of Noggin, BMPs must play an integral role in the formation of heterotopic ossification after trauma. Furthermore, the amount of heterotopic ossification that forms can be influenced by the presence of Noggin. Eight of the eleven animals had no radiographic evidence of heterotopic ossification at the proximal end of the cut tendon in the limb treated with Noggin, while the remaining three mice had less heterotopic ossification in the treated limb compared with that in the untreated limb. The focus of heterotopic ossification that formed on the distal stump of the cut tendon was not formally analyzed because of its variable nature and smaller size (only six of the eleven animals developed heterotopic ossification at the distal stump). However, the formation of heterotopic ossification at the distal stump did not seem to be as strongly influenced by Noggin, presumably because of the larger distance between the distal stump and the surgically implanted cells at the proximal end. The possibility that heterotopic ossification is only inhibited in the area in immediate contact with Noggin has important clinical implications. It is often desirable to inhibit heterotopic ossification in one area while also trying to promote bone-healing in a nearby area, such as after a total hip arthroplasty.

The weaknesses of this study include an inability to distinguish true bone formation from heterotopic ossification. Our histologic analysis was based on von Kossa staining for calcium deposits, a technique that is sensitive and specific for ossification but is not able to differentiate true bone formation, which is cellular in nature, from heterotopic ossification. However, our previous studies have shown that the structure of BMP-2 and BMP-4-induced bone is similar to the structure of true bone[35-37,55]. In addition, although there were no signs of infection or ill effects observed in any of the animals used in this study, we did not collect any long-term data demonstrating the safety of Noggin or the broad long-term inhibition of TGF-β superfamily members. Finally, while the retroviral vectors used to deliver the Noggin and the BMP-4 to the muscle-derived stem cells in this experiment have been used previously without any untoward effects, the use of gene therapy in a clinical setting should always be approached with caution and more research is needed to establish the safety of these procedures[35-37,50].

The clinical importance of finding new ways to inhibit heterotopic ossification lies in the fact that current methods of preventing or treating heterotopic ossification all have associated disadvantages. Radiation therapy carries an oncogenic risk, even with doses as small as 1000 cGy, and can also be associated with patient morbidity following total hip arthroplasty[56-59]. In addition, radiation damages cells, including muscle cells, and thereby impairs healing[60-62]. Bisphosphonates are able to delay the formation of heterotopic ossification, but, when treatment is discontinued, the process of ossification recurs[63,64]. Nonsteroidal anti-inflammatory drugs have been shown to prevent heterotopic ossification, but they can also cause considerable gastrointestinal bleeding[65-67]. More importantly, they systemically inhibit all bone-healing, which may be detrimental when trying to promote bone-healing elsewhere in the body[65-67]. Indirect gene therapy may offer a method to accurately deliver Noggin to a targeted area of the body and thereby inhibit heterotopic ossification without interfering with bone growth and bone-healing at other locations.

In conclusion, heterotopic ossification continues to pose a substantial problem in orthopaedic surgery. Currently, there is no ideal method of treatment. BMPs play a crucial and necessary role in the formation of heterotopic ossification induced by both demineralized bone matrix and trauma. The retroviral delivery of Noggin can inhibit heterotopic ossification caused by BMP-4, demineralized bone matrix, or trauma in an animal model. The use of gene therapy to deliver Noggin to a targeted area of the body may one day become an important tool for the prevention of heterotopic ossification. ■

NOTE: The authors thank Molly Voght, PhD, and Mark Chirumbole for their help with the statistical analysis.

David Hannallah, MD, MSc
Hairong Peng, MD, PhD
Brett Young, BSc
Arvydas Usas, MD
Brian Gearhart, BSc
Johnny Huard, PhD
Department of Orthopaedic Surgery (D.H., H.P., A.U., and J.H.) and Departments of Molecular Genetics and Biochemistry and Bio-Engineering (J.H.), University of Pittsburgh; Growth and Development Laboratory (D.H., H.P., B.Y, A.U., B.G., and J.H.), Children's Hospital of Pittsburgh, 4100 Rangos Research Center, 3705 Fifth Avenue, Pittsburgh, PA 15213-2582. E-mail address for J. Huard: jhuard@pitt.edu

In support of their research or preparation of this manuscript, one or more of the authors received grants or outside funding from the National Institutes of Health (R01-DE 13420-01A2-JH) as well as the William F. and Jean W. Donaldson endowed chair at the Children's Hospital of Pittsburgh, the Henry J. Mankin endowed chair at the University of Pittsburgh, and the Hirtzel Foundation. None of the authors received payments or other benefits or a commitment or agreement to provide such benefits from a commercial entity. No commercial entity paid or directed, or agreed to pay or direct, any benefits to any research fund, foundation, educational institution, or other charitable or nonprofit organization with which the authors are affiliated or associated.

This paper was the winner of the American Orthopaedic Association-Zimmer Travel Award for Orthopaedic Residents, 2002.

References

1. **Brumback RJ, Wells JD, Lakatos R, Poka A, Bathon GH, Burgess AR.** Heterotopic ossification about the hip after intramedullary nailing for fractures of the femur. *J Bone Joint Surg Am.* 1990;72:1067-73.
2. **DeLee J, Ferrari A, Charnley J.** Ectopic bone formation following low friction arthroplasty of the hip. *Clin Orthop.* 1976;121:53-9.
3. **Fahrer H, Koch P, Ballmer P, Enzler P, Gerber N.** Ectopic ossification following total hip arthroplasty: is diffuse idiopathic skeletal hyperostosis a risk factor? *Br J Rheumatol.* 1988;27:187-90.
4. **Lovelock JE, Pellegrini VD Jr.** Bone formation following carpal interposition arthroplasty. *Skeletal Radiol.* 1990;19:31-2.
5. **Soballe K, Christensen F, Kristensen SS.** Ectopic bone formation after total hip arthroplasty. *Clin Orthop.* 1988;228:57-62.
6. **Puzas JE, Miller MD, Rosier RN.** Pathologic bone formation. *Clin Orthop.* 1989;245:269-81.
7. **Connor JM, Evans DA.** Fibrodysplasia ossificans progressiva. The clinical features and natural history of 34 patients. *J Bone Joint Surg Br.* 1982; 64:76-83.
8. **Green DP, McCoy H.** Turnbuckle orthotic correction of elbow-flexion contractures after acute injuries. *J Bone Joint Surg Am.* 1979;61:1092-5.
9. **Viola RW, Hastings H 2nd.** Treatment of ectopic ossification about the elbow. *Clin Orthop.* 2000;370:65-86.
10. **Richards AM, Klaassen MF.** Heterotopic ossification after severe burns: a report of three cases and review of the literature. *Burns.* 1997;23:64-8.
11. **Naraghi FF, DeCoster TA, Moneim MS, Miller RA, Rivero D.** Heterotopic ossification. *Orthopedics.* 1996;19:145-51.
12. **Ahrengart L.** Periarticular heterotopic ossification after total hip arthroplasty. Risk factors and consequences. *Clin Orthop.* 1991;263:49-58.
13. **Crawford CM, Varghese G, Mani MM, Neff JR.** Heterotopic ossification: are range of motion exercises contraindicated? *J Burn Care Rehabil.* 1986;7: 323-7.
14. **Peterson SL, Mani MM, Crawford CM, Neff JR, Hiebert JM.** Postburn heterotopic ossification: insights for management decision making. *J Trauma.* 1989;29:365-9.
15. **Johns JS, Cifu DX, Keyser-Marcus L, Jolles PR, Fratkin MJ.** Impact of clinically significant heterotopic ossification on functional outcome after traumatic brain injury. *J Head Trauma Rehabil.* 1999;14:269-76.
16. **Lal S, Hamilton BB, Heinemann A, Betts HB.** Risk factors for heterotopic ossification in spinal cord injury. *Arch Phys Med Rehabil.* 1989;70: 387-90.
17. **Haque S, Eisen RN, West AB.** Heterotopic bone formation in the gastrointestinal tract. *Arch Pathol Lab Med.* 1996;120:666-70.
18. **Urist MR.** Bone: formation by autoinduction. *Science.* 1965;150:893-9.
19. **Musgrave DS, Bosch P, Lee JY, Pelinkovic D, Ghivizzani SC, Whalen J, Niyibizi C, Huard J.** Ex vivo gene therapy to produce bone using different cell types. *Clin Orthop.* 2000;378:290-305.
20. **Bosch P, Musgrave D, Ghivizzani S, Latterman C, Day CS, Huard J.** The efficiency of muscle-derived cell-mediated bone formation. *Cell Transplant.* 2000;9:463-70.
21. **Lieberman JR, Le LQ, Wu L, Finerman GA, Berk A, Witte ON, Stevenson S.** Regional gene therapy with a BMP-2-producing murine stromal cell line induces heterotopic and orthotopic bone formation in rodents. *J Orthop Res.* 1998;16:330-9.
22. **Gannon FH, Valentine BA, Shore EM, Zasloff MA, Kaplan FS.** Acute lymphocytic infiltration in an extremely early lesion of fibrodysplasia ossificans progressiva. *Clin Orthop.* 1998;346:19-25.
23. **Smith R, Athanasou NA, Vipond SE.** Fibrodysplasia (myositis) ossificans progressiva: clinicopathological features and natural history. *QJM.* 1996; 89:445-6.
24. **Shafritz AB, Kaplan FS.** Differential expression of bone and cartilage related genes in fibrodysplasia ossificans progressiva, myositis ossificans traumatica, and osteogenic sarcoma. *Clin Orthop.* 1998;346:46-52.
25. **Shafritz AB, Shore EM, Gannon FH, Zasloff MA, Taub R, Muenke M, Kaplan FS.** Overexpression of an osteogenic morphogen in fibrodysplasia ossificans progressiva. *N Engl J Med.* 1996;335:555-61.
26. **Chalmers J, Gray DH, Rush J.** Observations on the induction of bone in soft tissues. *J Bone Joint Surg Br.* 1975;57:36-45.
27. **Brunet LJ, McMahon JA, McMahon AP, Harland RM.** Noggin, cartilage morphogenesis, and joint formation in the mammalian skeleton. *Science.* 1998;280:1455-7.
28. **Semonin O, Fontaine K, Daviaud C, Ayuso C, Lucotte G.** Identification of three novel mutations of the noggin gene in patients with fibrodysplasia ossificans progressiva. *Am J Med Genet.* 2001;102:314-7.
29. **Lee JY, Qu-Petersen Z, Cao B, Kimura S, Jankowski R, Cummins J, Usas A, Gates C, Robbins P, Wernig A, Huard J.** Clonal isolation of muscle-derived cells capable of enhancing muscle regeneration and bone healing. *J Cell Biol.* 2000;150:1085-100.
30. **Rosenthal RK, Folkman J, Glowacki J.** Demineralized bone implants for nonunion fractures, bone cysts, and fibrous lesions. *Clin Orthop.* 1999; 364:61-9.
31. **Walton M, Rothwell AG.** Reactions of thigh tissues of sheep to blunt trauma. *Clin Orthop.* 1983;176:273-81.
32. **McClure J.** The effect of diphosphonates on heterotopic ossification in regenerating Achilles tendon of the mouse. *J Pathol.* 1983;139:419-30.
33. **Buck RC.** Regeneration of tendon. *J Pathol Bacteriol.* 1953;66:1-18.
34. **Rooney P, Grant ME, McClure J.** Endochondral ossification and de novo collagen synthesis during repair of the rat Achilles tendon. *Matrix.* 1992; 12:274-81.
35. **Wright V, Peng H, Usas A, Young B, Gearhart B, Cummins J, Huard J.** BMP4-expressing muscle-derived stem cells differentiate into osteogenic lineage and improve bone healing in immunocompetent mice. *Mol Ther.* 2002;6:169-78.
36. **Peng H, Chen ST, Wergedal JE, Polo JM, Yee JK, Lau KH, Baylink DJ.** Development of an MFG-based retroviral vector system for secretion of high levels of functionally active human BMP4. *Mol Ther.* 2001;4:95-104.
37. **Peng H, Wright V, Usas A, Gearhart B, Shen HC, Cummins J, Huard J.** Synergistic enhancement of bone formation and healing by stem cell-expressed VEGF and bone morphogenetic protein-4. *J Clin Invest.* 2002;110:751-9.
38. **Qu Z, Balkir L, van Deutekom JC, Robbins PD, Pruchnic R, Huard J.** Development of approaches to improve cell survival in myoblast transfer therapy. *J Cell Biol.* 1998;142:1257-67.
39. **Rando TA, Blau HM.** Primary mouse myoblast purification, characterization, and transplantation for cell-mediated gene therapy. *J Cell Biol.* 1994;125: 1275-87.
40. **Blau HM, Pavlath GK, Hardeman EC, Chiu CP, Silberstein L, Webster SG, Miller SC, Webster C.** Plasticity of the differentiated state. *Science.* 1985; 230:758-66.
41. **Yaffe D, Saxel O.** Serial passaging and differentiation of myogenic cells isolated from dystrophic mouse muscle. *Nature.* 1977;270:725-7.
42. **Tripp EJ, MacKay EH.** Silver staining of bone prior to decalcification for quantitative determination of osteoid in sections. *Stain Technol.* 1972;47:129-36.
43. **Smith WC, Harland RM.** Expression cloning of noggin, a new dorsalizing factor localized to the Spemann organizer in Xenopus embryos. *Cell.* 1992; 70:829-40.
44. **Zimmerman LB, De Jesus-Escobar JM, Harland RM.** The Spemann organizer signal noggin binds and inactivates bone morphogenetic protein 4. *Cell.* 1996;86:599-606.
45. **Valenzuela DM, Economides AN, Rojas E, Lamb TM, Nunez L, Jones P, Lp NY, Espinosa R 3rd, Brannan CI, Gilbert DJ.** Identification of mammalian noggin and its expression in the adult nervous system. *J Neurosci.* 1995; 15:6077-84.
46. **Capdevila J, Johnson RL.** Endogenous and ectopic expression of noggin suggests a conserved mechanism for regulation of BMP function during limb and somite patterning. *Dev Biol.* 1998;197:205-17.
47. **Merino R, Ganan Y, Macias D, Economides AN, Sampath KT, Hurle JM.** Morphogenesis of digits in the avian limb is controlled by FGFs, TGFbetas, and noggin through BMP signaling. *Dev Biol.* 1998;200:35-45.
48. **Gong Y, Krakow D, Marcelino J, Wilkin D, Chitayat D, Babul-Hirji R, Hudgins L, Cremers CW, Cremers FP, Brunner HG, Reinker K, Rimoin DL, Cohn DH, Goodman FR, Reardon W, Patton M, Francomano CA, Warman ML.** Heterozygous mutations in the gene encoding noggin affect human joint morphogenesis. *Nat Genet.* 1999;21:302-4.
49. **Aspenberg P, Jeppsson C, Economides AN.** The bone morphogenetic proteins antagonist Noggin inhibits membranous ossification. *J Bone Miner Res.* 2001;16:497-500.

50. **Hannallah D, Peterson B, Lieberman JR, Fu FH, Huard J.** Gene therapy in orthopaedic surgery. *J Bone Joint Surg Am.* 2002;84:1046-61.

51. **O'Connor JP.** Animal models of heterotopic ossification. *Clin Orthop.* 1998; 346:71-80.

52. **Michelsson JE, Granroth G, Andersson LC.** Myositis ossificans following forcible manipulation of the leg. A rabbit model for the study of heterotopic bone formation. *J Bone Joint Surg Am.* 1980;62:811-5.

53. **Schneider DJ, Moulton MJ, Singapuri K, Chinchilli V, Deol GS, Krenitsky G, Pellegrini VD Jr.** Inhibition of heterotopic ossification with radiation therapy in an animal model. *Clin Orthop.* 1998;355:35-46.

54. **Ekelund A, Brosjo O, Nilsson OS.** Experimental induction of heterotopic bone. *Clin Orthop.* 1991;263:102-12.

55. **Lee JY, Musgrave D, Pelinkovic D, Fukushima K, Cummins J, Usas A, Robbins P, Fu FH, Huard J.** Effect of bone morphogenetic protein-2-expressing muscle-derived cells on healing of critical-sized bone defects in mice. *J Bone Joint Surg Am.* 2001;83:1032-9.

56. **Brady LW.** Radiation-induced sarcomas of bone. *Skeletal Radiol.* 1979;4:72-8.

57. **Bonarigo BC, Rubin P.** Nonunion of pathologic fracture after radiation therapy. *Radiology.* 1967;88:889-98.

58. **Sacher GA.** *A review of the use of ionizing radiation for treatment of benign diseases: a report of the committee to review the use of ionizing radiation for the treatment of benign disease.* Department of Health, Education and Welfare (DHEW) Publication no. (FDA) 78-8043. Rockville, MD: United States Department of Health, Education and Welfare; 1977.

59. **Hutchison GB.** Late neoplastic changes following medical irradiation. *Cancer.* 1976;37(2 Suppl):1102-10.

60. **Shamberger R.** Effect of chemotherapy and radiotherapy on wound healing: experimental studies. *Recent Results Cancer Res.* 1985;98:17-34.

61. **Wang CC, Blitzer PH, Suit HD.** Twice-a-day radiation therapy for cancer of the head and neck. *Cancer.* 1985;55(9 Suppl):2100-4.

62. **Quinlan JG, Lyden SP, Cambier DM, Johnson SR, Michaels SE, Denman DL.** Radiation inhibition of mdx mouse muscle regeneration: dose and age factors. *Muscle Nerve.* 1995;18: 201-6.

63. **Hu HP, Kuijpers W, Slooff TJ, van Horn JR, Versleyen DH.** The effect of biphosphonate on induced heterotopic bone. *Clin Orthop.* 1991;272: 259-67.

64. **Thomas BJ, Amstutz HC.** Results of the administration of diphosphonate for the prevention of heterotopic ossification after total hip arthroplasty. *J Bone Joint Surg Am.* 1985;67:400-3.

65. **Friedlander G.** The influence of various physical modalities and drugs on bone regeneration and in-growth. In: Fitzgerald R, editor. *Noncemented total hip arthroplasty.* New York: Raven; 1988. p 135-41.

66. **Altman RD, Latta LL, Keer R, Renfree K, Hornicek FJ, Banovac K.** Effect of nonsteroidal antiinflammatory drugs on fracture healing: a laboratory study in rats. *J Orthop Trauma.* 1995;9:392-400.

67. **Dimar JR 2nd, Ante WA, Zhang YP, Glassman SD.** The effects of nonsteroidal anti-inflammatory drugs on posterior spinal fusions in the rat. *Spine.* 1996;21:1870-6.

EXHIBIT B

Modulation of bone morphogenetic protein signaling inhibits the onset and progression of ankylosing enthesitis

Rik J.U. Lories, Inge Derese, and Frank P. Luyten

Laboratory for Skeletal Development and Joint Disorders, Department of Rheumatology, University Hospitals Leuven, Katholieke Universiteit Leuven, Leuven, Belgium.

Joint ankylosis is a major cause of disability in the human spondyloarthropathies. Here we report that this process partially recapitulates embryonic endochondral bone formation in a spontaneous model of arthritis in DBA/1 mice. Bone morphogenetic protein (BMP) signaling appears to be a key molecular pathway involved in this pathological cascade. Systemic gene transfer of noggin, a BMP antagonist, is effective both as a preventive and a therapeutic strategy in the mouse model, mechanistically interfering with enthesial progenitor cell proliferation in early stages of the disease process. Immunohistochemical staining for phosphorylated smad1/5 in enthesial biopsies of patients with spondyloarthropathy reveals active BMP signaling in similar target cells. Our data suggest that BMP signaling is an attractive therapeutic target for interfering with structural changes in spondyloarthropathy either as an alternative or complementary approach to current antiinflammatory treatments.

Introduction

The human spondyloarthropathies are a group of chronic inflammatory joint disorders with a prevalence of about 0.3% (1), which primarily affect individuals between 20 and 40 years of age. Different diagnostic entities, based on clinical, genetic, and pathological characteristics, are classified within this disease concept (2). These consist of ankylosing spondylitis, psoriatic arthritis, reactive arthritis, arthritis associated with inflammatory bowel disease, and a juvenile and an undifferentiated form of arthritis. Clinical manifestations include arthritis and ankylosis, which cause severe and permanent disability. Increasing evidence suggests that an anatomical zone referred to as the enthesis, where tendons and ligaments attach to underlying bone, is a primary target of the pathological process (3, 4). Enthesitis, synovitis, and subchondral bone changes are associated with enthesial cell proliferation and heterotopic cartilage and bone formation, all of which eventually lead to joint space bridging, a process called ankylosing enthesitis. Together, these features are considered the hallmark of spondyloarthropathy (3–5).

Long-term treatment strategies for chronic joint diseases aim to prevent tissue damage and loss of joint function. So-called disease modifying treatments not only target symptom control but are also intended to influence the pathological process itself. In spondyloarthropathy, conventional therapies, such as nonsteroidal antiinflammatory drugs and immune modulators, are considered symptom-controlling rather than disease-modifying treatments (6). TNF inhibitory agents have been introduced as biologic response modifiers (7, 8). Despite their clinical efficacy and widespread use, and in contrast to what is seen in rheumatoid arthritis, the disease-modifying properties of these strategies remain unclear. In chronic joint diseases such as rheumatoid arthritis and in animal models of these diseases (9), inflammation is associated with bone loss and destruction. In spondyloarthropathy, new bone formation is characteristic. Coupling of inflammation and subsequent ankylosis have not been demonstrated. Progressive ankylosis may persist despite absence of clinical disease activity (10). It is possible that continued suppression of inflammation may result in accelerated bone formation and ankylosis once the pathological cascade has been triggered. Therapeutic strategies specifically targeting cartilage and bone formation may therefore be required, either as an alternative or a complementary approach to immune-suppressing drugs, for gaining full control of the disease (11).

Bone morphogenetic proteins (BMPs), discovered to be proteins that ectopically induce a cascade of endochondral bone formation (12), play a crucial role in skeletal (13, 14) and joint morphogenesis (15–18). BMPs are members of the TGF-β superfamily, a group of polypeptides capable of regulating a wide array of cellular processes such as proliferation, differentiation, lineage determination, motility, and death (19, 20). In their canonical pathway, BMPs induce ligand-dependent type I and type II receptor heterodimerization, leading to phosphorylation of smad-signaling molecules (smad1/5) that bind smad4 and then translocate to the nucleus. BMP signaling is controlled at many levels, including that of extracellular antagonists such as noggin (19). Reactivation of embryonic-signaling pathways has been suggested as an essential part of repair and homeostasis in health and disease (21, 22). However, untimely or unwanted activation of signaling cascades fundamental for normal development may promote disease processes such as spondyloarthropathies. Therefore, we hypothesized that BMP signaling could play a direct role in joint ankylosis.

To address this, we studied BMP signaling in a spontaneous model of arthritis. Grouped caging of male DBA/1 mice led to the development of arthritis affecting hind paws and characterized by ankylosing enthesitis (23–25). This feature clearly distinguishes the model from other animal models of different types of joint

Nonstandard abbreviations used: BMP, bone morphogenetic protein; PCNA, proliferating cell nuclear antigen; Sox9, sex-determining region Y-box 9; TBS, Tris-buffered saline.

Conflict of interest: The authors have declared that no conflict of interest exists. However, Rik Lories and Frank P. Luyten have submitted a patent application regarding the use of BMP inhibition in spondyloarthropathy.

Citation for this article: *J. Clin. Invest.* 115:1571–1579 (2005). doi:10.1172/JCI23738.

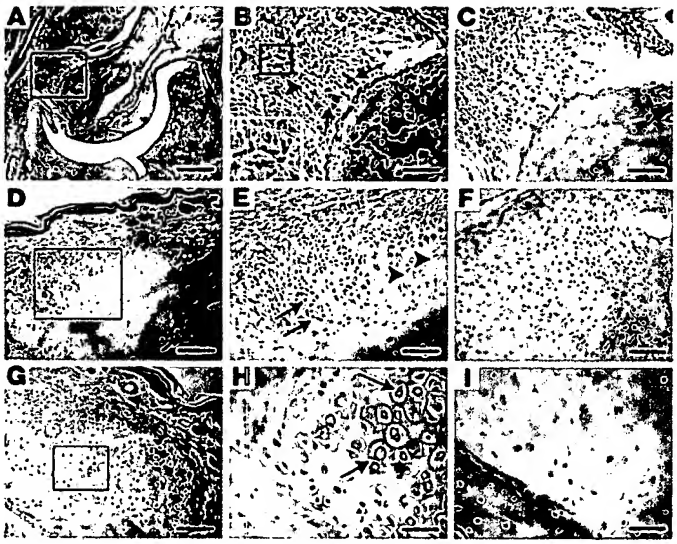

Figure 1
BMP immunohistochemistry in ankylosing enthesitis. (**A–C**) The first phase of ankylosing enthesitis is characterized by enthesial cell proliferation and cartilage differentiation; immunoreactivity for BMP2 is detected in spindle-shaped enthesial fibroblast-like cells (arrowheads, inset in **B**) and in more rounded early chondroblast-like cells (arrows) (**A**; **B**, detail of boxed area in **A**). At this stage of the disease process, no cartilage hypertrophy is seen. (**C**) Negative control staining using IgG. (**D–I**) Cartilage formation in ankylosing enthesitis shows BMP7-positive proliferating and prehypertrophic chondrocyte-like cells (**D**; **E**, detail of boxed area in **D**; arrows indicate zone of positive cells) and BMP6-positive hypertrophic chondrocyte-like cells (**G**; **H**, detail of boxed area in **G**; arrows indicate positive cells). No BMP7 expression is seen in hypertrophic chondrocyte-like cells (**E**, arrowheads). (**F** and **I**) Negative control staining using IgG. Scale bars: 200 μm in **A** and **D**; 100 μm in **G**; 80 μm in **E** and **F**; 50 μm in **B** and **C**; 25 μm in **H** and **I**.

diseases, such as rheumatoid arthritis and osteoarthritis, that are characterized by either synovial inflammation or progressive cartilage loss. Other features of the model include dactylitis and nail changes, symptoms characteristic of psoriatic arthritis (25). This model provides a tool for studying the mechanisms of joint ankylosis with potential relevance to the human spondyloarthropathies. In this report, we evaluate the effects of BMP signaling on initiation and progression of arthritis by gene transfer of noggin, a BMP antagonist.

Results

Distinct BMPs are expressed in ankylosing enthesitis. We used immunohistochemistry to identify specific BMPs, known to be involved in embryonic endochondral bone formation, in ankylosing enthesitis (Figure 1). The disease process was characterized by inflammation and proliferation at the enthesis, followed by cell differentiation into chondroblasts, prehypertrophic chondrocytes, and hypertrophic chondrocytes (24–27) (Supplemental Figure 1; supplemental material available online with this article; doi:10.1172/JCI23738DS1). The cartilage was progressively replaced by bone, which eventually led to joint ankylosis. Different BMPs were detected in distinct stages of ankylosing enthesitis as indicated by cell morphology (Figure 1). BMP2 was seen in spindle-shaped fibroblast-like cells in the proliferative zones as well as in more rounded chondroblasts in early disease stages (Figure 1, A and B). BMP2 was absent in prehypertrophic and hypertrophic chondrocytes (data not shown). In contrast, in later stages, BMP7 was largely restricted to prehypertrophic chondrocytes (Figure 1, D and E). BMP6 was found in hypertrophic chondrocytes (Figure 1, G and H).

Noggin gene transfer inhibits the onset and progression of spontaneous arthritis. We used intramuscular injections of plasmids that encode noggin cDNA under the control of a cytomegalovirus promoter to evaluate ubiquitous suppression of BMP signaling. Injection of 300 μg and 30 μg pcDNA3.1+noggin resulted in a dose-dependent increase in local mRNA expression (Figure 2, A and B). In the RT-negative control samples, only very discrete amounts of residual noggin cDNA were detected after injection of 300 μg pcDNA3.1+noggin. Protein was detectable in muscle and serum (Figure 2C). Injection of 300-μg pcDNA3.1+ empty vector into the contralateral muscle did not result in locally or systemically detectable noggin. We chose to repeat injections every 3 weeks to ensure gene expression during the course of the experiment (28, 29). To ascertain that repeated injections of noggin cDNA did not result in the formation of antibodies that could block its effect, mice were injected 4 times with 300 μg of pcDNA3.1+noggin at 3-week intervals. After 15 weeks, no specific antibodies were found in their serum (data not shown).

We studied the effect of BMP inhibition on clinical incidence and severity of spontaneous arthritis. Male mice were caged together at the age of 12 weeks and monitored for clinical signs of arthritis until the age of 25 weeks. Animals were treated every 3 weeks (weeks 12, 15, 18, and 21) with plasmid injections (either 300 μg pcDNA3.1+noggin, 30 μg pcDNA3.1+noggin, or similar amounts of empty pcDNA3.1+). Injections of both 300 μg and 30 μg of noggin cDNA reduced the incidence of arthritis as compared with injections of empty vector controls (Gehan-Wilcoxon test, $P < 0.05$) (Figure 2D). Similarly, pcDNA3.1+noggin reduced severity of arthritis as compared with empty vector (Mann-Whitney U test; $P < 0.05$) (Figure 2E). The effect of noggin treatment on clinical severity during the course of the disease was evaluated by calculating the area under the curve of the clinical severity score (Figure 2F). Both noggin treatment groups (300 μg and 30 μg plasmids) showed a reduction in time-integrated clinical severity scores (Mann-Whitney U test, $P < 0.05$). The effect was dose dependent. We noticed a slower disease onset and slightly reduced severity in the group that was treated with 300 μg empty vector as compared with the group treated with 30 μg empty vector. Yet this was not statistically significant. However, to exclude that the effect of pcDNA3.1+noggin treatment was due to nonspecific exogenous protein expression by gene transfer, additional mice were treated with pcDNA3.1+ coding for an irrelevant secreted protein (mouse Wnt5a with a mutated hydrophilic domain). No effect on arthritis was found (data not shown).

The effect of BMP inhibition as a therapeutic strategy was evaluated by pcDNA3.1+noggin or empty vector administration (300 μg) after symptoms of arthritis had developed. In a first set of experiments, individual mice were injected immediately after the

first symptoms (toe swelling or stiffness) were recognized. Mice were observed further for 3 weeks. Noggin plasmid treatment significantly reduced clinical disease progression, measured as the difference in clinical score between the beginning and end of the experiment, as compared with empty vector (Figure 3A) (Mann-Whitney U test, $P < 0.05$). In the noggin-treated group, 0 out of 6 mice showed disease progression (Figure 3B), and in 2 mice, improvement of arthritis was seen after treatment. In contrast, in the control group, disease progression was seen in 4 out of 8 mice (Figure 3B). In another set of experiments, individual mice were treated 10 days after the first onset of symptoms and further monitored for 3 weeks. Noggin gene therapy resulted in a significant reduction in clinical disease progression as compared with empty vector treatment (Figure 3C) (Mann-Whitney U test, $P < 0.05$). Of 9 mice, 4 in the noggin-treated group showed signs of clinical improvement, and in 1 animal, the clinical score increased (Figure 4D). In contrast, in the control group, 4 out of 8 mice showed an increase in clinical severity and none of the mice showed improvement of arthritis (Figure 4D).

Noggin modulates endochondral bone formation in ankylosing enthesitis. We studied the effect of exogenous noggin therapy on pathological bone formation by histological analysis in both the preventive and therapeutic experiments described above. Injection of pcDNA3.1+noggin (300 μg) every 3 weeks from the age of 12 weeks onward resulted in a significant difference in histological disease severity score as compared with injection of empty vector (Figure 4A) (Mann-Whitney U test, $P < 0.05$).

We analyzed the effect of noggin gene transfer in this experiment on different stages of endochondral bone formation (Table 1). In the pcDNA3.1+noggin-treated group, 5 out of 8 animals remained unaffected. Cell proliferation was seen in 3 out of 8 mice, but progression to cartilage formation was demonstrated in only 1 animal. Microscopic examination did not reveal bone formation or ankylosis. In contrast, 6 out of 8 animals in the control group were affected. Proliferation of enthesial cells was seen in all affected animals. Four animals showed signs of cartilage formation, and in 1 animal we found bone formation leading to ankylosis.

We also evaluated histological disease severity when noggin cDNA was administered after the first appearance of symptoms. Noggin treatment (300 μg plasmid) resulted in a significantly lower disease severity score as compared with empty vector treatment (Mann-Whitney U test, $P < 0.05$) (Figure 4B). All animals from both groups showed positive histopathological findings (Table 1). In the pcDNA3.1+noggin-treated group, 5 out of 6 animals showed signs of cell proliferation, but only 2 out of 6 showed ectopic cartilage and bone formation. Ankylosis was documented in 1 animal. In contrast, 8 out of 8 animals from the control group showed cell proliferation, 6 out of 8 showed cartilage and bone formation, and 3 out of 8 showed joint ankylosis. Together, these observations suggest that suppression of BMP signaling by noggin can block early stages of pathological endochondral bone formation.

Noggin gene transfer affects proliferation of progenitor cells. We studied the target cell population for BMP signaling in ankylosing enthesitis (Figure 5). Immunofluorescent staining for nuclear phosphorylated

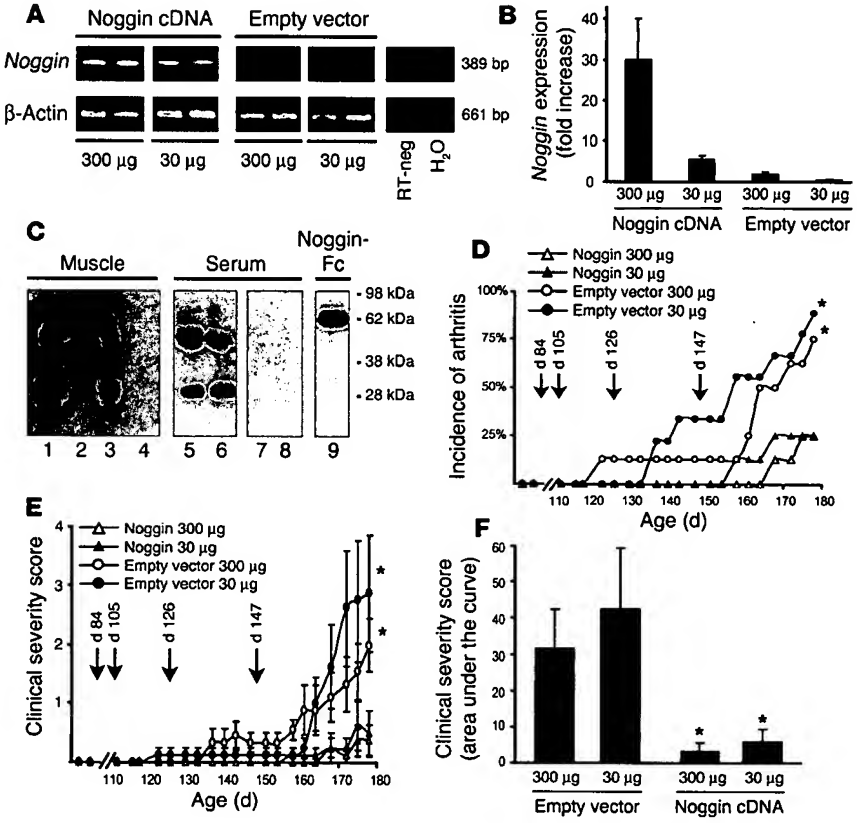

Figure 2

Noggin gene transfer prevents arthritis. (**A**) RT-PCR demonstrating enhanced expression of *noggin* 72 hours after cDNA gene transfer (300 μg and 30 μg). Little endogenous *noggin* is found. The RT-negative control (RT-neg) obtained from muscle injected with 300 μg pcDNA3.1+noggin shows that the RNA extraction procedure successfully removed most of the potentially contaminating cDNA. (**B**) Real-time PCR analysis of *noggin* expression 72 hours after cDNA gene transfer. Mean ± SD from 2 samples. (**C**) Immunoprecipitation and Western blot demonstrating expression of noggin 72 hours after intramuscular plasmid cDNA gene transfer. A 26-kDa band corresponding to noggin was found in 2 different mice after gene transfer in the injected tibialis anterior muscle (right muscle, lanes 1 and 3) but was absent in contralateral control muscle (left muscle, lanes 2 and 4). Noggin was also detected in the serum of both noggin plasmid-injected mice (lanes 5 and 6) but not in control mice (lanes 7 and 8). Lane 8 shows a positive control using recombinant noggin-Fc. (**D**) Noggin gene transfer significantly reduced incidence of spontaneous arthritis as compared with empty vector–treated animals. *Gehan-Wilcoxon test, $P < 0.05$. (**E**) Noggin gene transfer (300 μg or 30 μg) significantly reduced severity of spontaneous arthritis as compared with that in empty vector–treated animals. *Mann-Whitney U test; $P < 0.05$ at week 25. (**F**) Noggin gene transfer significantly reduced time-integrated clinical severity, expressed as area under the curve, as compared with that in control animals. *Mann-Whitney U test; $P < 0.05$. (**D** and **E**) Data are shown as mean ± SEM; $n = 8$ or 9 mice per group.

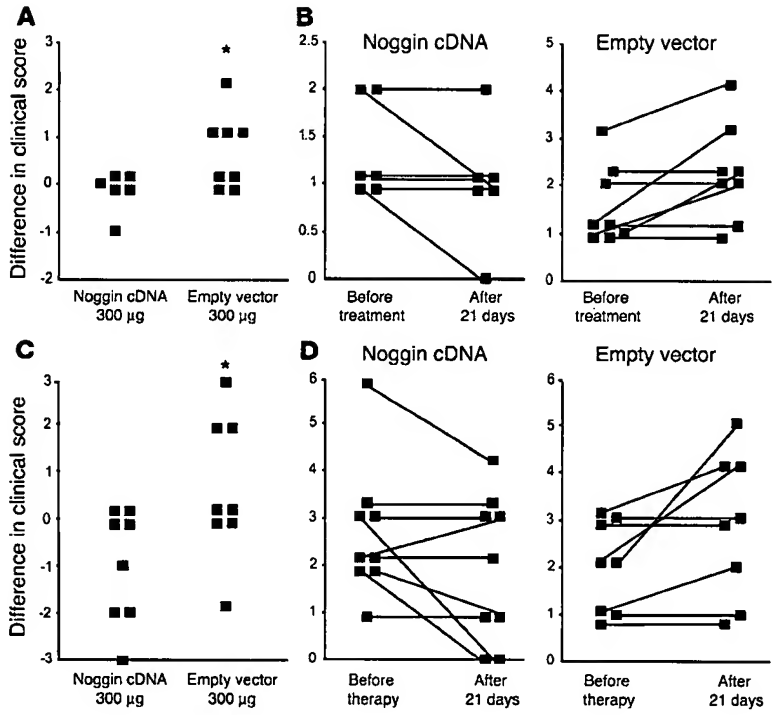

Figure 3
Noggin gene transfer influenced severity of established arthritis. DBA/1 mice were treated with noggin cDNA injection or empty vector immediately (**A–B**) or 10 days (**C–D**) after the first signs of arthritis had appeared. Disease progression, defined as the difference in clinical score between the beginning and the end of the experiment, was significantly reduced after noggin gene transfer as compared with that in empty vector controls. *Mann-Whitney *U* test; $P < 0.05$, 3 weeks after injection. In **B** and **D**, individual clinical scores before and after treatment are shown.

smad1/5, a marker of active BMP signaling, showed positive nuclei in the enthesial fibroblast-like cells and in cells showing early chondrogenic differentiation (Figure 5A). Phosphorylated-smad1/5 was not present in mature or hypertrophic chondrocytes.

To confirm that noggin gene transfer was inhibiting BMP signaling in affected joints, 3 different sets of interphalangeal joints were dissected (5 joints per group): normal joints, arthritic joints, and arthritic joints 6 days after gene transfer. The presence of phosphorylated-smad1/5 molecules was determined by Western blot and digital image analysis. Treatment with 300 μg pcDNA3.1+noggin resulted in a significant reduction in phosphorylated-smad1/5 6 days after treatment as compared with that in arthritic but nontreated joints (Kruskal-Wallis test, $P < 0.05$; Mann-Whitney *U* test, $P < 0.05$) (Figure 5B).

We hypothesized that BMPs were stimulating proliferation of enthesial progenitors before allowing cells to undergo chondrocytic differentiation. We therefore identified the target cell population for BMP signaling by double staining for proliferating cell nuclear antigen (PCNA), a marker of cell proliferation, and phosphorylated smad1/5 (Figure 5C). Colocalization was found in many but not all enthesial cells.

We further tested whether noggin gene transfer affected the local expression of other molecules that are probably involved in ankylosing enthesitis, such as PCNA (proliferation) and sex-determining region Y-box 9 (Sox9) (chondrogenesis) (Figure 6A), proinflammatory cytokines (TNF-α and IFN-γ) (Figure 6B), and BMP2, BMP6, and BMP7 (Figure 6C). Normal, affected, and arthritic joints 6 days after noggin gene therapy were tested. Significant differences in affected toes between normal and treated animals were shown for *PCNA* and *BMP2* (Kruskal-Wallis $P < 0.05$; Mann-Whitney *U* test, $P < 0.05$). Similar trends were seen in expression levels of *TNF-α* and *Sox9*, but this was not confirmed statistically. *BMP6* was significantly downregulated in treated samples versus untreated affected joints. No statistically meaningful differences were seen in *BMP7* and *IFN-γ* expression.

Active BMP signaling in human enthesial biopsies. To specifically test whether our findings in the mouse are relevant to new cartilage and bone formation in human disease, we studied activation of BMP signaling in enthesial biopsies obtained from Achilles tendons of spondyloarthropathy patients (Figure 7A). Histological analysis revealed progenitor cell proliferation and cartilage formation strikingly similar to that in the mouse model (Figure 7, B and C). Activation of BMP signaling was apparent in the proliferating and differentiating cell population as revealed by the presence of nuclear phosphorylated-smad1/5 (Figure 7D). As in the mouse model, in later stages, this staining was negative (Figure 7D). Double staining for PCNA and phosphorylated smad1/5 reflected our observations in mice (Figure 7, E–G). Immunoreactivity for BMP2, BMP7, and BMP6 was recognized in proliferating spindle-shaped cells and in prehypertrophic and mature chondrocytes, respectively (Supplemental Figure 2).

Discussion

In this study, we demonstrate that BMP signaling affects both the initiation and the progression of ankylosis in a model of anky-

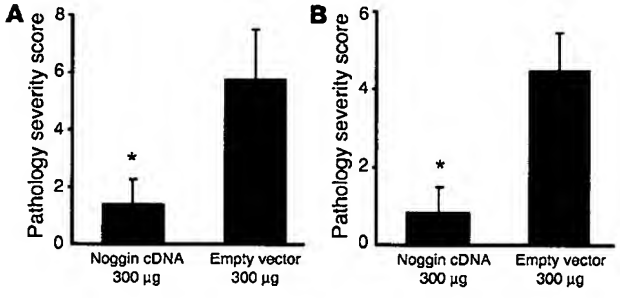

Figure 4
Noggin gene transfer ameliorated the pathological cascade in ankylosing enthesitis. Noggin or empty vector control gene transfer was performed either as a preventive strategy (**A**) or as a therapeutic strategy immediately after the first symptoms appeared (**B**). Noggin gene transfer significantly reduced pathological disease severity in treated animals as compared with empty vector–treated controls. *Mann-Whitney *U* test, $P < 0.05$. Data are shown as mean ± SEM of the cumulative score of all interphalangeal and metacarpophalangeal joints from the hind feet; each group consisted of 8 mice except the noggin cDNA–treated group in **B** ($n = 6$).

Table 1
Effect of noggin gene transfer on different features of ankylosing enthesitis

	Normal	Proliferation	Cartilage formation	Bone formation	Joint ankylosis
Prevention					
Empty vector	2/8 (25)	6/8 (75)	4/8 (50)	1/8 (12)	1/8 (12)
Noggin	5/8 (62)	3/8 (37)	1/8 (0.12)	0/8 (0)	0/8 (0)
Therapy					
Empty vector	0/8 (0)	8/8 (100)	6/8 (75)	6/8 (75)	3/8 (50)
Noggin	0/6 (17)	5/6 (83)	2/6 (33)	2/6 (33)	1/6 (17)

Data are shown as the number of animals exhibiting a specific trait as compared with the total number of animals in the group. Percentages are shown in parentheses.

losing enthesitis and spondyloarthropathy. BMP signaling has been studied in a mouse model of degenerative joint disease (30). Ectopic bone formation in this disorder may be a consequence of structural damage and is likely to be part of the body's response to local injury, either as an attempt to increase joint stability or as a secondary effect of growth factors trying to preserve joint homeostasis (31). Our data provide evidence that deregulation of specific embryonic signaling pathways can also contribute to pathology. Indeed, several arguments indicate that the process of enthesial bone formation leading to ankylosis, as seen in spondyloarthropathies and in this model, is different from osteophytes in osteoarthritis. First, progressive ankylosis in both spine and peripheral joints is a major contributor to disability. Second, ankylosing enthesitis presents frequently as clinically symptomatic arthritis. Third, in contrast to osteoarthritis, heterotopic endochondral bone formation takes place in tissue that is considered one of the primary disease targets (3, 5, 32). Therefore, inhibition of ankylosis may be an important and specific therapeutic target in spondyloarthropathy (11, 33).

To address the mechanisms driving joint ankylosis, we have used a spontaneous mouse model of arthritis. Although it was originally reported as another model of rheumatoid arthritis (23), subsequent studies involving microscopic analysis have clearly demonstrated that this model is characterized by ankylosing enthesitis (25, 27) rather than destructive synovitis. This model is particularly attractive since arthritis occurs in association with environmental factors such as stress that have also been implicated in spondyloarthropathy (24, 34). It also shows specific features of psoriatic arthritis (25) that have not been reported in other models of arthritis. The high incidence and reproducibility of arthritis in this model, in contrast to other models of ankylosis (35), highlight its usefulness for mechanistic studies in the process of ankylosis in spondyloarthropathy. As no animal model completely mimics human disease, different questions can be raised regarding the relevance of this model to human spondyloarthropathy. First, the absence of spine pathology in this model can at least partially be explained by differences in weight bearing between rodents and humans. So far, there are no indications that ectopic bone formation in spine and in peripheral joints is distinct. Both processes mimic predominantly endochondral bone formation (5, 36). Second, the inflammatory reaction associated with the proliferative and metaplastic process at the enthesis is still poorly defined. We have demonstrated that dactylitis or local inflammation at the enthesis, characterized by the presence of neutrophils and some mononuclear cells, precedes or coincides with connective tissue proliferation and differentiation (25). Remarkably, Nordling et al. demonstrated that anti-idiotypic anticollagen type II antibody treatment may prevent the onset of arthritis (37). Autoimmunity toward components of fibrocartilage has been proposed by different authors as directly relevant for the development of spondyloarthropathy (5, 38). Autoantibodies toward type II collagen have also been demonstrated in spondyloarthropathy patients (39). Interestingly, we have also shown that inhibition of IFN-γ delays the onset of disease (26). However, in contrast to the effect of noggin, no therapeutic effect of anti-IFN-γ strategies was seen once symptoms had occurred (26). The finding that the disease process is

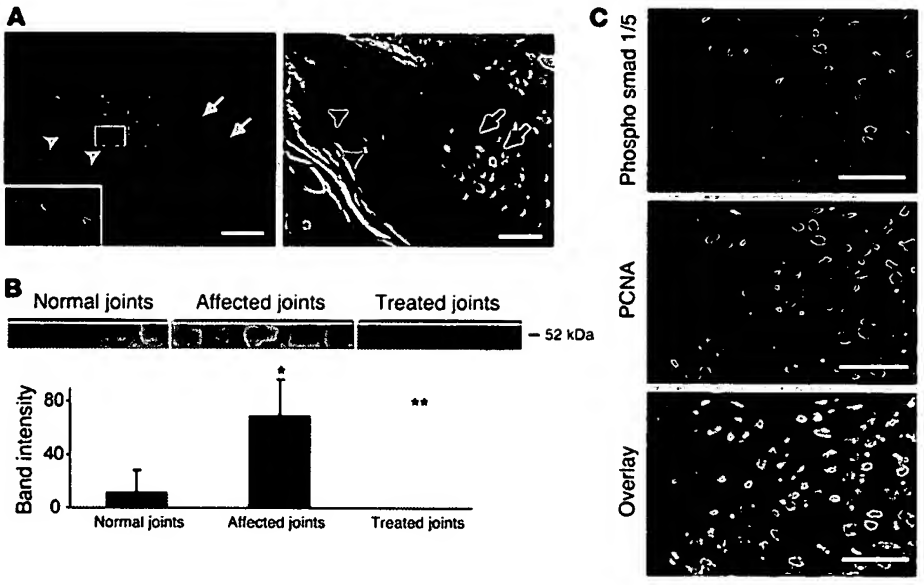

Figure 5
Noggin inhibited BMP signaling in spontaneous arthritis. (**A**) Immunofluorescent staining for phosphorylated smad1/5/8 demonstrating positive nuclei (red staining, arrowheads; detail in inset) in the zone of proliferating cells. The area corresponding to hypertrophic chondrocytes is negative (arrows). A representative, adjacent section stained with H&E is also shown. (**B**) Phosphorylation of smad1/5/8 was increased in arthritic as compared with healthy interphalangeal joints and was inhibited by noggin gene transfer as shown by semiquantitative Western blot ($n = 5$ animals per group, Kruskal-Wallis test $P < 0.05$; Mann-Whitney U test: $^*P < 0.05$ versus normal joints; $^{**}P < 0.05$ versus untreated affected joints). (**C**) Double immunofluorescense staining for phosphorylated smad1/5 (red) and PCNA (green) demonstrating nuclear colocalization (yellow in overlay). Scale bars: 50 μm.

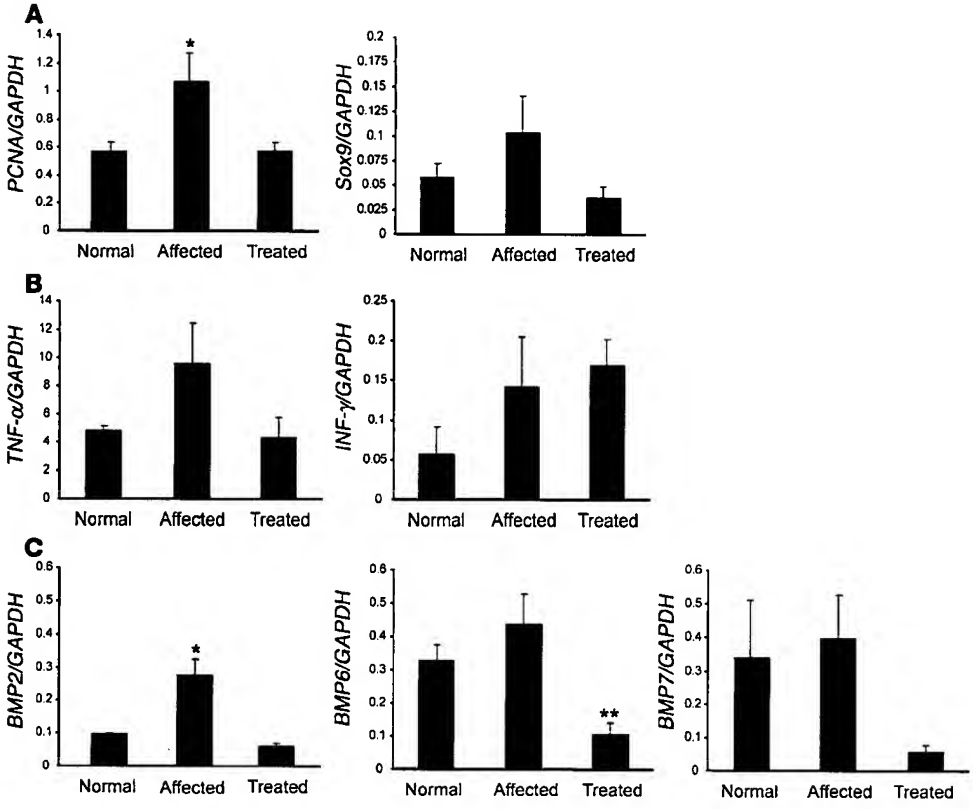

Figure 6
Systemic noggin gene transfer and gene expression in interphalangeal joints. Cell cycle and differentiation markers (**A**), proinflammatory cytokines (**B**), and BMPs (**C**) were studied by real-time PCR analysis. Data are expressed as amounts relative to the expression of *GAPDH*. $n = 5$ animals per group. *Kruskal-Wallis test, $P < 0.05$; Mann-Whitney U test, $P < 0.05$ for affected as compared with normal and treated animals. **Kruskal-Wallis test, $P < 0.05$; Mann-Whitney U test, $P < 0.05$ for treated as compared with affected animals. The y axes indicate expression levels relative to the expression of *GAPDH*.

apparently T cell independent seems to be in contrast with the proposed role for T cells in both psoriatic arthritis (40) and ankylosing spondylitis (5). In these experiments, however, T cell receptors $\alpha\beta^{-/-}$ and $\gamma\delta^{-/-}$ were used separately. Therefore, a role for T cells in the development of autoimmunity toward fibrocartilage components in this model cannot be excluded. Taken together, all these data support the concept of juxtaposed stages in the disease that are coupled but partially independent. Our model therefore seems representative of the process of ankylosis in spondyloarthropathy, which can be considered as a specific therapeutic target.

The somewhat surprising effects in the early stages of the disease highlight the importance of BMP signaling. This pathway is an essential part of the complex network regulating skeletal development (14–18). Endochondral bone formation is initiated by mesenchymal cell condensations. Cells within these condensations undergo chondrogenic differentiation, progressively acquiring the phenotypes of proliferating, prehypertrophic, and hypertrophic chondrocytes. In the later stages, the cartilaginous elements are replaced by bone (13). Studies in developmental models suggest that fine-tuned balances between BMPs and inhibitors such as noggin appear to influence different stages of endochondral bone formation. Retroviral over- and misexpression of noggin in the developing chick limb revealed a dual role for BMP signaling in early stages (41). Both cell condensation and differentiation of chondroprogenitor cells into chondrocytes were inhibited effectively, depending on the time of infection.

Various challenges regarding the role of BMPs in ankylosing enthesitis remain. First, understanding of the relative contribution of specific BMPs and inhibitors to the pathological cascade needs to be refined. Our data suggest an early role for BMP2 and later involvement of BMP6 and BMP7. The presence of additional ligands has not been studied. However, regardless of their presence, noggin has been demonstrated as an antagonist of the BMP2/4, the BMP5/6/7, and the growth and differentiation factor 5/6/7 groups (42). Therefore, noggin overexpression is likely to change the overall balance in BMP signaling in our model. Second, the identification of factors leading to the activation of the BMP-signaling pathway is of critical importance to understanding the links between inflammation and bone formation, but the exact mechanism remains unknown. We and other groups have demonstrated that specific BMPs, including BMP2 and BMP6, are upregulated by proinflammatory cytokines in cell populations obtained from the joint, providing circumstantial evidence that inflammatory changes and BMP expression are linked (43–45). Other explanations include increased expression of BMP receptors or BMP-signaling enhancers (46), through genetic or environmental factors, that lead to enhanced activation of the smad pathway.

It is well known that the biological response to BMPs is dependent on the target tissue (19). Injection of recombinant BMP2 into the knee joints of mice resulted in osteophyte formation in areas adjacent to the bone and did not result in cartilage formation in the synovium itself (47). Adenoviral infection of periost with BMP2 in vivo stimulated endochondral bone formation at the application site (48).

In summary, our findings support the concept that BMP signaling is an attractive therapeutic target for achieving disease modification in spondyloarthropathy. Symptom control by inhibition of inflammation may not be sufficient to stop the structural progression of disease and the resulting disability. Therefore, specific molecular targets involved in cartilage and bone forma-

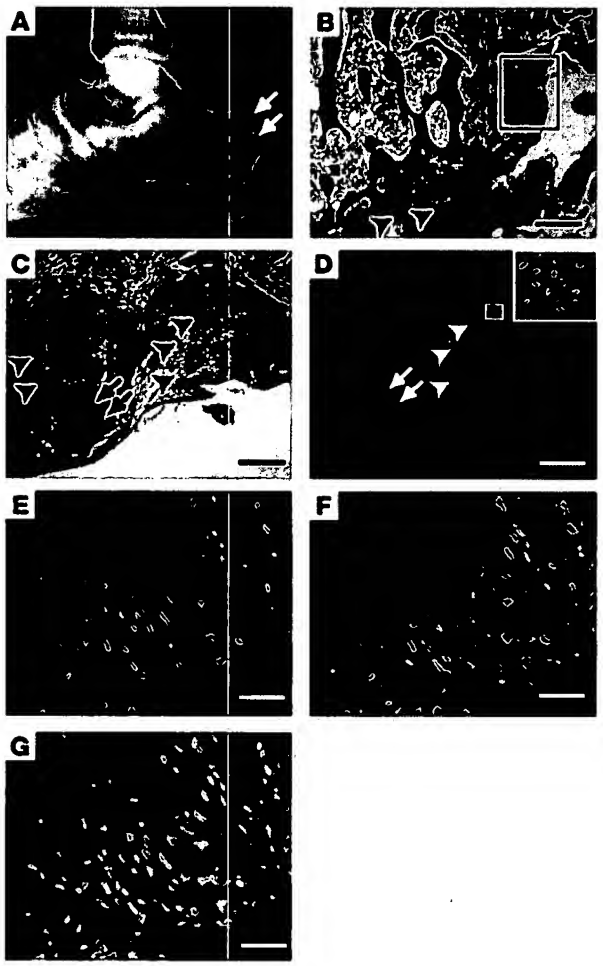

Figure 7
BMP signaling in human enthesitis in spondyloarthropathy. (**A**) X-ray image showing irregular borders and bony outgrowth (arrows) at the Achilles enthesis. (**B**) Overview of an enthesial biopsy stained with H&E, showing a normal attachment zone (arrowheads) and new tissue formation (boxed area). (**C**) Detail of boxed area in **B** showing proliferation (arrowheads) and cartilage formation (arrows). (**D**) Immunofluorescent staining for phosphorylated-smad1/5/8 showing positive proliferating cells (arrowheads, detail in inset) and negative chondrocytes (arrows). (**E–G**) Double immunofluorescence for phosphorylated-smad1/5 (**E**), PCNA (**F**), and overlay (**G**). Scale bars: **B**, 800 μm; **C** and **D**, 200 μm; **E** and **G**, 50 μm.

tion, including the BMPs and their transduction machinery, may provide a complementary or alternative therapeutic approach in patients with spondyloarthropathies. In the complex network of cell differentiation and lineage commitment, molecular networks may be crucial, and single-gene approaches to treating diseases may not be sufficient.

Methods

Animal experiments. Three sets of experiments were performed. First, male DBA/1 mice (Jackson Laboratory or Janvier) from different litters were mixed and caged together in groups of 4 to 6 mice at the age of 12 weeks. Full-length mouse noggin cDNA (a gift of R. Harland, University of California, Berkeley, California, USA) was cloned into pcDNA3.1+ vector (Invitrogen Corp.). Either 300 or 30 μg of pcDNA3.1+noggin or pcDNA3.1$^+$ was injected into the tibialis anterior muscles at weeks 12, 15, 18, and 21. Animals were sacrificed at 25 weeks. Second, after the first symptoms appeared in each mouse, pcDNA3.1+noggin (300 μg) or empty vector was injected immediately. Third, animals with clinical signs of arthritis were treated with pcDNA3.1+noggin (300 μg) or empty vector 10 days after the first symptoms were noted. In these experiments, individual mice were killed 3 weeks after injection of plasmid cDNA. The Ethics Committee for Animal Research (Katholieke Universiteit Leuven) approved all animal experiments. All experiments and analyses were run in a randomized and blinded fashion.

Mice were scored twice a week for clinical signs of arthritis as follows (26, 27): 0, no symptoms; 1, redness and swelling in one toe; 2, redness and swelling in more than one toe; 3, toe stiffness; and 4, deformity or ankle involvement. Both hind paws were evaluated, resulting in a maximum score of 8. For histological examination, hind paw forefeet were formalin-fixed, decalcified using Decal (Serva), paraffin embedded, and cut in a transverse plane. A histological score was developed previously (25, 26): 1, inflammatory cell infiltration; 2, enthesial fibroblast-like cell proliferation; 3, cartilage formation; 4, bone formation; and 5, ankylosis. In each mouse, a cumulative score for all interphalangeal and metatarsophalangeal joints of the 2 hind limbs was calculated by summation of the individual joint scores. Both clinical and pathological scores were found to be consistent and reproducible with little intra- and interobserver variability.

Human materials. Enthesial biopsies were obtained during surgery for refractory enthesitis. The Ethics Committee for Human Medical Research (Katholieke Universiteit Leuven) approved all procedures, and patient informed consent was obtained.

Immunohistochemistry and immunofluorescence. For immunohistochemistry and immunofluorescence, sections were quenched with 3% H_2O_2/H_2O or 50 mM NH_4Cl respectively and preincubated with donkey serum (20% in Tris-buffered saline [TBS]). Sections were incubated with polyclonal primary antibodies against BMP2 (Pfizer) (5 μg/ml), BMP7 (Pfizer) (10 μg/ml), BMP6 (Santa Cruz Biotechnology Inc.) (10 μg/ml), phosphorylated smad1/5 (PS1) (P. Ten Dijke, University of Leiden, Leiden, The Netherlands) (1/100) overnight at 4°C. Anti-BMP2 antibody was raised against peptide sequence Ac-REKRQAKHKARKRLKSSC-NH2. BLAST protein analysis (http://www.ncbi.nlm.nih.gov/BLAST) showed that this peptide is specific for BMP2 and is conserved across species (human, mouse, rat, xenopus). Anti-BMP7 antibody was raised against peptide sequence Ac-TGSKQRSQNRSKTPKNC-NH2. This peptide sequence is specific for human BMP7, as shown by BLAST protein analysis. The mouse and rat BMP7 sequence showed 1 amino acid difference (G instead of S in position 3). Anti-BMP6 was raised against a peptide sequence from the amino-terminus of human BMP6. Antiphosphorylated smad1/5 antibody recognizing the phosphorylated C-tail in Smad1 was generated by injection of peptide KKK-NPISSVS containing 2 C terminal phosphoserine residues coupled to keyhole limpet hemocyanin (49). Negative controls were performed with species-specific IgG (Jackson ImmunoResearch Laboratories Inc.) or preincubation of the antibodies with blocking peptides or proteins. After washing and a second blocking step, sections were incubated with horseradish peroxidase–conjugated secondary antibodies (Jackson ImmunoResearch Laboratories Inc.) (1/100). For immunofluoresence, secondary antibodies were Cy3-conjugated goat anti-rabbit antibody (1/100 dilution) or Cy2-conjugated anti-goat antibody (1/100 dilution) (Jackson ImmunoResearch Laboratories Inc.).

Western blot analysis. For phosphorylated smad1/5, interphalangeal joints were dissected, frozen, thawed twice, and stored in 6 M urea/10 mM

Tris/pH 7.8. Five-hundred ng protein, diluted in 4× NuPAGE-LDS buffer (Invitrogen Corp.) was analyzed under reducing conditions (2% mercaptoethanol and 0.1 M DTT) in NuPAGE-MES-SDS buffer (Invitrogen Corp.). Proteins were transferred onto a PVDF membrane in 0.4 M glycine/0.5 M Tris-base/0.01 M SDS and 200 ml/l methanol. Blots were probed with antibody PS1 (1/2500 in TBS-Triton/3% milk) and washed with TBS-Triton, and goat anti-rabbit horseradish peroxidase-conjugated secondary antibody (1/5000 in TBS-Triton/3% milk) (Jackson ImmunoResearch Laboratories Inc.) was added. For visualization, we used SuperSignal Pico Chemiluminescent Substrate (Pierce).

For noggin, tibialis anterior muscles were injected with 300 μg pcDNA3.1+noggin or empty vector. After 72 hours, muscles and blood were collected. Muscles were extracted in 1 M guanidium hydrochloride/50 mM Na-acetate overnight. Samples were desalted, lyophilized, and redissolved in 200-μl immunoprecipitation buffer (150 mM NaCl/1 % NP-40/2 mM EDTA/50 mM NaF/1 mM $Na_4P_2O_7$/20 mM Tris/pH 7.6). Samples and serum were incubated overnight at 4°C with 2 μg goat anti-noggin antibody. Protein A/G sepharose solution (Amersham Biosciences) was used for precipitation. Pellets were dissolved in loading buffer-8 M urea. Western blot was performed as above with goat anti-noggin polyclonal affinity purified antibody (R&D Systems) (1/5000) and horseradish peroxidase-conjugated mouse anti-goat (1/20000) (Jackson ImmunoResearch Laboratories Inc.). Recombinant noggin-Fc (R&D Systems) (10 ng) was used a positive control.

PCR. RNA was isolated from tibialis anterior muscle or interphalangeal joints using Trizol (Invitrogen Corp.) and reverse transcribed (Superscript III; Invitrogen Corp.). For conventional PCR, the following primers were used: β-*actin* forward primer 5′-TGACGGGGTCACCCACACTGTGCCCATCTA-3′; β-*actin* reverse primer 5′-CTAGAAGCATTTGCGGTGGACGATGGAGGG-3′; *noggin* forward primer 5′-GCATGGAGCGCTGCCCCAGC-3′; *noggin* reverse primer 5′-GAGCAGCGAGCGCAGCAGCG-3′. For β-*actin*, a 3-step PCR was performed with an annealing temperature of 60°C; for *noggin*, a 2-step PCR was performed with an annealing temperature of 72°C. For real-time PCR, gene expression was studied using Assay-on-Demand primer-probe systems (Applied Biosystems). Expression levels were normalized to *GAPDH* expression using the comparative threshold cycle method.

Statistics. Comparisons between groups were made by Kruskal-Wallis test and Mann-Whitney *U* test. For incidence, Gehan-Wilcoxon test was used.

Acknowledgments

The authors wish to thank Przemko Tylzanowski, Kurt de Vlam, Rene Westhovens, and Malcolm Moos for useful suggestions and critical appraisal of the data; Jenny Peeters and Erik-Jan Ververs for technical assistance; and Giovanni Matricali for enthesial biopsies. This work was supported by grant 0.390.03 from the Fund for Scientific Research – Flanders. R.J.U. Lories has received an Aspirant fellowship and is currently a postdoctoral fellow; both awards are from the Fund for Scientific Research – Flanders.

Received for publication October 26, 2004, and accepted in revised form April 12, 2005.

Address correspondence to: Frank P. Luyten, Department of Rheumatology, University Hospitals Leuven, Herestraat 49, B-3000 Leuven, Belgium. Phone: 32-16-346341; Fax: 32-16-346200; E-mail: Frank.Luyten@uz.kuleuven.ac.be.

Frank P. Luyten is the senior author.

1. Saraux, A., et al. 1999. Prevalence of rheumatoid arthritis and spondyloarthropathy in Brittany, France. *J. Rheumatol.* **26**:2622–2627.
2. Wright, V. 1978. Seronegative polyarthritis: a unified concept. *Arthritis Rheum.* **21**:619–633.
3. Ball, J. 1971. Enthesopathy of rheumatoid and ankylosing spondylitis. *Ann. Rheum. Dis.* **30**:213–223.
4. Benjamin, M., and McGonagle, D. 2001. The anatomical basis for disease localisation in seronegative spondyloarthropathy at entheses and related sites. *J. Anat.* **199**:503–526.
5. Francois, R.J., Braun, J., and Khan, M.A. 2001. Entheses and enthesitis: a histopathologic review and relevance to spondyloarthritides. *Curr. Opin. Rheumatol.* **13**:255–264.
6. van der Heijde, D., Braun, J., McGonagle, D., and Siegel, J. 2002. Treatment trials in ankylosing spondylitis: current and future considerations. *Ann. Rheum. Dis.* **61**:24–32.
7. Braun, J., et al. 2002. Treatment of active ankylosing spondylitis with infliximab: a randomised controlled multicentre trial. *Lancet.* **359**:1187–1193.
8. Mease, P.J., et al. 2000. Etanercept in the treatment of psoriatic arthritis and psoriasis: a randomised trial. *Lancet.* **356**:385–390.
9. Kong, Y.Y., et al. 1999. Activated T cells regulate bone loss and joint destruction in adjuvant arthritis through osteoprotegerin ligand. *Nature.* **402**:304–309.
10. Marzo-Ortega, H., Emery, P., and McGonagle, D. 2002. The concept of disease modification in spondyloarthropathy. *J. Rheumatol.* **29**:1583–1585.
11. Zhang, X., Aubin, J.E., and Inman, R.D. 2003. Molecular and cellular biology of new bone formation: insights into the ankylosis of ankylosing spondylitis. *Curr. Opin. Rheumatol.* **15**:387–393.
12. Urist, M.R. 1965. Bone: formation by autoinduction. *Science.* **150**:893–899.
13. Olsen, B.R., Reginato, A.M., and Wang, W.F. 2000. Bone development. *Annu. Rev. Cell Dev. Biol.* **16**:191–220.
14. Kronenberg, H.M. 2003. Developmental regulation of the growth plate. *Nature.* **423**:332–336.
15. Thomas, J.T., et al. 1996. A human chondrodysplasia due to a mutation in a TGF-beta superfamily member. *Nat. Genet.* **12**:315–317.
16. Thomas, J.T., et al. 1997. Disruption of human limb morphogenesis by a dominant negative mutation in CDMP1. *Nat. Genet.* **17**:58–64.
17. Polinkovsky, A., et al. 1997. Mutations in CDMP1 cause autosomal dominant brachydactyly type C. *Nat. Genet.* **17**:18–19.
18. Storm, E.E., et al. 1994. Limb alterations in brachypodism mice due to mutations in a new member of the TGF beta-superfamily. *Nature.* **368**:639–643.
19. Massague, J. 2000. How cells read TGF-beta signals. *Nat. Rev. Mol. Cell Biol.* **1**:169–178.
20. Waite, K.A., and Eng, C. 2003. From developmental disorder to heritable cancer: it's all in the BMP/TGF-beta family. *Nat. Rev. Genet.* **4**:763–773.
21. Steiling, H., et al. 2003. Fibroblast growth factor receptor signalling is crucial for liver homeostasis and regeneration. *Oncogene.* **22**:4380–4388.
22. Reddi, A.H. 2003. Cartilage morphogenetic proteins: role in joint development, homoeostasis, and regeneration. *Ann. Rheum. Dis.* **62**:73–78.
23. Nordling, C., Karlsson-Parra, A., Jansson, L., Holmdahl, R., and Klareskog, L. 1992. Characterization of a spontaneously occurring arthritis in male DBA/1 mice. *Arthritis Rheum.* **35**:717–722.
24. Holmdahl, R., Jansson, L., Andersson, M., and Jonsson, R. 1992. Genetic, hormonal and behavioural influence on spontaneously developing arthritis in normal mice. *Clin. Exp. Immunol.* **88**:467–472.
25. Lories, R.J., Matthys, P., de Vlam, K., Derese, I., and Luyten, F.P. 2004. Ankylosing enthesitis, dactylitis and onychoperiostitis in a mouse model of psoriatic arthritis. *Ann. Rheum. Dis.* **63**:595–598.
26. Matthys, P., et al. 2003. Dependence on interferon-gamma for the spontaneous occurrence of arthritis in DBA/1 mice. *Arthritis Rheum.* **48**:2983–2988.
27. Corthay, A., Hansson, A.S., and Holmdahl, R. 2000. T lymphocytes are not required for the spontaneous development of entheseal ossification leading to marginal ankylosis in the DBA/1 mouse. *Arthritis Rheum.* **43**:844–851.
28. Song, X.Y., Gu, M., Jin, W.W., Klinman, D.M., and Wahl, S.M. 1998. Plasmid DNA encoding transforming growth factor-β1 suppresses chronic disease in a streptococcal cell wall-induced arthritis model. *J. Clin. Invest.* **101**:2615–2621.
29. Zhang, Z.L., et al. 2003. Intramuscular injection of interleukin-10 plasmid DNA prevented autoimmune diabetes in mice. *Acta Pharmacol. Sin.* **24**:751–756.
30. Scharstuhl, A., Vitters, E.L., van der Kraan, P.M., and van Den Berg, W.B. 2003. Reduction of osteophyte formation and synovial thickening by adenoviral overexpression of transforming growth factor beta/bone morphogenetic protein inhibitors during experimental osteoarthritis. *Arthritis Rheum.* **48**:3442–3451.
31. Sandell, L.J., and Aigner, T. 2001. Cell biology of osteoarthritis. *Arthritis Res.* **3**:107–113.
32. McGonagle, D., Gibbon, W., and Emery, P. 1998. Classification of inflammatory arthritis by enthesitis. *Lancet.* **352**:1137–1140.
33. Dougados, M., et al. 2002. Conventional treatments for ankylosing spondylitis. *Ann. Rheum. Dis.* **61**:40–50.
34. Gooren, L.J.G., Giltay, E.J., van Schaardenburg, D., and Dijkmans, B.A.C. 2000. Gonadal and adrenal sex steroids in ankylosing spondylitis. *Rheum. Dis. Clin. North Am.* **26**:969–987.
35. Weinreich, S., Capkova, J., Hoebe-Hewryk, B., Boog, C., and Ivanyi, P. 1996. Grouped caging predisposes male mice to ankylosing enthesopathy. *Ann. Rheum.*

Dis. **55**:645–647.
36. Francois, R.J., Gardner, D.L., Degrave, E.J., and Bywaters, E.G. 2000. Histopathologic evidence that sacroiliitis in ankylosing spondylitis is not merely enthesitis. *Arthritis Rheum.* **43**:2011–2024.
37. Nordling, C., Kleinau, S., and Klareskog, L. 1992. Down-regulation of a spontaneous arthritis in male DBA/1 mice after administration of monoclonal anti-idiotypic antibodies to a cross-reactive idiotope on anti-collagen antibodies. *Immunology.* **77**:144–146.
38. Maksymowych, W.P. 2000. Ankylosing spondylitis–at the interface of bone and cartilage. *J. Rheumatol.* **27**:2295–2301.
39. Tani, Y., Sato, H., and Hukuda, S. 1997. Autoantibodies to collagens in Japanese patients with ankylosing spondylitis. *Clin. Exp. Rheumatol.* **15**:295–297.
40. Hohler, T., and Marker-Hermann, E. 2001. Psoriatic arthritis: clinical aspects, genetics, and the role of T cells. *Curr. Opin. Rheumatol.* **13**:273–279.
41. Pizette, S., and Niswander, L. 2000. BMPs are required at two steps of limb chondrogenesis: Formation of prechondrogenic condensations and their differentiation into chondrocytes. *Dev. Biol.* **219**:237–249.
42. Balemans, W., and Van Hul, W. 2002. Extracellular regulation of BMP signaling in vertebrates: a cocktail of modulators. *Dev. Biol.* **250**:231–250.
43. Fowler, M.J., Jr., et al. 1998. Induction of bone morphogenetic protein-2 by interleukin-1 in human fibroblasts. *Biochem. Biophys. Res. Commun.* **248**:450–453.
44. Lories, R.J.U., Derese, I., Ceuppens, J.L., and Luyten, F.P. 2003. Bone morphogenetic proteins 2 and 6, expressed in arthritic synovium, are regulated by proinflammatory cytokines and differentially modulate fibroblast-like synoviocyte apoptosis. *Arthritis Rheum.* **48**:2807–2818.
45. Fukui, N., Zhu, Y., Maloney, W.J., Clohisy, J., and Sandell, L.J. 2003. Stimulation of BMP-2 expression by pro-inflammatory cytokines IL-1 and TNF-alpha in normal and osteoarthritic chondrocytes. *J. Bone Joint Surg. Am.* **85**(Suppl. 3):59–66.
46. Lin, J., et al. 2005. Kielin/chordin-like protein, a novel enhancer of BMP signaling, attenuates renal fibrotic disease. *Nat. Med.* **11**:387–393.
47. van Beuningen, H.M., Glansbeek, H.L., van der Kraan, P.M., and van Den Berg, W.B. 1998. Differential effects of local application of BMP-2 or TGF-beta 1 on both articular cartilage composition and osteophyte formation. *Osteoarthr. Cartil.* **6**:306–317.
48. Uusitalo, H., et al. 2001. Induction of periosteal callus formation by bone morphogenetic protein-2 employing adenovirus-mediated gene delivery. *Matrix Biol.* **20**:123–127.
49. Persson, U., et al. 1998. The L45 loop in type I receptors for TGF-beta family members is a critical determinant in specifying Smad isoform activation. *FEBS Lett.* **434**:83–87.

EXHIBIT C

embryonic region, at the border of the serosa. The zygotic expression could then be maintained by an autoregulatory loop. To test this possibility, *otd-1*-binding sites in its regulatory region will have to be identified, and the effects of disrupting this site will have to be tested *in vitro* and *in vivo*.

As previously proposed[11,29], *bicoid* might have evolved from a duplicated *zerknüllt*-like gene, which was converted by mutation into a gene that codes for a K_{50}HD-containing protein—thus adopting the same DNA-binding specificity as Otd-1. During evolution of the higher Diptera, *otd* expression came under the regulation of the maternal gene *bicoid*, so that maternal Otd-1 function was not longer required. Thus, *otd* was restricted to become a gap gene in insects derived from this lineage. □

Methods

GenBank accession number AJ223627 (*Tribolium castaneum* mRNA for Orthodenticle-1 protein) was used in this study.

Antibody production and staining

A polyclonal antibody was produced by immunizing rabbits with bacterially expressed *Tribolium* Orthodenticle-1 protein (Eurogentec). The coding region of the protein used in immunization corresponds to position 760–1474 of the mRNA[15], which was cloned into the *Pvu*II site of the PRSET A vector (Invitrogen). Immunohistochemistry for Otd-1 and Engrailed (using the 4D9 antibody) expression, was carried out as described previously[15]. *In situ* hybridizations were performed according to ref. 19; the embryos shown in Fig. 1a–f are from the same immunohistochemical reaction and were processed identically.

RNA interference

dsRNA was produced as described[30] using the Maxi-Script Kit (Ambion). The *otd-1* dsRNA was produced from a complementary-DNA deletion clone (ΔPst), representing the 3′ part of the RNA (position 1215–1991)[15], which does not contain the homeobox. The cDNA clone that contains the complete open reading frame, and another deletion construct, ΔXho, which represents the 5′ part of the RNA (position 1–918)[15], included the homeobox and were used as controls (not shown). *Tribolium hb* dsRNA was produced from a 2.4-kilobase cDNA clone[19]. Eggs were collected at intervals of 2 h and were microinjected using a standard injection apparatus. At the time of injection, embryos were at an early stage of nuclear division. For parental RNAi, female pupae were immobilized with heptane glue in a Petri dish lid, and injected by free hand under a stereomicroscope, using a glass capillary held by a needle holder connected to an air-filled syringe. dsRNA (500 ng μl^{-1}) was injected to produce *otd-1*^{RNAi} or *hb*^{RNAi} embryos, and equal amounts of both dsRNA preparations (1 $\mu g\,\mu l^{-1}$) were injected to produce *otd-1/hb*^{RNAi} embryos. *Distal-less* dsRNA (900 base pairs) was injected at a concentration of 1 $\mu g\,\mu l^{-1}$ as a control. Only the appendage-specific phenotype[17] was obtained in all of the analysed cuticles ($n = 43$), irrespective of the higher number of molecules injected.

Received 2 September 2002; accepted 25 February 2003; doi:10.1038/nature01536.

1. Gao, Q. & Finkelstein, R. Targeting gene expression to the head: the *Drosophila orthodenticle* gene is a direct target of the Bicoid morphogen. *Development* **125**, 4185–4193 (1998).
2. St Johnston, D. & Nüsslein-Volhard, C. The origin of pattern and polarity in the *Drosophila* embryo. *Cell* **68**, 201–220 (1992).
3. Lall, S. & Patel, N. H. Conservation and divergence in molecular mechanisms of axis formation. *Annu. Rev. Genet.* **35**, 407–437 (2001).
4. Sommer, R. & Tautz, D. Segmentation gene expression in the housefly *Musca domestica*. *Development* **113**, 419–430 (1991).
5. Schröder, R. & Sander, K. A comparison of transplantable *bicoid* activity and partial *bicoid* homeobox sequences in several *Drosophila* and blowfly species (Calliphoridae). *Wilhelm Roux Arch. Dev. Biol.*, **203**, 34–43 (1993).
6. Stauber, M., Jäckle, H. & Schmidt-Ott, U. The anterior determinant *bicoid* of *Drosophila* is a derived Hox class 3 gene. *Proc. Natl Acad. Sci. USA* **96**, 3786–3789 (1999).
7. Brown, S. J. *et al.* A strategy for mapping *bicoid* on the phylogenetic tree. *Curr. Biol.* **11**, R43–R44 (2001).
8. Dubnau, J. & Struhl, G. RNA recognition and translational regulation by a homeodomain protein. *Nature* **379**, 694–699 (1996).
9. Rivera-Pomar, R., Niessing, D., Schmidt-Ott, U., Gehring, W. J. & Jäckle, H. RNA binding and translational suppression by *bicoid*. *Nature* **379**, 746–749 (1996).
10. Simpson-Brose, M., Treisman, J. & Desplan, C. Synergy between the *hunchback* and *bicoid* morphogens is required for anterior patterning in *Drosophila*. *Cell* **78**, 855–865 (1994).
11. Dearden, P. & Akam, M. Axial patterning in insects. *Curr. Biol.* **9**, R591–R594 (1999).
12. Wimmer, E., Carleton, A., Harjes, P., Turner, T. & Desplan, C. *bicoid*-independent formation of thoracic segments in *Drosophila*. *Science* **287**, 2476–2479 (2000).
13. Tautz, D., Friedrich, M. & Schröder, R. Insect embryogenesis—what is ancestral and what is derived? *Development*, (Suppl.), 193–199 (1994).
14. Cohen, S. & Jürgens, G. *Drosophila* headlines. *Trends Genet.* **7**, 267–272 (1991).
15. Li, Y. *et al.* Two *orthodenticle*-related genes in the short-germ beetle *Tribolium castaneum*. *Dev. Genes Evol.* **206**, 35–45 (1996).
16. Brown, S. J., Mahaffey, J., Lorenzen, M., Denell, R. & Mahaffey, J. Using RNAi to investigate orthologous homeotic gene function during development of distantly related insects. *Evol. Dev.* **1**, 11–15 (1999).
17. Bucher, G., Scholten, J. & Klingler, M. Parental RNAi in *Tribolium* (Coleoptera). *Curr. Biol.* **12**, R85–R86 (2002).
18. Frohnhöfer, H. G. & Nüsslein-Volhard, C. Organization of anterior pattern in the *Drosophila* embryo by the maternal gene *bicoid*. *Nature* **324**, 120–125 (1986).
19. Wolff, C., Sommer, R., Schröder, R., Glaser, G. & Tautz, D. Conserved and divergent expression aspects of the *Drosophila* segmentation gene *hunchback* in the short germ band embryo of the flour beetle *Tribolium*. *Development* **121**, 4227–4236 (1995).
20. Falciani, F. *et al.* Class 3 Hox genes in insects and the origin of *zen*. *Proc. Natl Acad. Sci. USA* **93**, 8479–8484 (1996).
21. Lehmann, R. & Nüsslein-Volhard, C. *hunchback*, a gene required for segmentation of an anterior and posterior region of the *Drosophila* embryo. *Dev. Biol.* **119**, 402–417 (1987).
22. Pultz, M., Pitt, J. & Alto, N. Extensive zygotic control of the anteroposterior axis in the wasp *Nasonia vitripennis*. *Development* **126**, 701–710 (1999).
23. Niessing, D. *et al.* Homeodomain position 54 specifies transcriptional versus translational control by Bicoid. *Mol. Cell* **5**, 395–401 (2000).
24. Draper, B. W., Mello, C. C., Bowerman, B., Hardin, J. & Priess, J. R. MEX-3 is a KH domain protein that regulates blastomere identity in early *C. elegans* embryos. *Cell* **87**, 205–216 (1996).
25. Isaacs, H., Andreazzoli, M. & Slack, J. Anteroposterior patterning by mutual repression of *orthodenticle* and *caudal*-type transcription factors. *Evol. Dev.* **1**, 143–152 (1999).
26. Gamberi, C., Peterson, D. S., He, L. & Gottlieb, E. An anterior function for the *Drosophila* posterior determinant Pumilio. *Development* **129**, 2699–2710 (2002).
27. Lall, S., Ludwig, M. Z. & Patel, N. H. *nanos* plays a conserved role in axial patterning outside of the Diptera. *Curr. Biol.* **13**, 224–229 (2003).
28. Patel, N. *et al.* Grasshopper *hunchback* expression reveals conserved and novel aspects of axis formation and segmentation. *Development* **128**, 3459–3472 (2001).
29. Stauber, M., Prell, A. & Schmidt-Ott, U. A single *Hox3* gene with composite *bicoid* and *zerknüllt* expression characteristics in non-Cyclorrhaphan flies. *Proc. Natl Acad. Sci. USA* **99**, 274–279 (2002).
30. Fire, A. *et al.* Potent and specific genetic interference by double-stranded RNA in *Caenorhabditis elegans*. *Nature* **391**, 806–811 (1998).

Supplementary Information accompanies the paper on *Nature*'s website (http://www.nature.com/nature).

Acknowledgements I thank T. Mader for excellent technical assistance, A. Beermann, H. Dove, F. Maderspacher, R. Reuter and C. Wolff for critically reading drafts of the manuscript, E. A. Wimmer for discussions and for pointing out the existence of an NRE site in the *otd-1* sequence, and the Deutsche Forschungsgemeinschaft for financial support.

Competing interests statement The author declares that he has no competing financial interests.

Correspondence and requests for material should be addressed to the author (e-mail: reinhard.schroeder@uni-tuebingen.de).

The BMP antagonist noggin regulates cranial suture fusion

Stephen M. Warren*, Lisa J. Brunet†, Richard M. Harland†, Aris N. Economides‡ & Michael T. Longaker*

** Department of Surgery, Stanford University School of Medicine, Stanford, California 94305-5148, USA*
† Department of Molecular and Cell Biology, Division of Biochemistry and Molecular Biology, University of California, Berkeley, California 94720-3204, USA
‡ Regeneron Pharmaceuticals, Inc., Tarrytown, New York 10591-6707, USA

During skull development, the cranial connective tissue framework undergoes intramembranous ossification to form skull bones (calvaria). As the calvarial bones advance to envelop the brain, fibrous sutures form between the calvarial plates[1]. Expansion of the brain is coupled with calvarial growth through a series of tissue interactions within the cranial suture complex[2]. Craniosynostosis, or premature cranial suture fusion, results in an abnormal skull shape, blindness and mental retardation[3]. Recent studies have demonstrated that gain-of-function mutations in fibroblast growth factor receptors (*fgfr*) are associated with syndromic forms of craniosynostosis[4,5]. Noggin, an antagonist of bone morphogenetic proteins (BMPs), is required for embryonic neural tube, somites and skeleton patterning[6–8]. Here we show that *noggin* is expressed postnatally in the suture mesenchyme of patent, but not fusing, cranial sutures, and that *noggin* expression is suppressed by FGF2 and syndromic *fgfr*

signalling. Since *noggin* misexpression prevents cranial suture fusion *in vitro* and *in vivo*, we suggest that syndromic *fgfr*-mediated craniosynostoses may be the result of inappropriate downregulation of *noggin* expression.

In the mouse, the posterior frontal cranial suture fuses in the first 45 days of life, whereas all other sutures, including the sagittal and coronal, remain patent[9]. The dura mater regulates cranial suture fusion through multiple pathways[9], including signalling by transforming growth factor-β1 (refs 9, 10) and fibroblast growth factor-2 (FGF2)[11] from the posterior frontal dura mater. To address whether posterior frontal suture fusion is indeed an active process, when compared with sagittal or coronal suture patency, we examined other factors known to promote bone formation, such as BMPs[12,13].

Surprisingly, we found abundant BMPs in both fusing and patent cranial sutures on gene chip analysis and in quantitative real-time polymerase chain reaction with reverse transcription (RT–PCR) (data not shown). Immunohistochemistry localized BMP4 protein to the suture mesenchyme and osteogenic fronts of the posterior frontal suture 1 week before the onset of fusion, as well as to patent sutures (Fig. 1a and b). The presence of BMP4 in fusing and non-fusing sutures suggested that there might be suture-specific regulation of BMP activity by secreted BMP antagonists[6,7,14–16].

We therefore screened for BMP antagonist messenger RNAs before (day 15), during (days 35 and 42), and after (day 50) the period of predicted suture fusion using *in situ* hybridization. We did not detect *dan/cerberus* family antagonists (*gremlin*, *dcr4* (GenBank accession number AA289245), *prdc*[17], *sost*[18], *dcr7* (GenBank accession number BC021458) or *cerberus*) in either patent or fusing sutures; however, we detected *noggin* in patent sutures (data not shown). To facilitate the temporal and spatial analysis of *noggin* expression, we used in-frame *lacZ/noggin* transgenic mice[6]. Stage-specific *lacZ* staining revealed *noggin* expression in the patent sagittal and coronal sutures before, during, and after the period of predicted suture fusion (Fig. 1c). In marked contrast, there was almost no *noggin* expression in the fusing posterior frontal suture complex as early as day 15 (Fig. 1c).

Because BMP4 is present in both fusing and patent sutures, and osteoblasts line the osteogenic fronts of these sutures, we examined the effects of BMP4 on Noggin expression in osteoblasts. Primary calvarial osteoblasts treated with BMP4 expressed Noggin protein in a dose-dependent manner (Fig. 2a). If BMP4 induces Noggin expression, how can the posterior frontal suture fuse? Significantly, only the posterior frontal dura mater expresses FGF2 mRNA and protein *in vivo*[9] and produces high levels of FGF2 in culture (Fig. 2b). FGF2 might therefore regulate BMP4-induced Noggin expression in calvarial osteoblasts[19]. Interestingly, FGF2 disrupts Noggin induction in a dose-dependent fashion (Fig. 2c). This suggests that environments with a low FGF2 concentration (that is, sagittal or

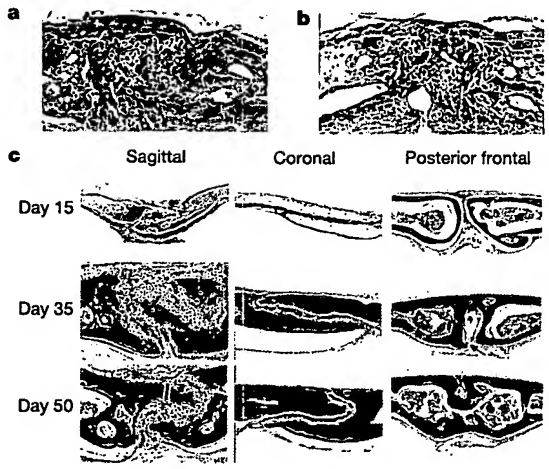

Figure 1 BMP4 and *noggin* expression in patent and fusing sutures. **a**, Photomicrograph of BMP4 immunolocalization in 18-day-old patent sagittal suture. Note staining in the suture mesenchyme and cells lining the osteogenic fronts. Controls, from which primary antibodies were omitted, yielded no detectable staining. **b**, Photomicrograph of BMP4 immunolocalization in 18-day-old posterior frontal suture, 1 week before the onset of suture fusion. Note the staining in the suture mesenchyme and cells lining the osteogenic fronts. Controls, from which primary antibodies were omitted, yielded no detectable staining. **c**, Ontogeny of *noggin* expression in the patent sagittal and coronal sutures compared with the fusing posterior frontal suture. Sections from sutures in *lacZ/noggin* transgenic mice were stained on the indicated days (day 15 is before onset of posterior frontal suture; day 35 is during posterior frontal suture fusion; day 50 is after posterior frontal suture fusion). The posterior frontal suture fuses in an endocranial to ectocranial direction. Arrow indicates initial endocranial bridging (posterior frontal day 35).

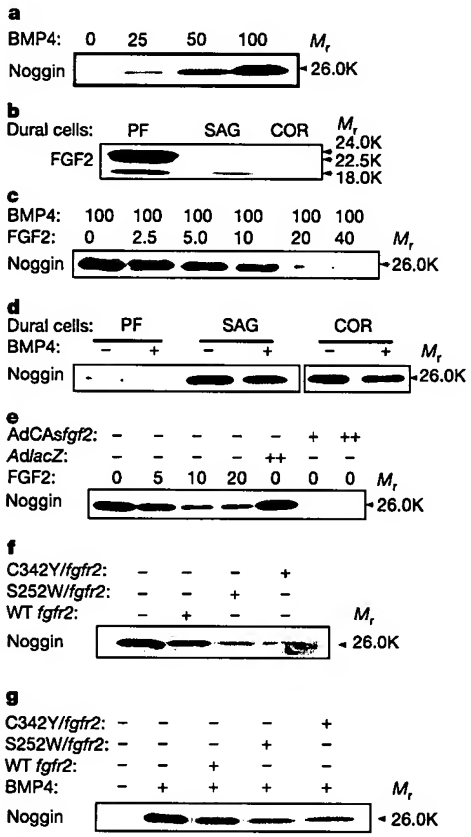

Figure 2 BMP4-induced Noggin expression in primary osteoblasts and dural cells is suppressed by FGF2 and *fgfr2* gain-of-function mutations. **a**, Western analysis of BMP4-induced (concentrations are shown in ng ml^{-1}) Noggin in primary calvarial osteoblasts. **b**, FGF2 western analysis of cultured posterior frontal (PF), sagittal (SAG) and coronal (COR) dura mater. **c**, Noggin western analysis on primary calvarial osteoblasts treated with BMP4 and FGF2 (concentrations of both are shown in ng ml^{-1}). **d**, Noggin western analysis of cultured posterior frontal (PF), sagittal (SAG) and coronal (COR) dura mater. Minus signs, untreated dura mater; plus signs, treatment with 100 ng ml^{-1} BMP4. **e**, Noggin western analysis of cultured coronal dura mater after treatment with FGF2 (concentrations shown in ng ml^{-1}) or transfection with an adenovirus containing *lacZ* (Ad*lacZ*; 100 (++) multiplicity of infection (MOI)) or *fgf2* (AdCAs*fgf2*; 50 (+) and 100 (++) MOI, respectively). **f**, Noggin western analysis on sagittal dura mater transduced with a retrovirus containing wild-type *fgfr2* (WT *fgfr2*), Apert mutated *fgfr2* (S252W/*fgfr2*) or Crouzon mutated *fgfr2* (C342Y/*fgfr2*). **g**, Noggin western analysis on BMP4 (25 ng ml^{-1})-treated osteoblasts transduced with a retrovirus containing wild-type *fgfr2* (WT *fgfr2*), Apert mutated *fgfr2* (S252W/*fgfr2*) or Crouzon mutated *fgfr2* (C342Y/*fgfr2*).

coronal sutures) might not suppress BMP-induced Noggin expression, but environments high in FGF2 (that is, posterior frontal suture) reduce Noggin expression and enable suture fusion. These findings *in vitro* correlate with murine expression patterns *in vivo* for FGF2 (ref. 9) and Noggin in posterior frontal, sagittal and coronal sutures (Fig. 1c).

Whereas BMP4 stimulates Noggin expression in calvarial osteoblasts, the suture-specific dura mater is an independent source of Noggin; thus, the dura mater might be directly patterning cranial suture fate by interrupting BMP signalling. Cultured dura mater cells from patent sutures expressed high levels of Noggin protein without BMP stimulation, whereas the dura mater from the fusing posterior frontal suture expressed almost undetectable levels of Noggin. Treating these dural cell cultures with BMP4 had little impact on Noggin protein production (Fig. 2d), indicating that Noggin expression might be near maximal in sagittal and coronal dural cell cultures. Furthermore, treatment with BMP4 does not overcome endogenous FGF2-mediated Noggin suppression in the posterior frontal dura mater (Fig. 2d). Interestingly, when signalling mediated by FGF receptors (FGFRs) was disrupted with a dominant-negative FGFR1 adenoviral construct, posterior frontal dural cells did not express Noggin (data not shown). However, complete abrogation of FGF2 signalling is difficult, and the failure of our dominant-negative construct to restore Noggin expression might indicate that levels of the truncated FGFR1 receptor were insufficient to competitively inhibit wild-type receptors.

While blocking FGF signalling[20] or FGF2 activity[21] prevents cranial suture fusion or osteogenesis, respectively, our findings suggest that exogenous FGF signalling is capable of suppressing Noggin expression during cranial suture fusion. For example, treatment with FGF2 suppressed Noggin production from coronal (Fig. 2e) and sagittal (data not shown) dura mater in a dose-dependent fashion. Taken together, these findings suggest that FGF2 guides suture fate (patency versus fusion) by regulating suture-specific Noggin production in osteoblasts and dura mater and, in turn, suture-specific BMP activity. Moreover, these data suggest a possible mechanism for syndromic craniosynostoses arising from *fgfr* gain-of-function mutations.

Because constitutive FGFR signalling is associated with syndromic forms of premature cranial suture fusion, we investigated the role of Noggin in a previously established model of FGF-mediated coronal synostosis[20]. In this model, injection of an FGF2-expressing adenovirus into perinatal coronal dura mater led to FGF2 over-expression, pathological osteogenesis and suture fusion within 30 days. Just as the application of FGF2 protein suppressed Noggin production in coronal dura mater in culture, infection with the FGF2-expressing adenovirus completely ablated Noggin expression (Fig. 2e). Injection of this FGF2-expressing adenovirus into the coronal dura mater of neonatal *lacZ/noggin* transgenic mice led to the suppression of Noggin expression in all animals (Fig. 3) and pathological coronal suture fusion (ref. 20, and data not shown). Taken together, our cell culture and *in vivo* data suggest that increased FGFR signalling might lead to suture fusion by suppressing Noggin production in the dura mater and osteoblasts of normally patent cranial sutures.

Because FGF2 misexpression led to Noggin suppression in coronal sutures, we investigated the effects of Apert (S252W) and Crouzon (C342Y) syndrome *fgfr2* gain-of-function mutations on Noggin production in dural cell and osteoblast cultures[22]. Although infection with a wild-type *fgfr2* retrovirus did not substantially affect Noggin expression, both Apert and Crouzon syndrome *fgfr2* mutants markedly downregulated Noggin protein production in sagittal dura mater (Fig. 2f). The Apert and Crouzon *fgfr2* constructs also downregulated BMP4-induced Noggin expression in calvarial osteoblasts (Fig. 2g). Because both Apert and Crouzon syndrome *fgfr* gain-of-function mutations promote pathological suture fusion, these findings provide an important link between the murine models and the gain-of-function *fgfr* mutations associated with syndromic forms of human craniosynostosis.

Having demonstrated that Noggin is normally expressed in the patent suture complex and that posterior frontal dura mater-derived FGF2 suppresses Noggin, we proposed that forced

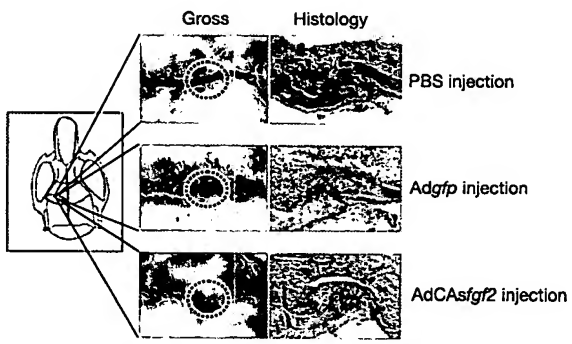

Figure 3 FGF2 suppresses *noggin* expression in coronal dura mater *in vivo*. Gross (×5 original magnification) and histological (×100 original magnification) views of stained *lacZ/noggin* transgenic 9-day-old coronal sutures after microinjection of PBS, 10^9 PFU of an adenovirus containing *gfp* (Ad*gfp*) or 10^9 PFU of an adenovirus containing *fgf2* (AdCAs*fgf2*). Animals were microinjected on day 3 of life. Injection of PBS ($n = 9$) or Ad*gfp* ($n = 11$) did not affect *noggin* expression. In marked contrast, AdCAs*fgf2* ($n = 13$) led to *noggin* suppression in all animals transfected. The dotted circle denotes area of microinjection.

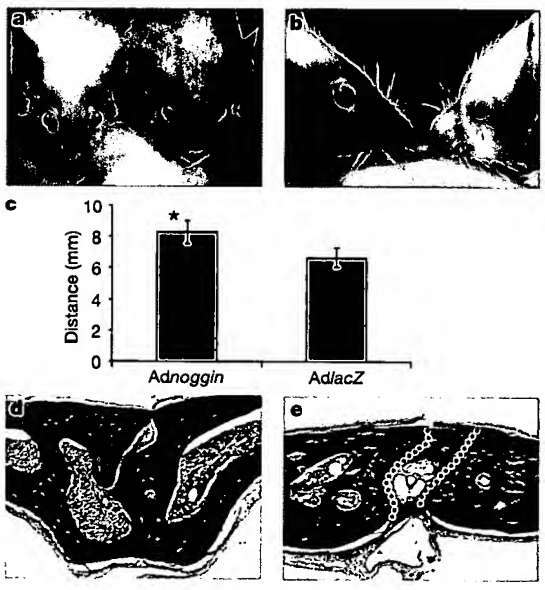

Figure 4 Noggin misexpression maintains posterior frontal suture patency *in vivo*. **a**, Anterior view of 53-day-old CD-1 mice. The posterior frontal sutures of these mice were injected with 10^9 PFU of an adenovirus containing *lacZ* (left, $n = 12$) or *noggin* (right, $n = 9$) on day 3 of life. **b**, Lateral view of mice injected with Ad*lacZ* (left) and Ad*noggin* (right). Ad*noggin*-injected animals had a marked reduction in midface projection. **c**, The distance between the eyes of Ad*noggin*-injected mice was significantly greater than that of Ad*lacZ*-injected mice (intercanthal distance 8.28 ± 0.7 mm versus 6.68 ± 0.6 mm, $^*P < 0.0001$) owing to increased frontal bone growth perpendicular to the posterior frontal suture. **d**, Histological section (×100 original magnification) of the posterior frontal suture of Ad*lacZ*-injected mouse. The posterior frontal suture is fused. **e**, Histological section (×100 original magnification) of the posterior frontal suture of an Ad*noggin*-injected mouse. Dotted lines indicate osteogenic fronts of widely patent posterior frontal suture.

expression of *noggin* would maintain posterior frontal suture patency. We first examined the effects of *noggin* misexpression in a previously established *in vitro* organ culture model[23]. Using a *noggin*-expressing adenovirus, 22-day-old posterior frontal sutures were infected and placed in organ culture. After 30 days, all posterior frontal sutures mock-infected or infected with *lacZ* virus were fused. In marked contrast, all posterior frontal sutures infected with the *noggin* virus were widely patent (Supplementary Information).

To test the effects of *noggin* misexpression *in vivo*, the posterior frontal sutures of 3-day-old CD-1 mice were injected with PBS, a *lacZ* adenovirus (Ad*lacZ*) or a *noggin* adenovirus (Ad*noggin*). After 50 days, the Ad*noggin*-infected mice had short broad snouts and widely spaced eyes (Fig. 4a and b). The distance between the eyes of Ad*noggin*-infected mice was significantly greater than that of Ad*lacZ*-injected mice (intercanthal distance 8.28 ± 0.7 mm versus 6.68 ± 0.6 mm, $P < 0.0001$; Fig. 4c) owing to increased frontal bone growth perpendicular to the posterior frontal suture. Histological analysis demonstrated that all mice injected with PBS ($n = 11$) and Ad*lacZ* virus ($n = 12$) had normally fused posterior frontal sutures, whereas the posterior frontal sutures of all Ad*noggin*-injected mice ($n = 9$) were widely patent (Fig. 4d and e). This result demonstrates that *noggin* misexpression at an early stage of suture development has profound consequences on cranial suture fate.

Homozygous *noggin*$^{-/-}$ mice die at birth with multiple defects that include joint fusion of the appendicular skeleton[6]. While human *noggin* mutations have been linked to the fusion of finger joints (proximal symphalangism)[24], nothing was previously known about the role of *noggin* in calvarial joint (suture) biology until the opposing activity of Noggin and BMP4 in the dorsal lip of amphibian gastrulae led us to examine whether Noggin antagonized BMP4 in postnatal cranial sutures[14]. Here we have demonstrated that Noggin, a high-affinity secreted BMP antagonist, is present only in patent sutures and is decisively regulated by FGF signalling. Because Noggin enforces suture patency, syndromic *fgfr*-mediated craniosynostoses might result from inappropriate Noggin suppression. Finally, ectopic *noggin* expression prevents the fusion of mouse posterior frontal sutures, raising the possibility that therapeutic Noggin could be exploited to control postnatal skeletal development. □

Methods

Gene chip analysis

Total RNA was isolated and pooled from posterior frontal and sagittal sutures ($n = 20$ per time point) with associated dura mater from Sprague–Dawley rats at times before, during and after programmed posterior frontal suture fusion. Synthesis of cDNA, *in vitro* transcription and biotin labelling of cRNA, and hybridization to the R34U A Chips (Affymetrix) were performed in accordance with Affymetrix protocols. Expression data were analysed with Microarray Suite 5.0 (Affymetrix) and Genespring 4.2 (Silicon Genetics) software. Overall chip intensities were scaled to an artificial mean to permit chip-to-chip comparisons and normalized to day 30 (post-fusion) sutures.

Quantitative real-time RT–PCR

RNA was harvested with the Ambion RNAqueous for PCR kit in accordance with the manufacturer's instructions, including incubation with DNase I to remove any genomic contamination. Taqman (Applied Biosystems, Foster City, California) primer and probe sets for *bmp2*, *bmp4* and *bmp7* were designed with PrimerExpress Software (Applied Biosystems) and screened for appropriate amplification by using end-point RT–PCR analysis. Rodent glyceraldehyde-3-phosphate dehydrogenase (*gapdh*) primer and probe reagents were purchased from Applied Biosystems. Quantification was performed with the ABI Prism 7900HT Sequence Detection System (Applied Biosystems) in a two-step non-multiplexed assay in accordance with the relative standard method. Transcript quantification was performed in triplicate for every sample and reported relative to *gapdh*.

Immunohistochemistry

Immunohistochemistry was performed on 18-day-old mice as described previously[25]. Sections were de-waxed in xylene, blocked in 10% goat serum, incubated in polyclonal BMP4 antibody (R&D Systems) or PBS alone (control), followed by a biotinylated anti-rabbit antibody, and amplified with an avidin–biotin enzyme complex (ABC kit; Vector Laboratories). Detection was performed with 0.05% 3,3-diaminobenzidine chromophore (Sigma) and 0.03% hydrogen peroxide in 0.1 M Tris-HCl, pH 7.4. Sections were lightly counterstained with haematoxylin.

In situ hybridization

Calvaria were harvested, decalcified and embedded as described previously[26]. Antisense *gremlin*, *dcr4*, *prdc*, *sost*, *dcr7*, *cerberus* and *noggin* riboprobes were labelled with ^{35}S-UTP and *in situ* hybridization was performed with standard protocols[27]. Sections were counterstained with Hoechst 33258 (5 μg ml^{-1}) to reveal nuclei.

LacZ staining

Calvaria were stained as described previously[6]. Whole calvaria were fixed in 4% paraformaldehyde for 20 min and placed in standard staining solution (5 mM potassium ferricyanide, 5 mM potassium ferrocyanide, 2 mM $MgCl_2$, 0.4% 5-bromo-4-chloro-4-indolyl-β-D-galactopyranoside in PBS) overnight at 4 °C. The following day, samples were incubated for 4–6 h at 37 °C (wild-type littermates served as controls). Stained calvaria were dehydrated through an alcohol series and embedded in paraffin. Sections were cut at 5 μm thickness and lightly counterstained with haematoxylin and eosin.

Western blot analysis

Dura mater or osteoblast cultures were grown to confluence, starved in low-serum medium for 24 h and then treated with various doses of BMP4 and/or FGF2. Medium was collected 24 h after cytokine treatment and incubated with immobilized heparin–Sepharose beads (Pharmacia). Bound proteins were eluted by heating at 95 °C. Denatured samples were fractionated by 10% SDS–polyacrylamide-gel electrophoresis, transferred to a poly(vinylidene difluoride) membrane and probed with RP57-16 anti-Noggin antibody[28]. Blots were exposed to a horseradish-peroxidase-conjugated goat anti-rat IgG and developed with ECL chemiluminescent reagents (Amersham Pharmacia Biotech). All membranes were stained with Ponceau S to ensure equivalent loading and transfer.

Retroviral infection

The pLSXN/*fgfr2* constructs were co-transfected with an ecotropic packaging vector into HEK-293 cells. Supernatants were collected, passed through a 0.45 μm filter and frozen at −80 °C. Osteoblasts and dural cells were infected in the presence of 8 μg ml^{-1} Polybrene (Sigma) and selected in medium containing G418 (400 μg ml^{-1}).

Adenoviral infection *in vitro*

Adenoviruses were prepared as previously described[20]. Calvaria from 22-day-old CD-1 mice were isolated and washed. The posterior frontal sutures were injected with PBS ($n = 6$), Ad*lacZ* (10^9 plaque-forming units (PFU), $n = 7$) or Ad*noggin* (10^9 PFU, $n = 5$). Infected and control calvaria were placed on a 3.0-μm culture well insert and fed with standard BGJb medium (pH 7.4). All sutures were harvested after 30 days in culture and immediately fixed in 4% paraformaldehyde. Calvaria were photographed, processed, embedded and sectioned.

Adenoviral infection *in vivo*

To determine the effects of FGF2 on *noggin* expression, the coronal sutures of 3-day-old transgenic *lacZ*/*noggin* mice were injected with PBS ($n = 9$), an adenovirus containing green fluorescent protein (Ad*gfp*, 10^9 PFU, $n = 11$) or an adenovirus containing *fgf2* (AdCAs*fgf2*, 10^9 PFU, $n = 13$). Animals were harvested 6 days after injection.

To determine the effects of *noggin* expression on suture patency, the posterior frontal sutures of 3-day-old CD-1 mice were injected with PBS ($n = 11$), an adenovirus containing *lacZ* (10^9 PFU, $n = 12$) or an adenovirus containing *noggin* (10^9 PFU, $n = 9$). Previous work has documented widespread infection by such viruses, with expression detectable for 30 days (ref. 20). At 50 days after injection, animals were harvested and photographed, and intercanthal distances were measured with digital calipers with an accuracy of 0.01 mm (Model CD-6 CS, Mitutoyo, Kanagawa, Japan). A paired *t*-test was performed to determine statistical significance. After measurement, the skulls were processed, embedded and sectioned.

Received 2 October 2002; accepted 7 March 2003; doi:10.1038/nature01545.

1. Slavkin, H. C. *Developmental Craniofacial Biology* (Lea & Febiger, Philadelphia, 1979).
2. Thilander, B. Basic mechanisms in craniofacial growth. *Acta Odontol. Scand.* **53**, 144–151 (1995).
3. McCarthy, J. G., Epstein, F. J. & Wood-Smith, D. in *Plastic Surgery* (ed. McCarthy, J. G.) 3013–3053 (W.B. Saunders Co., Philadelphia, 1990).
4. Cohen, M. M. Jr Craniosynostoses: phenotypic/molecular correlations. *Am. J. Med. Genet.* **56**, 334–339 (1995).
5. Wilkie, A. O. M. Craniosynostosis: genes and mechanisms. *Hum. Mol. Genet.* **6**, 1647–1656 (1997).
6. Brunet, L. J., McMahon, J. A., McMahon, A. P. & Harland, R. M. Noggin, cartilage morphogenesis, and joint formation in the mammalian skeleton. *Science* **280**, 1455–1457 (1998).
7. McMahon, J. A. *et al.* Noggin-mediated antagonism of BMP signaling is required for growth and patterning of the neural tube and somite. *Genes Dev.* **12**, 1438–1452 (1998).
8. Capdevila, J. & Johnson, R. L. Endogenous and ectopic expression of noggin suggests a conserved mechanism for regulation of BMP function during limb and somite patterning. *Dev. Biol.* **197**, 205–217 (1998).
9. Warren, S. M. *et al.* New developments in cranial suture research. *Plast. Reconstr. Surg.* **107**, 523–540 (2001).
10. Opperman, L. A., Nolen, A. A. & Ogle, R. C. TGF-beta 1, TGF-beta 2, and TGF-beta 3 exhibit distinct patterns of expression during cranial suture formation and obliteration *in vivo* and *in vitro*. *J. Bone Miner. Res.* **12**, 301–310 (1997).
11. Greenwald, J. A. *et al.* Regional differentiation of cranial suture-associated dura mater *in vivo* and *in vitro*: implications for suture fusion and patency. *J. Bone Miner. Res.* **15**, 2413–2430 (2000).
12. Wozney, J. M. *et al.* Novel regulators of bone formation: Molecular clones and activities. *Science* **242**, 1528–1534 (1988).
13. Wang, E. A. *et al.* Recombinant human bone morphogenetic protein induces bone formation. *Proc. Natl Acad. Sci. USA* **87**, 2220–2224 (1990).

14. Zimmerman, L. B., De Jesus-Escobar, J. M. & Harland, R. M. The Spemann organizer signal noggin binds and inactivates bone morphogenetic protein 4. *Cell* 86, 599–606 (1996).
15. Hsu, D. R., Economides, A. N., Wang, X., Eimon, P. M. & Harland, R. M. The *Xenopus* dorsalizing factor gremlin identifies a novel family of secreted proteins that antagonize BMP activities. *Mol. Cell* 1, 673–683 (1998).
16. Capdevila, J., Tsukui, T., Rodriquez Esteban, C., Zappavigna, V. & Izpisua Belmonte, J. C. Control of vertebrate limb outgrowth by the proximal factor Meis2 and distal antagonism of BMPs by gremlin. *Mol. Cell* 4, 839–849 (1999).
17. Minabe-Saegusa, C., Saegusa, H., Tsukahara, M. & Noguchi, S. Sequence and expression of a novel mouse gene PRDC (protein related to DAN and cerberus) identified by a gene trap approach. *Dev. Growth Differ.* 40, 343–353 (1998).
18. Brunkow, M. E. *et al.* Bone dysplasia sclerosteosis results from loss of the SOST gene product, a novel cystine knot-containing protein. *Am. J. Hum. Genet.* 68, 577–589 (2001).
19. Gazzerro, E., Gangji, V. & Canalis, E. Bone morphogenetic proteins induce the expression of noggin, which limits their activity in cultured rat osteoblasts. *J. Clin. Invest.* 102, 2106–2114 (1998).
20. Greenwald, J. A. *et al. In vivo* modulation of FGF biological activity alters cranial suture fate. *Am. J. Pathol.* 158, 441–452 (2001).
21. Moore, R., Ferretti, P., Copp, A. & Thorogood, P. Blocking endogenous FGF-2 activity prevents cranial osteogenesis. *Dev. Biol.* 243, 99–114 (2002).
22. Mansukhani, A., Bellosta, P., Sahni, M. & Basilico, C. Signaling by fibroblast growth factors (FGF) and fibroblast growth factor receptor 2 (FGFR2)-activating mutations blocks mineralization and induces apoptosis in osteoblasts. *J. Cell Biol.* 149, 1297–1308 (2000).
23. Bradley, J. P. *et al.* Studies in cranial suture biology: *in vitro* cranial suture fusion. *Cleft Palate–Craniofac. J.* 33, 150–156 (1996).
24. Dixon, M. E., Armstrong, P., Stevens, D. B. & Bamshad, M. Identical mutations in NOG can cause either tarsal/carpal coalition syndrome or proximal symphalagism. *Gen. Med.* 3, 349–353 (2001).
25. Roth, D. A. *et al.* Studies in cranial suture biology. I. Increased immunoreactivity for transforming growth factor-beta (β1, β2, β3) during rat cranial suture fusion. *J. Bone Miner. Res.* 12, 311–321 (1997).
26. Bradley, J. P., Levine, J. P., Roth, D. A., McCarthy, J. G. & Longaker, M. T. Studies in cranial suture biology. IV. Temporal sequence of posterior frontal cranial suture fusion in the mouse. *Plast. Reconstr. Surg.* 98, 1039–1045 (1996).
27. Albrecht, U., Helms, J. A. & Lin, H. in *Molecular and Cellular Methods in Developmental Toxicology* (ed. Daston, G. P.) 23–48 (CRC Press, Boca Raton, 1997).
28. Paine-Saunders, S., Viviano, B. L., Economides, A. N. & Saunders, S. Heparan sulfate proteoglycans retain noggin at the cell surface: A potential mechanism for shaping bone morphogenetic protein gradients. *J. Biol. Chem.* 277, 2089–2096 (2002).

Supplementary Information accompanies the paper on *Nature*'s website (http://www.nature.com/nature).

Acknowledgements We thank C. J. Tabin, I. Thesleff, D. M. Kingsley and N. Quarto for comments and suggestions on this manuscript, and K. D. Fong, J. A. Mathy and R. P. Nacamuli for their technical assistance. The human *fgfr2*, *fgfr2*/S252W (Apert) and *fgfr2*/C342Y (Crouzon) retroviral constructs were provided by A. Mansukhami and C. Basilico (New York University). This work was supported by NIH grants (R.M.H. and M.T.L.) and a Lyndon Peer/PSEF Fellowship (S.M.W.).

Competing interests statement The authors declare that they have no competing financial interests.

Correspondence and requests for materials should be addressed to M.T.L. (e-mail: longaker@stanford.edu).

The exocyst complex is required for targeting of Glut4 to the plasma membrane by insulin

Mayumi Inoue, Louise Chang, Joseph Hwang, Shian-Huey Chiang & Alan R. Saltiel

Life Sciences Institute, Departments of Internal Medicine and Physiology, University of Michigan Medical Center, Ann Arbor, Michigan 48109, USA

Insulin stimulates glucose transport by promoting exocytosis of the glucose transporter Glut4 (refs 1, 2). The dynamic processes involved in the trafficking of Glut4-containing vesicles, and in their targeting, docking and fusion at the plasma membrane, as well as the signalling processes that govern these events, are not well understood. We recently described tyrosine-phosphorylation events restricted to subdomains of the plasma membrane that result in activation of the G protein TC10 (refs 3, 4). Here we show that TC10 interacts with one of the components of the exocyst complex, Exo70. Exo70 translocates to the plasma membrane in response to insulin through the activation of TC10, where it assembles a multiprotein complex that includes Sec6 and Sec8. Overexpression of an Exo70 mutant blocked insulin-stimulated glucose uptake, but not the trafficking of Glut4 to the plasma membrane. However, this mutant did block the extracellular exposure of the Glut4 protein. So, the exocyst might have a crucial role in the targeting of the Glut4 vesicle to the plasma membrane, perhaps directing the vesicle to the precise site of fusion.

To search for potential effectors of TC10 that have a role in insulin-stimulated glucose transport, we screened a yeast two-hybrid complementary-DNA library derived from 3T3L1 adipocytes with a constitutively active mutant form of human TC10α[5], and identified two clones encoding the full-length sequence of Exo70, a component of the exocyst complex, which has been implicated in the tethering or docking of secretory vesicles[6,7]. To explore the specificity of the interaction of TC10 with Exo70, we co-transfected 293T cells with myc-tagged Exo70 and haemagglutinin (HA)-tagged, constitutively active forms of mouse TC10α, Rho1, Rac1 or Cdc42 cDNAs[8–11] (Fig. 1a). Exo70 could be co-precipitated with TC10, but not with Rho, Rac or Cdc42, indicating that its interaction with TC10 is specific. TC10β could also be co-precipitated with Exo70 (data not shown). To evaluate whether Exo70 is a potential effector of TC10, we incubated lysates derived from cells expressing different forms of HA-tagged TC10 with a glutathione *S*-transferase (GST)–Exo70 fusion protein, to examine binding *in vitro* (Fig. 1b). Exo70 bound to the constitutively active mutant TC10α(Q67L), but not to the dominant-interfering TC10α(T23N). Identical results were obtained with the corresponding mutants TC10β(T25N) and TC10β(Q69L) (data not shown). To confirm that the interaction of TC10 with Exo70 was GTP-dependent, lysates expressing TC10 were loaded with GDP or a non-hydrolysable form of GTP (GTPγS) *in vitro*, and incubated with GST–Exo70. Exo70 bound weakly to the GDP-bound form of TC10, and strongly to the GTP-bound, activated state of the protein. These data show that Exo70 interacts with TC10 in a GTP-dependent manner.

To study the function of Exo70 in glucose transport, we sought to map its TC10 binding site through a series of deletion mutants. Exo70 has only one putative protein–protein interaction region, a coiled-coil domain in the amino terminus (Fig. 1c). We deleted amino acids 1–384 of Exo70, and also prepared constructs expressing only amino acids 1–384, 1–99 or 100–384, and evaluated the ability of the mutants to bind constitutively active TC10α(Q67L) in a co-precipitation experiment. Whereas wild-type Exo70 (Exo70-WT) bound to TC10, Exo70(385–653) (Exo70-C) did not. Moreover, an Exo70 fragment containing only amino acids 1–384 (Exo70-N) bound to TC10, whereas Exo70 containing amino acids 1–99, which comprised the coiled-coil domain, bound weakly, and Exo70 containing residues 100–384 also bound weakly. These data indicate that amino acids 1–384 of Exo70 are both necessary and sufficient for binding to TC10, but that this interaction requires more than the coiled-coil domain (Fig. 1d and Supplementary Fig. 1).

We analysed the intracellular localization of Exo70 by immunohistochemistry, and evaluated its potential regulation by insulin and TC10. 3T3L1 adipocytes were transfected with myc–Exo70 plus or minus TC10 and its mutants. As shown in Fig. 2a, b, myc–Exo70 was distributed diffusely throughout the intracellular region. Co-expression of TC10 or its inactive mutant TC10(T23N) did not influence the localization of overexpressed myc–Exo70. By contrast, Exo70 was localized at the plasma membrane when co-expressed with the constitutively active mutant TC10(Q67L), indicating that TC10 activation stimulates the translocation of Exo70. We also examined whether the amino-terminal fragment of Exo70 (Exo70-N) translocated to the plasma membrane after expression of active TC10. Unlike the wild-type form of the protein, this fragment did

EXHIBIT D

INTRODUCTORY COMMENTS

This supplement to *The Journal of Bone and Joint Surgery* consists of articles based on presentations delivered at the Fourth International Conference on Bone Morphogenetic Proteins, held in Sacramento, California, in October 2002. Many of these articles, particularly those on the clinical applications of recombinant human bone morphogenetic proteins (rhBMPs), will be of special interest to orthopaedic surgeons. For example, Einhorn[1] summarizes the results of prospective, randomized clinical trials of the use of rhBMPs in the treatment of tibial nonunions and open tibial shaft fractures. On the basis of the results of the tibial nonunion study[2], the United States Food and Drug Administration has issued a Humanitarian Device Exemption for the use of an OP-1 (rhBMP-7) implant as "an alternative to the patient's own bone (autograft) in recalcitrant long bone nonunions where autograft is unfeasible and alternative treatments have failed."[3]

Sandhu and Khan[4] present a comprehensive review of preclinical experimental studies and prospective, randomized clinical trials of the effects of rhBMP implants on the rate and characteristics of fusion following posterolateral intertransverse process arthrodesis and following anterior lumbar interbody arthrodesis with use of lordotic tapered cages. On the basis of the results of a pilot study, the Orthopaedic and Rehabilitation Devices panel of the Food and Drug Administration recommended the approval of a multicenter clinical trial of rhBMP2/type-I collagen implants in lordotic tapered cages for anterior interbody arthrodeses. The Food and Drug Administration has now approved the use of the rhBMP-2/type-I collagen implant in a lordotic tapered cage for single-level anterior interbody arthrodesis in the treatment of degenerative disc disease.

The clinical application of BMPs appears to have entered a new phase, wherein the usefulness of rhBMP/carrier combinations in the treatment of orthopaedic problems will be progressively established and these devices will become available for an increasing variety of clinical applications. For example, Einhorn[1] also considers the possibility of using a single percutaneous injection of rhBMP to accelerate and enhance the healing of closed fractures. This procedure would require the use of an injectable carrier with properties different from those of the type-I collagen carrier devices implanted during the operative treatment of open fractures. Seeherman et al.[5] provide an in-depth analysis of the problems associated with the development of an injectable carrier, describe the attributes and properties of an ideal injectable carrier, and extensively evaluate the performance of a number of rhBMP/carrier candidate combinations, including injectable calcium phosphate cement (α-BSM).

The basic-science articles in this supplement examine the molecular mechanisms by which the BMPs exert their biologic functions. The BMPs elicit the chemotaxis, proliferation, and differentiation of mesenchymal stem cells into cartilage and then bone[6]. BMP signal transduction triggers these events. BMP signal transduction involves the binding of the BMP to its serine/threonine kinase receptors; the activation of the transcription factors Smads 1, 5, and 8; and the translocation of the activated Smads to the cell nucleus, where they activate the genes involved in cartilage and bone formation. However, the BMPs differ greatly in their osteoinductive activity. One recent study suggested that BMP-2, BMP-6, and BMP-9 most potently induce the osteoblast differentiation of mesenchymal stem cells[7]. Articles in this supplement describe the conditions that selectively favor chondrogenesis or osteogenesis[8,9].

BMP signal transduction is regulated by BMP antagonists, such as Noggin, which bind to the BMP extracellularly and block the binding of the BMP to its receptors. Recently, it was shown that BMP-4 is overexpressed in patients with fibrodysplasia ossificans progressiva[10,11] and that whereas cells from normal human subjects exhibit increased expression of BMP antagonists on exposure to high concentrations of BMP-4, cells from patients with fibrodysplasia ossificans progressiva do not[12]. These observations led to the development of a procedure involving gene transfer of an engineered Noggin mutein that prevents BMP-4-induced heterotopic ossification in the mouse[13]. Thus, studies that shed light on the pathogenesis of a genetic disorder in humans were based on knowledge of the molecular mechanisms that mediate and regulate BMP activity. The results of these studies led in turn to the development of a new modality of therapy to prevent pathological ossification.

The basic-science articles in this supplement include an abundance of new, useful information about the molecular mechanisms that mediate and regulate the effects of the BMPs. This information provides the foundation for the development of new modalities of treatment for skeletal disease.

—Lawrence C. Rosenberg, MD
Deputy Editor for Research
The Journal of Bone and Joint Surgery

References

1. **Einhorn TA.** Clinical applications of recombinant human BMPs: early experience and future development. *J Bone Joint Surg Am.* 2003;85 Suppl 3:82-8.
2. **Friedlaender GE, Perry CR, Cole JD, Cook SD, Cierny G, Muschler GF, Zych GA, Calhoun JH, LaForte AJ, Yin S.** Osteogenic protein-1 (bone morphogenetic protein-7) in the treatment of tibial nonunions. *J Bone Joint Surg Am.* 2001;83 Suppl 1 (Pt 2):S151-8.
3. **Food and Drug Administration.** Document H010002—OP-1TM Implant. Oct. 17, 2001. www.fda.gov/OHRMS/DOCKETS/98fr/03-7817.pdf.
4. **Sandhu HS, Khan SN.** Recombinant human bone morphogenetic protein-2: use in spinal fusion applications. *J Bone Joint Surg Am.* 2003;85 Suppl 3: 89-95.
5. **Seeherman H, Li R, Wozney J.** A review of preclinical program development for evaluating injectable carriers for osteogenic factors. *J Bone Joint Surg Am.* 2003;85 Suppl 3:96-108.
6. **Reddi AH.** Role of morphogenetic proteins in skeletal tissue engineering and regeneration. *Nat Biotechnol.* 1998;16:247-52.
7. **Cheng H, Jiang W, Phillips FM, Haydon RC, Peng Y, Zhou L, Luu HH, An N, Breyer B, Vanichakarn P, Szatkowski JP, Park JY, He T-C.** Osteogenic activity of the fourteen types of human bone morphogenetic proteins (BMPs). *J Bone Joint Surg Am.* 2003;85:1544-52.
8. **Hatakeyama Y, Nguyen J, Wang X, Nuckolls GH, Shum L.** Smad signaling in mesenchymal and chondroprogenitor cells. *J Bone Joint Surg Am.* 2003;85 Suppl 3:13-8.
9. **ten Dijke P, Fu J, Schaap P, Roelen BAJ.** Signal transduction of bone morphogenetic proteins in osteoblast differentiation. *J Bone Joint Surg Am.* 2003;85 Suppl 3:34-8.
10. **Shafritz AB, Shore EM, Gannon FH, Zasloff MA, Taub R, Muenke M, Kaplan FS.** Overexpression of an osteogenic morphogen in fibrodysplasia ossificans progressiva. *N Engl J Med.* 1996;335:555-61.
11. **Gannon FH, Kaplan FS, Olmsted E, Finkel GC, Zasloff MA, Shore E.** Bone morphogenetic protein 2/4 in early fibromatous lesions of fibrodysplasia ossificans progressiva. *Hum Pathol.* 1997;28:339-43.
12. **Ahn J, Serrano de la Pena L, Shore EM, Kaplan FS.** Paresis of a bone morphogenetic protein-antagonist response in a genetic disorder of heterotopic skeletogenesis. *J Bone Joint Surg Am.* 2003;85:667-74.
13. **Economides AN, Glaser DL, Wang L, Liu X, Kimble RD, Fandl JP, Wilson JM, Stahl N, Kaplan FS, Shore EM.** In vivo somatic cell gene transfer of an engineered Noggin mutein prevents BMP4-induced heterotopic ossification in the mouse. *J Bone Joint Surg Am.* In press.

EXHIBIT E

0013-7227/03/$15.00/0
Printed in U.S.A.

Endocrinology 144(5):1972–1978

doi: 10.1210/en.2002-220918

Skeletal Overexpression of Noggin Results in Osteopenia and Reduced Bone Formation

R. D. DEVLIN, Z. DU, R. C. PEREIRA, R. B. KIMBLE, A. N. ECONOMIDES, V. JORGETTI, AND E. CANALIS

Department of Research (R.D.D., Z.D., R.C.P., E.C.), Saint Francis Hospital and Medical Center, Hartford, Connecticut 06105-1299; The University of Connecticut School of Medicine (Z.D., E.C.), Farmington, Connecticut 06030; Regeneron Pharmaceuticals, Inc. (A.N.E.), Tarrytown, New York 10591; and Laboratorio de Fisiopatolgia Renal (V.J.), Universidade de São Paulo, São Paulo, Brazil

Skeletal cells synthesize bone morphogenetic proteins (BMPs) and BMP antagonists. Noggin is a glycoprotein that binds BMPs selectively and antagonizes BMP actions. Noggin expression in osteoblasts is induced by BMPs and noggin opposes the effects of BMPs on osteoblastic differentiation and function *in vitro*. However, its effects *in vivo* are not known. We investigated the direct *in vivo* effects of noggin on bone remodeling in transgenic mice overexpressing noggin under the control of the osteocalcin promoter. Noggin transgenics suffered long bone fractures in the first month of life. Total, vertebral, and femoral bone mineral densities were reduced by 23–29%. Static and dynamic histomorphometry of the femur revealed that noggin transgenic mice had decreased trabecular bone volume, number of trabeculae, and bone formation rate. Osteoblast surface and number of osteoblasts/trabecular area were not significantly decreased, indicating impaired osteoblastic function. Osteoclast surface and number were normal/decreased, there was no increase in bone resorption, and the tissue had the appearance of woven bone. Vertebral microcomputed tomography scanning confirmed decreased trabecular bone volume and trabecular number. In conclusion, transgenic mice overexpressing noggin in the bone microenvironment have decreased trabecular bone volume and impaired osteoblastic function, leading to osteopenia and fractures. (*Endocrinology* 144: 1972–1978, 2003)

SKELETAL CELLS SYNTHESIZE a number of growth factors including bone morphogenetic proteins (BMP)-2, -4, and -6 (1, 2). BMPs are unique because they induce the differentiation of mesenchymal cells toward cells of the osteoblastic lineage and enhance the function of the osteoblast, playing an autocrine role in osteoblast formation and function (3–7).

BMPs bind to specific receptors and signal either by activating the P38 MAPK pathway or by phosphorylating the cytoplasmic proteins mothers against decapentalegic (Smad) 1 and 5, which form heterodimers with Smad 4, and following nuclear translocation regulate transcription (8–10). BMP activity is modulated by intracellular and extracellular antagonists, including pseudoreceptors that compete with signaling receptors, inhibitory Smads that block signaling, intracellular binding proteins that bind Smad 1 and 5, and factors that induce ubiquitination and proteolysis of signaling Smads (11–15). In addition, a large number of extracellular proteins that bind BMPs and prevent their binding to signaling receptors have emerged. They include the components of the Spemann organizer, noggin, chordin, and follistatin, members of the Dan/Cerberus family, and twisted gastrulation (16–23). The antagonists tend to be specific for BMPs and have been used to block BMP action and study its role in selected tissues.

Noggin is one of the BMP antagonists that has been studied in greater detail. Noggin is a secreted glycoprotein with a molecular mass of 64 kDa, originally characterized as a component of the Spemann organizer and shown to induce dorsalization and the formation of neural tissue (16–18). Noggin binds with various degrees of affinity BMP-2, -4, -5, -6, and -7, and growth and differentiation factors 5 and 6, but not other members of the TGFβ family of peptides (17, 24). Homozygous null mutations of the noggin gene in mice result in serious developmental skeletal abnormalities and joint lesions, and heterozygous gene mutations in humans result in multiple joint lesions (25, 26). These findings indicate embryonic and adult detrimental consequences secondary to the lack of noggin, either directly or indirectly due to tissue overexposure to BMPs. The phenotypic lethality of noggin null mice has not allowed the definition of an adult skeletal phenotype in this model.

Osteoblasts express noggin following BMP treatment and the addition of noggin to osteoblasts and stromal cell cultures decreases the stimulatory effects of BMPs on osteoblastic function and impairs osteoblastogenesis and osteoclastogenesis (7, 27). However, the consequences of noggin overexpression in the bone microenvironment *in vivo* are not known. The intent of this study was to investigate the direct effects of noggin on bone remodeling. For this purpose, we created transgenic mice overexpressing noggin under the control of the osteoblastic specific osteocalcin promoter, and determined their skeletal phenotype.

Abbreviations: BMC, Bone mineral content; BMD, bone mineral density; BMP, bone morphogenetic protein; BV/TV, trabecular relative bone volume; μCT, microcomputed tomography; d, deoxy; L3, lumbar 3; Tb.Th., trabecular thickness.

Materials and Methods

Osteocalcin/noggin construct

Noggin was expressed under the control of the osteocalcin promoter so that transcription would occur specifically in cells of the osteoblastic

lineage (28). For this purpose, a 1.7-kb fragment of the rat osteocalcin promoter (Dr. R. Derynck, San Francisco, CA) was used to direct transcription of a 0.7-kb fragment coding for murine noggin (16, 29). The second intron of the rabbit β-globin gene (0.6 kb) was included between the osteocalcin promoter and noggin coding sequences, which were followed by a 0.2-kb fragment containing polyadenylation coding sequences from the bovine GH gene. Before the generation of transgenic mice, the *in vitro* activity of the osteocalcin promoter construct was demonstrated by documenting its ability to direct green fluorescent protein gene expression in transiently transfected MC3T3 cells by fluorescence microscopy (30, 31). The ability of the construct to drive noggin *in vitro* was confirmed by transiently transfecting the transgene construct into ROS17/2 osteosarcoma cells and identification of noggin transgene mRNA (by Northern blot analysis) and protein (by Western blot analysis; data not shown).

Generation of transgenic mice

Microinjection of linearized DNA into pronuclei of fertilized oocytes from CD-1 outbred albino mice (Charles River Laboratories, Inc., Cambridge, MA), and transfer of microinjected embryos into pseudopregnant mice were carried out at the transgenic facility of The University of Connecticut Health Center (Farmington, CT). Positive founders for osteocalcin driven noggin transgene were identified by Southern blot analysis of tail DNA (32). Founder mice were bred to wild-type CD-1 outbred albino mice. Heterozygous and nontransgenic littermates from the F1 and subsequent generations were selected by Southern blotting of genomic DNA. Heterozygous mice were intercrossed but failed to generate a homozygous offspring, possibly due to embryonic lethality. Transgenic mice overexpressing noggin were compared with wild-type littermates. All animal experiments were approved by the Animal Care and Use Committee of Saint Francis Hospital and Medical Center.

Northern blot analysis and RT-PCR

Calvarial or femoral RNA was isolated by the acid guanidium thiocyanate-phenol-chloroform extraction method followed by purification with an RNeasy column (QIAGEN, Valencia, CA; Ref. 33). RNA was quantitated by spectrometry. For Northern blot analysis, equal amounts of RNA were loaded on a formaldehyde agarose gel following denaturation. The gel was stained with ethidium bromide to visualize ribosomal RNA and confirm equal RNA loading of the samples. The RNA was blotted onto GeneScreen Plus charged nylon (Perkin-Elmer, Norwalk, CT) and uniformity of transfer confirmed by revisualization of ethidium bromide-stained ribosomal RNA. A 1.0-kb murine noggin cDNA (Regeneron Pharmaceuticals, Inc.), and a 752-bp murine 18S ribosomal RNA (American Type Culture Collection, Manassas, VA) were purified by agarose gel electrophoresis. cDNAs were labeled with [α-^{32}P]-deoxy (d)-CTP (50 μCi at a specific activity of 3000 Ci/mmol; Perkin-Elmer) using Ready-To-Go DNA-labeling beads (dCTP) kit (Amersham Pharmacia Biotech, Piscataway, NJ), in accordance with manufacturer's instructions. Hybridizations were carried out at 42 C for 16–72 h, followed by two post-hybridization washes at room temperature for 15 min in 1× saline sodium citrate and a wash at 65 C for 20 to 30 min in 0.5× or 1× saline sodium citrate. The bound radioactive material was visualized by autoradiography on X-AR5 film (Eastman Kodak Co., Rochester, NY), employing Cronex Lightning Plus (Perkin-Elmer) or Biomax MS (Eastman Kodak Co.) intensifying screens.

For RT-PCR, 1 μg of deoxyribonuclease I-treated total RNA from bone extracts was reverse transcribed with murine Moloney leukemia virus reverse transcriptase (Invitrogen, Rockville, MD) in the presence of 20 μM reverse primer corresponding to an 18-bp fragment of bovine GH polyadenylation sequence present in the noggin vector. One microliter of reverse transcription reaction was amplified by 30 cycles of PCR at 64 C annealing temperature in the presence of 20 μM 5′ to 3′ primer spanning bp +355 to +375 of noggin coding sequence, [α-^{32}P]-dCTP and 2.5 U of *Taq* polymerase to yield a product of a 388-bp predicted size. The products of the PCR were resolved by electrophoresis on a 6% polyacrylamide gel and visualized by autoradiography. Northern analysis and RT-PCR shown are representative of three samples.

X-ray analysis and bone mineral density (BMD)

Radiography was performed on mice anesthetized with tribromoethanol (Sigma, St. Louis, MO) on a Faxitron x-ray system (model MX 20, Faxitron X-Ray Corp., Wheeling, IL). Total, vertebral and femoral bone mineral content (BMC; grams), skeletal area (square centimeters), and BMD (grams per square centimeter) were measured on anesthetized mice using the PIXImus small animal DEXA system (GE Medical Systems/Lunar Corp., Madison, WI; Ref. 34). Calibrations were performed with a phantom of a defined value, and quality assurance measurements were performed before each use. The coefficient of variation for total BMD is less than 1% (n = 9).

Microcomputed tomography (μCT) scanning

μCT scanning of trabecular vertebral bone of transgenic and wild-type mice was determined using a μCT-20 system (μCT-20; Scanco Medical, Zurich, Switzerland; Ref. 35). Tridimensional analysis was performed to calculate morphometric indices of the lumbar spine (L3), including bone volume density [bone volume (BV)/tissue volume (TV), %], bone surface (BS) to volume ratio (BS/TV, mm^2/mm^3 = 1/mm) trabecular thickness (Tb.Th., μm), trabecular number (1/mm), and trabecular separation (mm).

Bone histomorphometric analysis

Static and dynamic histomorphometry was carried out in mice following calcein injections, 20 mg/kg, 7 d, and 2 d before the mice were killed by CO_2 asphyxiation. Femora were dissected and fixed in 70% ethanol. After dehydration, bone samples were embedded in methyl methacrylate and 5-μm-thick longitudinal sections were cut on a Jung polycut (Reichert-Jung, Heidelberg, Germany) or a Microm microtome (Microm, Richards-Allan Scientific, Kalamazoo, MI) and stained with Masson, Masson-Goldner trichrome or toluidine blue stains. Static parameters of bone formation and resorption were measured at a standardized site using a BioQuant image analysis system (Nashville, OH), and an OsteoMeasure morphometry system (Osteometrics, Atlanta, GA). Trabecular relative bone volume (BV/TV, %), Tb.Th. (micrometers) and trabecular number (per millimeter), and trabecular osteoblast and osteoclast surfaces (percentage) were measured. To determine the number of osteoblasts and osteoclasts/bone or trabecular area (square millimeters), the number of cells present in 20 fields of 180 μm^2 each of bone area were counted. For dynamic histomorphometry, mineral apposition rate (micrometers per day) was measured on unstained sections under UV light, using a B-2A set long pass filter consisting of an excitation filter ranging from 450–490 nm, a barrier filter at 515 nm, and a dichroic mirror at 500 nm. Bone formation rate (cubed micrometers per square micrometers per day) was calculated. The terminology and units used are those recommended by the Histomorphometry Nomenclature Committee of the American Society for Bone and Mineral Research (36).

Statistical analysis

Results are expressed as means ± SEM. Statistical significance was determined by Student's *t* test.

Results

Generation of transgenic mice and examination of transgene expression

Two transgenic lines with analogous skeletal phenotype were generated, and one was studied in detail and is described. For this purpose, a founder expressing four to six copies of the transgene was used to generate heterozygous mice, which were compared with wild-type littermates. Attempts to generate a homozygous offspring were unsuccessful, suggesting that high levels of noggin expression may compromise viability. However, there was no evidence of heterozygous lethality following heterozygote-wild-type matings, which generated the expected 50% heterozygous/50% wild-type offspring. RT-PCR of RNA extracted from

calvariae (Fig. 1) and femora (not shown) demonstrated the presence of noggin transgene in bone from transgenic mice and not in wild-type littermate controls. Noggin mRNA was not detected by Northern blot analysis of calvariae from 6-, 10-, or 28-wk-old wild-type mice. In contrast, noggin transcripts were clearly detectable in calvariae from noggin transgenic mice, although their levels declined as the animals aged (Fig. 1). This is probably a function of decreased activity of the osteocalcin promoter in older mice (28).

Weight, x-rays, and BMD

Transgenic heterozygous mice overexpressing noggin were smaller than wild-type littermates and the decrease in weight was sustained for a 6-month period (Table 1). The phenotype appeared limited to the skeleton because noggin expression was under the control of the osteocalcin promoter, and no obvious abnormalities were noted in extraskeletal tissues. Contact radiography of noggin transgenics revealed the presence of osteopenia and fractures of long bones at 4–5 wk of age (Fig. 2). Fractures occurred in tibiae, humeri, and occasionally in femora, but they were not detected in other bones. Of the fractures detected, tibial fractures were the most common and noted in virtually all transgenic mice overexpressing noggin. The osteopenia was sustained and fractures of long bones of upper and lower extremities occurred for 8–12 wk, and at 24 wk lucent areas of what appeared poorly healed fractures were noted. Accordingly, transgenic mice overexpressing noggin had significant and sustained decreases in BMC when compared with wild-type controls (Table 1). At 5–24 wk of age, total BMC was 28–37% lower in noggin transgenics than in wild-type control mice. Although noggin transgenics had reduced skeletal area, total BMD in 5- to 24-wk-old noggin transgenics was 15–24% ($P < 0.05$) lower than in wild-type controls, indicating a sustained decrease in total BMD (Table 1). This decrease was generalized and observed in total, vertebral, and femoral bones (Table 2). At 5 wk of age, the decrease in BMD in transgenic

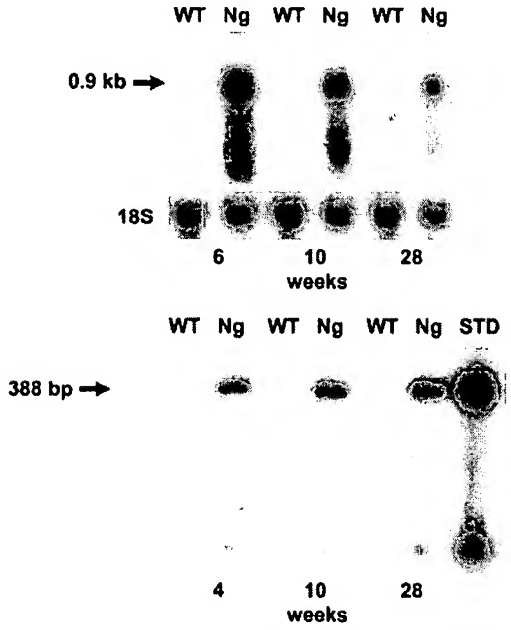

FIG. 1. Expression of noggin mRNA by Northern blot analysis (*upper panel*) and noggin transgene mRNA by RT-PCR (*lower panel*) in extracted calvariae from noggin transgenic (Ng) and wild-type (WT) control mice. Total RNA was extracted from calvariae of noggin transgenics and wild-type controls of the indicated ages. In the *upper panel*, RNA was resolved by gel electrophoresis, transferred to a nylon membrane, hybridized with [α-^{32}P]-labeled mouse noggin and 18S cDNAs, and visualized by autoradiography. In the *lower panel*, RNA was reverse transcribed, amplified by PCR in the presence of [α-^{32}P]-dCTP, resolved by gel electrophoresis, and visualized by autoradiography. *Right lane* represents osteocalcin noggin plasmid standard (STD).

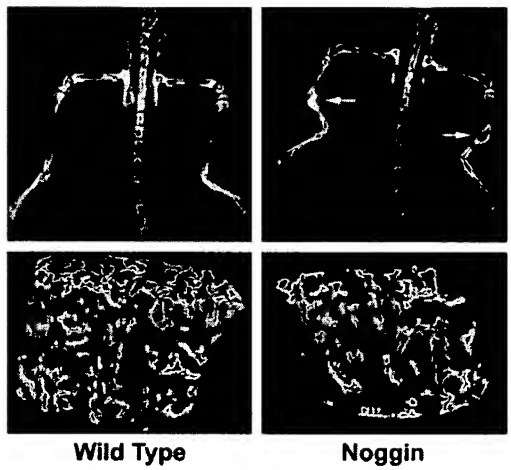

FIG. 2. The *upper panel* shows a representative skeletal radiograph of a 4-wk-old heterozygous transgenic overexpressing noggin and a wild-type littermate control mouse. *Arrows* indicate fractures and calluses. The *lower panel* shows a representative μCT scan of trabecular bone of an L3 vertebral body from a 4.5-wk-old heterozygous transgenic overexpressing noggin, with a BV/TV of 12.1%, and a wild-type littermate control, with a BV/TV of 26.7%. Images were obtained at a resolution of 18 μm, and the cortical shell was artificially removed for a better display of trabecular bone.

TABLE 1. Weight, total BMC, bone area, and BMD of 5- to 24-wk-old transgenics overexpressing noggin and wild-type littermate mice

Weeks	Weight		BMC		Skeletal area		BMD	
	Wild-type	Noggin	Wild-type	Noggin	Wild-type	Noggin	Wild-type	Noggin
5	20.6 ± 0.6	13.3 ± 0.7[a]	0.324 ± 0.01	0.206 ± 0.01[a]	8.2 ± 0.2	6.3 ± 0.2[a]	0.040 ± 0.001	0.033 ± 0.001[a]
8	28.0 ± 2.2	19.5 ± 1.3[a]	0.456 ± 0.04	0.316 ± 0.02[a]	9.1 ± 0.5	7.5 ± 0.3[a]	0.050 ± 0.001	0.042 ± 0.001[a]
12	37.8 ± 1.6	25.6 ± 1.1[a]	0.611 ± 0.01	0.383 ± 0.02[a]	10.6 ± 0.2	8.7 ± 0.3[a]	0.058 ± 0.003	0.044 ± 0.001[a]
24	31.4 ± 1.8	26.0 ± 0.3[a]	0.620 ± 0.05	0.444 ± 0.01[a]	10.6 ± 0.4	9.2 ± 0.1[a]	0.058 ± 0.002	0.049 ± 0.002[a]

Weight (g), BMC (g), skeletal area (cm^2), and BMD (g/cm^2) were obtained from 5-, 8-, 12-, and 24-wk-old noggin heterozygous transgenic mice and wild-type littermates. Values are means ± SEM (n = 3–14).

[a] Significantly different from wild-type controls, $P < 0.05$.

TABLE 2. BMD of 5- to 24-wk-old transgenic overexpressing noggin and wild-type littermate mice

Weeks	Total		Femoral		Vertebral	
	Wild-type	Noggin	Wild-type	Noggin	Wild-type	Noggin
5	0.040 ± 0.001	0.033 ± 0.001[a]	0.053 ± 0.002	0.038 ± 0.003[a]	0.042 ± 0.001	0.030 ± 0.002[a]
8	0.050 ± 0.001	0.042 ± 0.001[a]	0.067 ± 0.003	0.049 ± 0.002[a]	0.058 ± 0.002	0.042 ± 0.002[a]
12	0.058 ± 0.003	0.044 ± 0.001[a]	0.081 ± 0.002	0.058 ± 0.002[a]	0.066 ± 0.002	0.039 ± 0.002[a]
24	0.058 ± 0.002	0.049 ± 0.002[a]	0.079 ± 0.003	0.061 ± 0.002[a]	0.065 ± 0.006	0.045 ± 0.001[a]

BMD was obtained from 5, 8, 12, and 24-wk-old noggin heterozygous transgenic mice and wild-type littermates. BMD is expressed as g/cm^2 and values are means ± SEM (n = 3–14) of total, vertebral, and femoral BMD.

[a] Significantly different from wild-type controls, $P < 0.05$.

TABLE 3. Three-dimensional microstructural parameters of vertebral bones from 4.5-wk-old mice overexpressing noggin and wild-type littermate mice

	Wild-type	Noggin
BV/TV (%)	22.6 ± 2.2	12.0 ± 1.4[a]
Trabecular thickness (mm)	0.052 ± 0.002	0.046 ± 0.009
Trabecular number (1/mm)	5.7 ± 0.2	4.3 ± 0.3[a]
Trabecular separation (mm)	0.17 ± 0.01	0.24 ± 0.02[a]
Bone surface to volume ratio (1/mm)	37.7 ± 2.9	45.0 ± 1.8[a]

Morphometric indices were obtained by μCT scanning of vertebral bones from 4.5-wk-old noggin heterozygous transgenic mice and wild-type littermates. Values are means ± SEM (n = 6–7).

[a] Significantly different from wild-type controls, $P < 0.05$.

mice was 17% for total BMD, and 28 and 29% for femoral and vertebral BMD.

μCT scanning, static and dynamic histomorphometry

μCT scanning of the L3 vertebral body revealed decreased bone volume due to decreased trabecular number (Table 3 and Fig. 2). Static and dynamic parameters of bone formation and parameters of bone resorption were determined by histomorphometric analysis of the femur. Cancellous bone volume was reduced 70% in noggin transgenic mice, and this was due to a reduction in the number of trabeculae, rather than a reduction in trabecular thickness (Table 4 and Fig. 3). Histomorphometric analysis revealed normal osteoblast and osteoclast surfaces in noggin transgenic mice. In accordance, the number of osteoblasts per trabecular area was not significantly altered in noggin transgenics at either 4 wk (Table 4) or 8 wk of age, when osteoblast number/trabecular area was (mean ± SE; n = 7–8) 86 ± 8/mm^2 in wild-type and 114 ± 18/mm^2 in transgenics. The number of osteoclasts/trabecular area was decreased in noggin transgenics at 4 wk (Table 4), but not at 8 wk, when osteoclast number was 4.1 ± 1.6 in wild-type and 6.3 ± 1.5 (n = 7–8, $P > 0.05$) in transgenics. The decrease in osteoclasts/bone area observed at 4 wk of age in noggin transgenics was related to the reduction in trabecular bone resulting in areas of bone tissue without trabeculae, and therefore without cells. Mineral apposition and bone formation rates were reduced by 85% in transgenic mice, indicative of a decrease in osteoblastic function (Table 4 and Fig. 3).

In noggin transgenic mice, dual labeling with calcein resulted in diffuse broad labels, at times disorganized, characteristic of woven bone, suggesting abnormal or incomplete mineralization (Fig. 3). In some areas, mineralization fronts were visible, and were used to calculate mineral apposition rate (Table 4). In addition to the effects on trabecular bone, noggin transgenics displayed decreased bone formation in cortical bone. Cortical bone formation rate in 4-wk-old wild-type was (mean ± SEM; n = 7–9) 2.6 ± 0.3 and in transgenic mice was 1.1 ± 0.3 μm/μm^2·d, $P < 0.05$. Growth plate architecture appeared normal, although in accordance with the generalized decrease in bone size, growth plate height and width were decreased in noggin transgenics by 20%, $P < 0.05$. Consistent with the activity of the osteocalcin promoter, the phenotypic impact of noggin overexpression, as determined by bone histomorphometry, occurred in the first 4–8 wk of life and then declined (Fig. 3 and Table 5). Dual calcein labeling of 12 wk and 6-month-old transgenics revealed normal and organized mineralization fronts and absence of woven bone (not shown).

Discussion

Our findings demonstrate that transgenic mice overexpressing noggin under the control of the osteocalcin promoter develop decreased trabecular bone volume and osteopenia. The skeletal phenotype, as determined by histomorphometry, was evident at 4 and 8 wk of age, a time of marked expression of the osteocalcin promoter, but it was not observed in older animals, presumably due to a decrease in the activity of the osteocalcin promoter (28). However, the decrease in bone mineral content, the osteopenia and poor healing of fractures persisted for 6 months. The osteopenia could be due to more persistent changes in cortical bone, but it is more likely due to early changes in bone structure with a consequent decrease in bone mineral content. Abnormal mineralization would be consistent with the marked initial disruption of the bone structure, and poor healing of fractures could be due to a suppression of BMP activity by noggin because BMPs play a role in fracture healing (37). However, fractures caused misalignment of bone structures that were not corrected, and this also could affect their healing. The decrease in trabecular bone volume observed in noggin transgenic mice was secondary to a decrease in trabecular number. This appeared to be due to decreased osteoblastic activity because mineral apposition rate was decreased and the number of osteoblasts per trabecular area was not decreased significantly. Furthermore, osteoclast number was not increased and bone resorption was not visibly affected. The substantial decrease in trabecular bone resulted in areas of tissue without trabeculae or cells in noggin transgenics. However, the number of osteoblasts/bone area was not significantly decreased, although the number of

TABLE 4. Femoral trabecular bone histomorphometry in 4-wk-old transgenic overexpressing noggin and wild-type littermate mice

	Wild-type	Noggin
Trabecular relative bone volume (%)	8.3 ± 2.4	2.1 ± 0.5[a]
Trabecular osteoblast surface (%)	42.5 ± 4.4	42.4 ± 6.3
Number of osteoblasts/trabecular area (mm^2)	254 ± 24	204 ± 19
Trabecular osteoclast surface (%)	24.3 ± 1.4	25.2 ± 8.0
Number of osteoclasts/trabecular area (mm^2)	13.4 ± 2.3	5.6 ± 1.2[a]
Trabecular thickness (μm)	22.1 ± 2.4	18.8 ± 3.1
Trabecular number (per mm)	3.4 ± 0.7	1.0 ± 0.2[a]
Trabecular spacing (μm)	688 ± 2	3573 ± 1896
Mineral apposition rate (μm/d)	1.27 ± 0.15	0.22 ± 0.16[a]
Bone formation rate ($\mu m^3/\mu m^2$/d)	0.28 ± 0.03	0.04 ± 0.04[a]

Bone histomorphometry was performed on femora from 4-wk-old noggin heterozygous transgenic mice and wild-type littermates. Values are means ± SEM (n = 7–8).

[a] Significantly different from wild-type controls, $P < 0.05$.

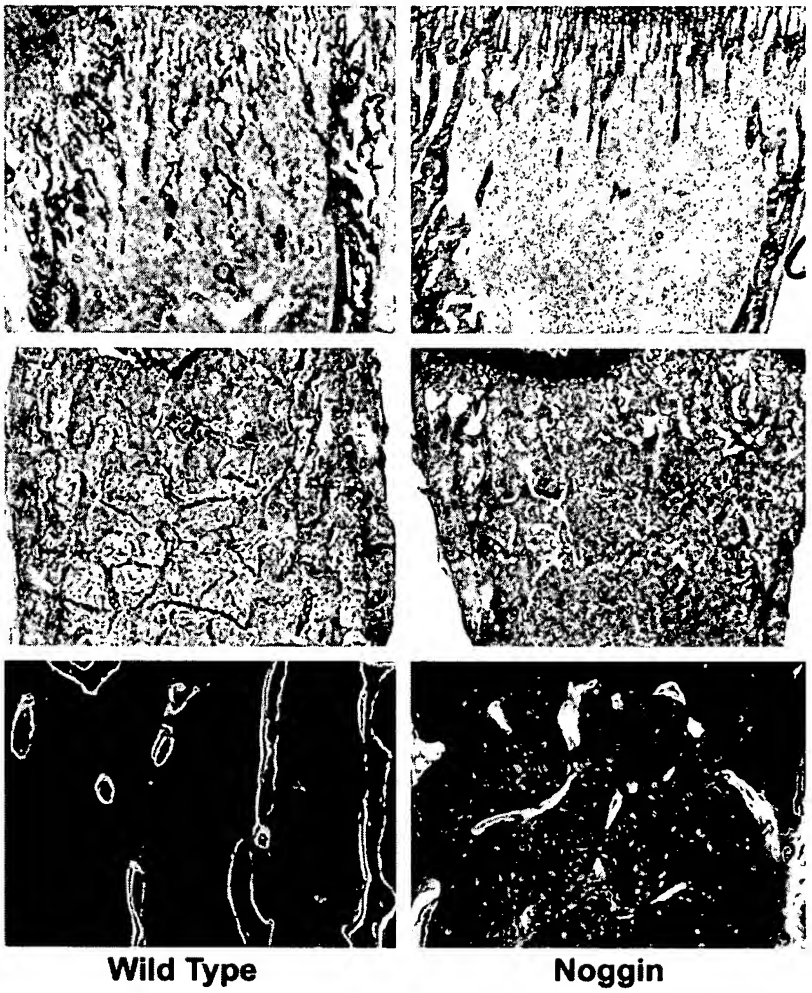

FIG. 3. Representative undecalcified sections of femora from heterozygous transgenics overexpressing noggin and wild-type littermate controls. In the *upper panel*, toluidine blue-stained sections were obtained from 4-wk-old mice (final magnification, ×100). In the *middle* and *lower panels*, toluidine blue-stained and unstained sections were obtained from the same area of 8-wk-old mice given sequential doses of calcein. Stained sections were visualized at a final magnification of ×40 and unstained sections were visualized by UV light microscopy at a final magnification of ×100.

osteoclasts present in a predefined area of bone were decreased.

The decreased osteoblastic function observed in noggin transgenics confirms previous *in vitro* observations, demonstrating that the addition of noggin to cultured calvariae results in decreased bone collagen synthesis and alkaline phosphatase activity (7). The mechanism of the impaired osteoblastic function in noggin transgenics could involve the binding and sequestering of BMPs by noggin in the bone microenvironment. There was no evidence of systemic effects of noggin, outside the skeleton, and immunoreactive noggin, as determined by ELISA, was undetectable in serum (not shown). The phenotypic changes observed are in agreement with what would be predicted from blocking the known effects of BMPs on osteoblastic function. BMPs have modest mitogenic activity in bone and have a more prevalent

TABLE 5. Selected histomorphometric parameters in 4- to 24-wk-old transgenic overexpressing noggin and wild-type littermate mice

Weeks	Trabecular bone volume (%)		Trabecular number (per mm)		Mineral apposition rate (μm/d)	
	Wild-type	Noggin	Wild-type	Noggin	Wild-type	Noggin
4	8.3 ± 2.4	2.1 ± 0.5[a]	3.4 ± 0.7	1.0 ± 0.2[a]	1.27 ± 0.15	0.22 ± 0.16[a]
8	11.9 ± 1.7	5.0 ± 0.7[a]	4.1 ± 0.5	2.1 ± 0.3[a]	1.00 ± 0.07	0.24 ± 0.07[a]
12	11.2 ± 2.2	9.8 ± 2.8	3.3 ± 0.5	3.0 ± 0.6	0.90 ± 0.16	0.81 ± 0.21
24	6.8 ± 2.5	5.7 ± 3.6	2.3 ± 0.5	1.8 ± 0.8	Not determined	Not determined

Bone histomorphometry was performed on femora from 4- to 24-wk-old noggin heterozygous transgenic mice and wild-type littermates. Values are means ± SEM (n = 3–8).

[a] Significantly different from wild-type controls, $P < 0.05$.

impact on the differentiated function of the osteoblast (4–7). However, noggin effects independent of BMPs are possible and were not excluded. Previous work has shown that BMPs induce the differentiation of mesenchymal cells toward cells of the osteoblastic lineage (38). However, our results suggest a more significant effect on osteoblastic function than in number in noggin transgenics. This is possibly due to the model used in the present study because the osteocalcin promoter becomes active only following osteoblastic cell maturation. Consequently, noggin is not overexpressed before the formation of mature osteoblasts, and in this model it might not affect the differentiation of immature cells. Recent work from our laboratory has demonstrated that stromal cells overexpressing noggin under the control of the cytomegalovirus promoter and primary cultures of stromal cells from noggin transgenic mice fail to differentiate into mature osteoblasts (39). This would confirm a dual role for BMPs in osteoblastic differentiation and function.

Our studies also demonstrate that a decrease in trabecular bone volume and osteoblastic function by noggin overexpression can be translated into significant and generalized osteopenia and fractures in the mouse. This would suggest a role for BMPs in the maintenance of a normal bone structure. The validity of the transgenic model used has been substantiated by a number of studies including the demonstration of an increase in bone formation by overexpressing IGF-I under the control of the osteocalcin promoter, and confirmation of the known anabolic actions of IGF I *in vitro* (40). The present studies suggest that noggin may act by trapping BMPs in a manner analogous to that described for IGF I and its binding proteins. Although we have postulated a need to temper the activity of locally produced skeletal growth factors, it is important to note that overexpression of proteins binding skeletal growth factors can have seriously detrimental consequences, such as osteopenia and fractures. For instance, transgenic mice overexpressing IGF binding protein 5 under the control of the osteocalcin promoter display decreased bone formation and osteopenia (31).

In conclusion, our studies demonstrate that *in vivo* skeletal overexpression of noggin, under the control of the osteocalcin promoter, causes decreased trabecular volume and severe osteopenia. This appears secondary to impaired osteoblastic function.

Acknowledgments

The authors thank Dr. R. Derynck for an osteocalcin promoter construct, and Regeneron Pharmaceuticals, Inc. for noggin cDNA. The authors thank Drs. Stephen Clark and Anne Delany for helpful discussions, Mr. Vincenzo Buccilli, Ms. Lisa Stadmeyer, and Ms. Sheila Rydziel for technical assistance, and Ms. Karen Berrelli and Ms. Nancy Wallach for secretarial assistance.

Received September 3, 2002. Accepted January 8, 2003.

Address all correspondence and requests for reprints to: Ernesto Canalis, M.D., Department of Research, Saint Francis Hospital and Medical Center, 114 Woodland Street, Hartford, Connecticut 06105-1299. E-mail: ecanalis@stfranciscare.org.

This work was supported by Grant AR-21707 from the National Institute of Arthritis and Musculoskeletal and Skin Diseases.

References

1. **Margolis RN, Canalis E, Partridge NC** 1996 Anabolic hormones in bone: basic research and therapeutic potential. J Clin Endocrinol Metab 81:872–877
2. **Pereira RC, Rydziel S, Canalis E** 2000 Bone morphogenetic protein-4 regulates its own expression in cultured osteoblasts. J Cell Physiol 182:239–246
3. **Celeste AJ, Iannazzi JA, Taylor RC, Hewick RM, Rosen V, Wang EA, Wozney JM** 1990 Identification of transforming growth factor B family members present in bone-inductive protein purified from bovine bone. Proc Natl Acad Sci USA 87:9843–9847
4. **Hughes FJ, Collyer J, Stanfield M, Goodman SA** 1995 The effects of bone morphogenetic protein-2, -4, and -6 on differentiation of rat osteoblast cells *in vitro*. Endocrinology 136:2671–2677
5. **Thies RS, Bauduy M, Ashton BA, Kurtzberg L, Wozney JM, Rosen V** 1992 Recombinant human bone morphogenetic protein-2 induces osteoblastic differentiation in W-20–17 stromal cells. Endocrinology 130:1318–1324
6. **Schmitt JM, Hwang K, Winn SR, Hollinger JO** 1999 Bone morphogenetic proteins: an update on basic biology and clinical relevance. J Orthop Res 17:269–278
7. **Gazzero E, Gangji V, Canalis E** 1998 Bone morphogenetic proteins induce the expression of noggin, which limits their activity in cultured rat osteoblasts. J Clin Invest 102:2106–2114
8. **Yamashita H, ten Dijke P, Heldin C-H, Miyazono K** 1996 Bone morphogenetic protein receptors. Bone 19:569–574
9. **Derynck R, Zhang Y, Feng X-H** 1998 Smads: transcriptional activators of TGF-β responses. Cell 95:737–740
10. **Nohe A, Hassel S, Ehrlich M, Neubauer F, Sebald W, Henis YI, Knaus P** 2002 The mode of bone morphogenetic protein (BMP) receptor oligomerization determines different BMP-2 signaling pathways. J Biol Chem 277:5330–5338
11. **Onichtchouk D, Chen Y-G, Dosch R, Gawantka V, Delius H, Massague J, Niehrs C** 1999 Silencing of TGFβ signaling by the pseudoreceptor BAMBI. Nature 401:480–485
12. **Imamura T, Takase M, Nishihara A, Oeda E, Hanai J-I, Kawabata M, Miyazono K** 1997 Smad6 inhibits signaling by the TGF-β superfamily. Nature 389:622–626
13. **Wang W, Mariani FV, Harland RM, Luo K** 2000 Ski represses bone morphogenic protein signaling in *Xenopus* and mammalian cells. Proc Natl Acad Sci USA 97:14394–14399
14. **Yoshida Y, Tanaka S, Umemori H, Minowa O, Michihiko U, Ikematsu N, Hosoda E, Imamura T, Kuno J, Yamashita T, Miyazono K, Noda M, Noda T, Yamamoto T** 2000 Negative regulation of BMP/Smad signaling by Tob in osteoblasts. Cell 103:1085–1097
15. **Zhang Y, Chang C, Gehling DJ, Hemmati-Brivanlou A, Derynck R** 2001 Regulation of Smad degradation and activity by Smurf2, and E3 ubiquitin ligase. Proc Natl Acad Sci USA 98:974–979
16. **Valenzuela DM, Economides AN, Rojas E, Lamb TM, Nunez L, Jones P, Ip NY, Espinosa R, Brannan CI, Gilbert DJ, Copeland NG, Jenkins NA, LeBeau MM, Harland RM, Yancopoulos GD** 1995 Identification of mammalian noggin and its expression in the adult nervous system. J Neurosci 15:6077–6084
17. **Zimmerman LB, DeJesus-Escobar JM, Harland RM** 1996 The Spemann organizer signal noggin binds and inactivates bone morphogenetic protein 4. Cell 86:599–606
18. **Smith WC, Harland RM** 1992 Expression cloning of noggin, a new dorsalizing

factor localized to the Spemann organizer in Xenopus embryos. Cell 70: 829–840
19. **Sasai Y, Lu B, Steinbeisser H, Geissert D, Gont LK, De Robertis EM** 1994 *Xenopus chordin:* a novel dorsalizing factor activated by organizer-specific homeobox genes. Cell 79:779–790
20. **Fainsod A, Deibler K, Yelin R, Marom K, Epstein M, Pillemer G, Steinbeisser H, Blum M** 1997 The dorsalizing and neural inducing gene *follistatin* is an antagonist of BMP-4. Mech Dev 63:39–50
21. **Pearce JJH, Penny G, Rossant J** 1999 A mouse cerberus/Dan-related gene family. Dev Biol 209:98–110
22. **Ross JJ, Shimmi O, Vilmos P, Petryk A, Kim H, Gaudenz K, Hermanson S, Ekker SC, O'Connor MB, Marsh JL** 2001 Twisted gastrulation is a conserved extracellular BMP antagonist. Nature 410:479–482
23. **Chang C, Holtzman DA, Chau S, Chickering T, Woolf EA, Holmgren LM, Bodorova J, Gearing DP, Holmes WE, Brivanlou AH** 2001 Twisted gastrulation can function as a BMP antagonist. Nature 410:483–487
24. **Aspenberg P, Jeppsson C, Economides AN** 2001 The bone morphogenetic proteins antagonist noggin inhibits membranous ossification. J Bone Miner Res 16:497–500
25. **Brunet LJ, McMahon JA, McMahon AP, Harland RM** 1998 Noggin, cartilage morphogenesis, and joint formation in the mammalian skeleton. Science 280: 1455–1457
26. **Gong Y, Krakow D, Marcelino J, Wilkin D, Chitayat D, Babul-Hirji R, Hudgins L, Cremers CW, Cremers FP, Brunner HG, Reinker K, Rimoin DL, Cohn DH, Goodman FR, Reardon W, Patton M, Francomano CA, Warman ML** 1999 Heterozygous mutations in the gene encoding noggin affect human joint morphogenesis. Nat Genet 21:302–304
27. **Abe E, Yamamoto M, Taguchi Y, Lecka-Czernik B, O'Brien CA, Economides AN, Stahl N, Jilka RL, Manolagas SC** 2000 Essential requirement of BMPs-2/4 for both osteoblast and osteoclast formation in murine bone marrow cultures from adult mice: antagonism by noggin. J Bone Miner Res 15:663–673
28. **Frenkel B, Caparelli C, Van Auken M, Baran D, Bryan J, Stein JL, Stein GS, Lian JL** 1997 Activity of the osteocalcin promoter in skeletal sites of transgenic mice and during osteoblast differentiation in bone marrow-derived stromal cell cultures: effects of age and sex. Endocrinology 138:2109–2116
29. **Erlebacher A, Derynck R** 1996 Increased expression of TGF-β2 in osteoblasts results in an osteoporosis-like phenotype. J Cell Biol 132:195–210
30. **Chalfie M, Tu Y, Euskirchen G, Ward WW, Prasher DC** 1994 Green fluorescent protein as a marker for gene expression. Science 263:802–805
31. **Devlin RD, Du Z, Buccilli V, Jorgetti V, Canalis E** 2002 Transgenic mice overexpressing insulin-like growth factor binding protein-5 display transiently decreased osteoblastic function and osteopenia. Endocrinology 143:3955–3962
32. **Irwin N** 1989 Molecular cloning. Sambrook J, Fritsch EF, Maniatis T, eds. Cold Spring Harbor, NY: Cold Spring Harbor Laboratory Press; 9.32–9.36
33. **Chomczynski P, Sacchi N** 1987 Single step method of RNA isolation by acid guanidium thiocyanate-phenol-chloroform extraction. Anal Biochem 162: 156–159
34. **Nagy TR, Prince CW, Li J** 2001 Validation of peripheral dual-energy x-ray absorptiometry for the measurement of bone mineral in intact and excised long bones of rats. J Bone Miner Res 16:1682–1687
35. **Ruegsegger P, Koller B, Muller R** 1996 A microtomographic system for the nondestructive evaluation of bone architecture. Calcif Tissue Int 58:24–29
36. **Parfitt AM, Mathews CHE, Villaneuva AR, Kleerekoper M, Frame B, Rao DS** 1987 Bone histomorphometry: standardization of nomenclature, symbols, and units. Report of the ASBMR Histomorphometry Nomenclature Committee. J. Bone Miner Res 2:595–610
37. **Bouxsein ML, Turek TJ, Blake CA, D'Augusta D, Li X, Stevens M, Seeherman HJ, Wozney JM** 2001 Recombinant human bone morphogenetic protein-2 accelerates healing in a rabbit ulnar osteotomy model. J Bone Joint Surg Am 83-A:1219–1230
38. **Spinella-Jaegle S, Roman-Roman S, Faucheu C, Dunn F-W, Dawai S, Gallea S, Stiot V, Blanchet AM, Courtois B, Baron R, Rawadi G** 2001 Opposite effects of bone morphogenetic protein-2 and transforming growth factor-β1 on osteoblast differentiation. Bone 29:323–330
39. **Gazzerro E, Du Z, Devlin RD, Rydziel S, Priest L, Economides AN, Canalis E,** Noggin arrests stromal cell differentiation *in vitro.* Bone, in press
40. **Zhao G, Monier-Faugere MC, Langub MC, Geng Z, Nakayama T, Pike JW, Chernausek SD, Rosen CJ, Donahue L-R, Malluche HH, Fagin JA, Clemens TL** 2000 Targeted overexpression of insulin-like growth factor I to osteoblasts of transgenic mice: increased trabecular bone volume without increased osteoblast proliferation. Endocrinology 141:2674–2682